HISTORY MATCHING AND OPTIMIZATION USING STOCHATIC METHODS: APPLICATIONS TO CHEMICAL FLOODING

A Dissertation

by

ZHENG ZHANG

Submitted to the Office of Graduate and Professional Studies of
Texas A&M University
in partial fulfillment of the requirements for the degree of

DOCTOR OF PHILOSOPHY

Chair of Committee,	Akhil Datta-Gupta
Committee Members,	Michael King
	Christine Ehlig-Economides
	Yalchin Efendiev
Head of Department,	A. Daniel Hill

December 2014

Major Subject: Petroleum Engineering

ABSTRACT

A typical lifecycle of an oil and gas field is characterized by three stages: primary recovery by natural depletion, secondary recovery by fluid injection, and enhanced oil recovery (EOR). The primary goal of reservoir management is to increase hydrocarbon recovery while reducing capital and operational expenditures. Two key techniques for the success of reservoir management are model calibration and production optimization. History matching is used to calibrate existing geological models against to measured data and predict the range of future recovery. Production optimization on calibrated reservoir models provides economic assessment of different field development plans and suggests optimal strategies to maximize recovery and minimize cost.

We first presented the workflow of history matching in chemical flooding. Evolutionary algorithms are the method of choice due to its capability of calibrating various parameter types and its global search nature. Chemical flooding simulator UTCHEM, developed by The University of Texas at Austin, is coupled during the history matching process to consider complex mechanisms such as phase behavior, chemical and physical transformations, etc.

Next, we implemented the proposed workflow to calibrate models in multiple stages that can efficiently reduce large amounts of uncertain parameters in alkaline-surfactant-polymer (ASP) flooding. Each stage of model calibration will follow an order of field scale, and then individual well scale, with consideration of behaviors brought by ASP flooding, such as surfactant/polymer adsorption. The proposed multi-stage history matching workflow is powerful to deliver better history matching results and significantly reduce the uncertainty of large numbers of parameters involved in chemical flooding.

Lastly, we extended the evolutionary workflows for multi-objective optimization via introducing the concept of Pareto optimality. Pareto front method is proposed to handle conflicting objective functions such as oil production and chemical efficiency instead of

weighted sum method in optimizing ASP flooding. Non-dominated Sorting Genetic Algorithm (NSGA-II) is used to search for Pareto optimal solutions.

The robustness and practical feasibility of our approaches have been demonstrated through both synthetic and field examples.

DEDICATION

To my beloved husband, my parents, my sister and my nephew for their endless love and support.

ACKNOWLEDGEMENTS

I would like to gratefully and sincerely thank my academic advisor, Dr. Akhil Datta-Gupta for his academic guidance, patience, understanding, and financial support. Without his mentorship, I could not have finished my PhD study and research. His immense knowledge, rigorous attitude to study and amiable personality have been and will always be a model for me.

I would like to thank Dr. King for innovative ideas and thoughtful suggestions during our meetings and discussions. I would like to thank other committee members, Dr. Ehlig-Economides, Dr. Efendiev, for their insightful comments that have improved this dissertation. I would like to thank Dr. Nasrabadi to contribute and substitute for Dr. Ehlig-Economides during the defense. I would like to thank Dr. Mojdeh Delshad from University of Texas at Austin for providing chemical flooding cases.

I would like to thank BHP Billiton (Petroleum) and Total E&P USA for providing me internship opportunities. I would like to thank Reza Fassihi, Doug Peck, Rick Walker, Ed Turek, Martin Cohen, Yann Bigno, and Frederic Brigaud for their precious trust and support during the summers, from which I obtained valuable experience.

Special thanks to all my colleagues in the MCERI group at Texas A&M University, for your help and support. Your excellence and hard-working spirit encouraged me to become more diligent. I appreciate every joyful moment with you all.

NOMENCLATURE

σ	interfacial tension, N/m
N_T	trapping number
S_r	residual saturation
S_r^{low}	residual saturation at low trapping number
S_r^{high}	residual saturation at high trapping number
k_r	endpoint of relative permeability curve
n	exponent of relative permeability curve
N_c	capillary number
u	displacing velocity, m/s
μ	viscosity, cp
IFT	Interfacial Tension
T_l	capillary desaturation curve parameter for each phase
CDC	Capillary Desaturation Curve
GA	Genetic Algorithm
UF	Utility Factor

TABLE OF CONTENTS

Page

LIST OF FIGURES

Page

LIST OF TABLES

Page

CHAPTER I
INTRODUCTION AND STUDY OBJECTIVES

A typical lifecycle of an oil and gas field is characterized by three stages: primary recovery by natural depletion, secondary recovery by fluid injection, and enhanced oil recovery (EOR). The primary goal of reservoir management is to increase hydrocarbon recovery while reducing capital and operational expenditures. Two key techniques for the success of reservoir management are model calibration and production optimization. History matching is used to calibrate existing geological models against to measured data and predict the range of future recovery. Production optimization on calibrated reservoir models provides economic assessment of different field development plans and suggests optimal strategies to maximize recovery and minimize cost.

1.1 Overview of History Matching and Production Optimization

In order to maximize oil and gas recovery, it is critical to have a clear understanding of the static properties and dynamic behavior of the field. This is achieved by reservoir simulations on full field models which consist of many wells over usually decades. These geological models are typically constructed by static data including well logs, core measurements, and seismic data. Consisting of large numbers of subsurface uncertainties, models derived exclusively from static data often fail to reproduce the observed dynamic production history and consequently will most likely give poor recovery prediction. Therefore, integrating historical dynamic production data is a vital step to develop reliable reservoir performance models. The process is referred to as history matching or model calibration.

Traditionally, manual history matching has commonly been conducted on a single deterministic model by sequential trial-and-error adjustments of model parameters: from global, then to flow units, followed by local parameters (Williams et al. 2004; Williams

et al. 1998). This manual process is tedious and for large fields it becomes impractical to investigate complex relationships between the model responses and different reservoir input parameters.

Over past decades, assisted history matching (AHM) has been an active area of research. It is different from manual history matching in that computer software is employed to adjust the reservoir parameters rather than direct intervention of engineers. AHM can be thought of as a minimization problem, whose objective function includes the sum of squared difference between observed data and computed data. The goal of AHM is to minimize objective functions by varying model input parameters. In particular, model calibration on geological properties has gained a lot of attention in literature. Most of them commonly focus on adjustment of fine-scale reservoir permeability in order to match dynamic production data, where gradient-based methods and sensitivity-based methods are preferred to derivative-free methods. Gradient-based methods such as adjoint methods are computationally expensive and typically converge slowly (Gill 1981; McCormick 1972). Sensitivity-based methods are attractive because of faster convergence compared to gradient-based methods (Bissell et al. 1992). The essential part of sensitivity-based history matching is the computation of the partial derivatives of the production responses with respect to the reservoir parameters of interest. The streamline-based generalized travel time inversion (GTTI) technique has proven to be an efficient technique for in water-flooding reservoirs (Cheng et al. 2005; Cheng et al. 2008; Datta-Gupta 2001) because analytical sensitivities can be efficiently obtained in the same forward simulation run when the residual objective function is evaluated. The GTTI history matching approach has been applied successfully in a large number of field applications (Cheng et al. 2004; Hohl et al. 2006; Qassab et al. 2003; Rey et al. 2009).

However, most of deterministic approaches mentioned above generally start with a single initial geological model. Therefore, they strongly depend on quality of the initial model. Field experience shows that misrepresentation of large-scale features such as fault communications and pore volumes can result in unphysical model updates in fine

scale reservoir permeability. This is due to the local search nature of the deterministic technique and its deficiency in handling various scale uncertainties. In contrast, global search algorithms avoid the problem of convergence to local optimum nearest to the initial starting point (Cheng et al. 2008) and are able to reconcile multi-scale uncertainties simultaneously. Global search techniques such as simulated annealing (SA) (Galassi 2009; Kirkpatrick 1983; Ouenes and Bhagavan 1994), Markov chain Monte Carlo (MCMC) (Ma et al. 2006; Sambridge and Mosegaard 2002) and genetic algorithms (GA) (Holland 1992) have been known to be effective for history matching problems. The advantage of these stochastic search techniques is that they require neither complicated differential equations nor a smooth response space. The primary challenge is that they require large number of flow simulations, which can be computationally prohibitive when the parameter space is very large. Consequently, sensitivity analysis is introduced to rank the importance of model parameters and screen insignificant ones, and the proxy model is introduced as a surrogate to avoid simulations for less likely model candidates (Cheng et al. 2008; Pan and Horne 1998; White and Royer 2003; Yeten et al. 2005; Yeten et al. 2002).

Most existing applications of stochastic model calibrations in literature are for conventional reservoirs with water flooding. One particular application that has received relatively less attention is enhanced oil recovery. Although in recent years chemical EOR are gaining more and more popularity, most model calibration work of chemical flooding are still done in a manual manner with limited number of uncertainties. As more and more EOR mechanisms are being investigated through pilot tests on conventionally water-flooded reservoirs, relatively little attention is paid to systematically and automatically calibrating EOR parameters.

1.2 Objectives and Dissertation Outline

The primary goal of this dissertation is to study the applicability of stochastic methods in management of chemical flooding. We will now outline the stages of this dissertation and the specific objective in Chapter II-IV.

In Chapter II, we will present the workflow of history matching chemical flooding. Evolutionary algorithms are the method of choice due to its capability of calibrating various parameter types and its global search nature. Chemical flooding simulator UTCHEM, developed by The University of Texas at Austin, is coupled with genetic algorithm during the history matching process to consider complex mechanisms such as phase behavior, chemical and physical transformations, etc.

In Chapter III we implement the proposed workflow to calibrate model in multiple stages that can efficiently constrain large numbers of uncertain parameters in alkaline-surfactant-polymer (ASP) flooding. First, uncertain parameters regarding capillary desaturation, relative permeability, and adsorption and their effects on oil recovery are studied. Then, a multi-stage model calibration is applied to adjust related parameters according to the individual objective function for each stage of the ASP process. Each stage of model calibration will follow a sequence of field scale, and then individual well scale, with consideration of physical mechanisms brought by ASP flooding, such as surfactant/polymer adsorption.

In Chapter IV, the evolutionary workflows introduced in Chapter II will be extended for multi-objective optimization via introducing the concept of Pareto optimality. Pareto front method is proposed to handle conflicting objective functions such as oil production and chemical efficiency instead of weighted sum method in optimizing ASP flooding. A field application will be demonstrated to illustrate the improved workflow.

In the Appendix, we discussed a different application of history matching by evolutionary algorithm. This application involves unconventional reservoirs, and was carried out as a summer internship project with BHP Billiton.

CHAPTER II
ASSISTED HISTORY MATCHING USING GENETIC ALGORITHM FOR CHEMICAL FLOODING

Chemical enhanced oil recovery (EOR) methods have been widely used in recent years as the demands for energy grows globally, because it can potentially recover the remaining oil after conventional waterflooding by mobilizing trapped oil in porous media due to capillary forces. Another reason is the increasing oil price relative to the chemicals price in recent years. A successful chemical flooding application requires accurate and reliable numerical models no matter in core scale, pilot scale, or field scale. History matching is one of the key techniques to achieve this goal.

We proposed a general workflow for assisted history matching in chemical flooding using Genetic Algorithm (GA), due to its global search nature and its power of calibrating various parameter types. During the assisted history matching process, the chemical flooding simulator UTCHEM, developed by The University of Texas at Austin, is coupled to cover complex mechanisms such as phase behavior, interfacial tension, relative permeability, capillary trapping, adsorption, cation exchange, etc. The coupling can generalize the workflow by solving various chemical flooding methods in core scale, pilot scale and field scale.

2.1 History Matching Using Genetic Algorithm

Our goal here is to calibrate static parameters for integration of dynamic data. In chemical flooding, static parameters usually consist of various types of parameters, such as the endpoints and exponents of relative permeability curves, surfactant and polymer adsorption parameters, permeability reduction parameters, etc. The dynamic data to be matched usually includes pressure drop (for coreflooding), oil recovery, oil cut, surfactant concentration, etc.

In our work, we used Genetic Algorithm, one of the evolutionary algorithms, to realize model calibration and data integration. Genetic Algorithm has been widely used to solve complicate history matching problem (Schulze-Riegert et al. 2002; Williams et al. 2004; Yin et al. 2010). The principle of evolutionary algorithms is inspired by Darwin's theory about evolution in natural world – survival of the fittest to an environment. The genetic information of the survivals is transferred to their children by crossover and mutation. To apply this theory on history matching problem, the key procedures are explained as follows.

- Define an objective function. In history matching problem, objective function is usually defined as the difference between the observed values and calculated values, i.e.,

$$f = \sum_{i=1}^{n} w_i \left(f_i^{obs}(\mathbf{x}) - f_i^{cal}(\mathbf{x}) \right)^2 \qquad \text{.....(2.1)}$$
$$\sum_{w=1}^{n} w_i = 1$$

  where **x** refers to the list of uncertain parameters, *w* denotes weighting factor for each objective, and *n* is the number of objectives. The definition of objective function is used to quantify the quality of history matching by evaluating each proposed model. However, in multi-objective problem, it is quite challenging to select proper weights for objectives which may also be in difference scales, for example, total oil production misfit in STB, bottom-hole pressure misfit in psi. To solve this problem, objective function is improved by summation of logarithm misfit:

$$f = \sum_{i=1}^{n} \ln \left| f_i^{obs}(\mathbf{x}) - f_i^{cal}(\mathbf{x}) \right| \qquad \text{.....(2.2)}$$

In this way, several misfit terms can be reconciled during history matching process.

- Select uncertain parameters by sensitivity analysis. It is not reasonable to calibrate all possible parameters to do history matching. Hence, to start with, sensitivity analysis should be conducted to identify key parameters and their ranges and study how they affect the quality of history matching. The objective function is defined to evaluate the quality of history matching. Smaller objective function means that the proposed model can provide solution closer to history data. Given a set of potential uncertain parameters, simulations will be performed under their given high and low values. The effect of each parameter on the objective function is ranked. Parameters with higher ranks mean that they are sensitivity to the objective function and are kept. In contrast, less sensitive parameters with lower ranks will be discarded.
- Construct initial proxy by Latin Hypercube Sampling. To initialize population, Latin Hypercube Sampling (LHS), one of experimental design methods, is used with a space filling design with respect to the sensitive parameters from previous step. The advantage of LHS over simple random sampling is that it will stratify each marginal distribution maximally and provide a full coverage of the range of each variable, as shown in **Fig. 2.1**. Also, unlike full factorial design or D-optimal design, it requires fewer experiments.

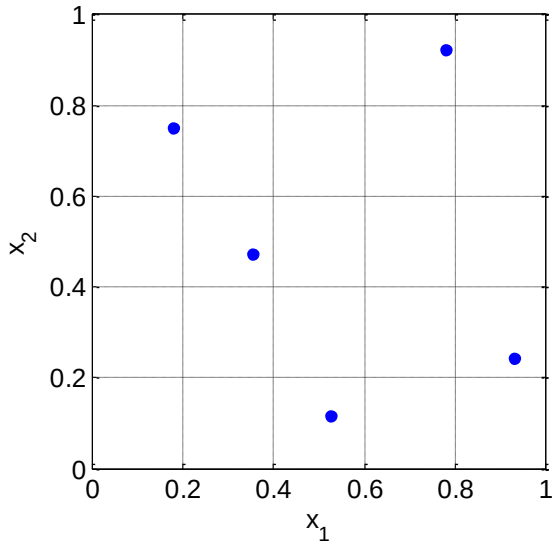

Fig. 2.1 Two-variable Latin Hypercube Sampling design of 5 experiments (Yin 2011)

- Construct response surface by krigging. Response surface proxy serves as an approximate representation of a real system. When a new experiment is generated, only the minimum on the surface is selected for further simulation. The experiment with better fitness will be added into population and improve the response surface, so that the proxy model will more and more approach to the true response. Response surface also serves as a filter to avoid unnecessary and expensive computation when evaluating a random sample. Models whose objective function is higher than defined threshold will not go through actual simulation.
- Select models based on fitness. During history matching process, objective function is minimized while the fitness function $g_i(\mathbf{x})$ of genomes is maximized, as defined in **Eq. 2.3**. In our work, the selection of models is based on Roulette-wheel algorithm, which defines the probability of the model:

$$P(x) = \frac{g_l(x)}{\sum_{l=1}^{n} g_l(x)} = \frac{\exp(-f_l(x))}{\sum_{l=1}^{n} \exp(-f_l(x))} \quad \text{.....(2.3)}$$

- Reproduce population by Genetic Algorithm. Genetic Algorithm uses binary strings of 0's and 1's to represent a list of parameters. The full binary strings representing whole set of parameters is called a genome. Under each iteration, populations will be evolved from original ones (parents) to new ones (offspring) by GA operators: crossover and mutation. Crossover recombines fitter parents and produce good and even better offspring by exchanging between two genomes from a randomly chosen position. Mutation operator is a key process to introduce diversity to a generation by randomly flipping some bits in a genome.

The outline of model calibration using genetic algorithm is summarized in **Fig. 2.2**. To start with, the evolution is initialized from a population of individuals randomly generated by Latin Hypercube Sampling. The objective function of current population is evaluated. Based on the values of objective function, a set of the population is selected to reproduce a new generation by genetic operators (crossover, and/or mutation) for next iteration of the algorithm. The proxy model is constructed by krigging to filter the model whose objective function is higher than the unacceptable threshold without running the actual simulation. The optimization process terminates when the maximum number of generations is produced or the fitness level of the solution stops improving.

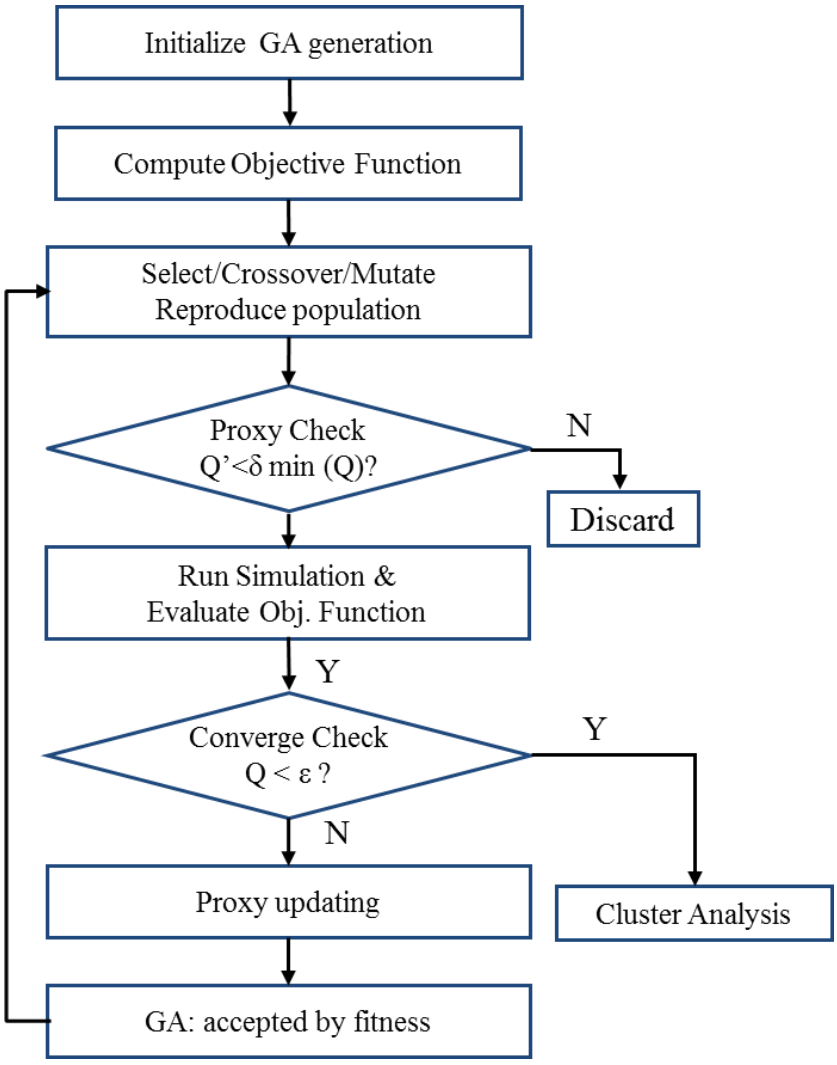

Fig. 2.2 Flowchart of Genetic Algorithm with proxy

2.2 Chemical Flooding Simulation by UTCHEM

During the process of model calibration, we used UTCHEM as forward simulator to run simulations. UTCHEM, developed by the University of Texas at Austin, is currently one of the most advanced chemical flood simulator to capture ASP mechanisms. Pope and Nelson (1978) developed a one-dimensional, compositional simulator, which considered phase behavior, interfacial tension, and polymer viscosity, and processes involved such

as two- and three-phase behavior, fractional flow, adsorption, cation exchange, etc. In 1981, Wang et al. (1981) extended the simulator to a two-dimensional, multicomponent, multiphase, compositional simulator for micellar/polymer flooding simulation, with more factors such as reservoir heterogeneity, crossflow, dispersion, injection rate, and process variables such as slug size, salinity gradient, and mobility ratio included. Datta-Gupta (1985) enhanced the simulator to solve three-dimensional problems with detailed physical property description and phase relationship. This becomes the predecessor of UTCHEM. Bhuyan et al. (1990) included the geochemical reactions in UTCHEM to consider in-situ soap generation.

UTCHEM is widely used to simulate multiphase, multicomponent, three-dimensional in the displacement processes at both laboratory and field scales. The balance equations include the mass conservation equation for each species, pressure equation for up to four fluid phases, and energy conservation equation for temperature. The pressure equation is formulated by an overall mass balance on volume-occupying components (water, oil, surfactant, co-solvent, and air), substituting Darcy's law for the phase flux terms. The pressures of other phases are computed by adding the capillary pressure between phases. The energy balance equation is developed by the assumption that energy is a function of temperature and energy flux in the aquifer or reservoir is only caused by advection and heat conduction. Significant achievements of UTCHEM are its focus on the accurate physical and chemical models. The major physical phenomena modeled in UTCHEM covers phase behavior, interfacial tension, relative permeability, capillary trapping, adsorption, etc. The chemical reaction includes ion-exchange reactions with the matrix, precipitation/dissolution of minerals, acid reactions with oil, etc. Important aspects, such as phase behavior, interfacial tension, trapping number and adsorption, which are also relevant to our research, are introduced as follows. Description regarding other physical and chemical modeling in UTCHEM can be found in Delshad et al. (1995).

2.2.1 Phase Behavior

An important part of the research effort on chemical flooding simulation by The University of Texas at Austin is the phase behavior model. The surfactant/oil/water phase behavior is based on the work by Winsor (1954), Healy and Reed (1974), Nelson and Pope (1978), Prouvost et al. (1985), and others. A microemulsion phase behavior considers up to five components: surfactant, co-surfactant, hydrocarbon, water and NaCI. Usually the number of components is reduced by combining one or more components into pseudocomponents in order to extend the phase behavior studies to a wide range of compositions. For example, water and NaCI are commonly combined into the brine pseudocomponents, and the hydrocarbon phase represents a mixture of hydrocarbons. In most cases, the surfactant and co-surfactant are treated as a pseudocomponent and called as "surfactant". The concentrations of these three pseudocomponents are used as the coordinates on a ternary diagram, as depicted in **Fig. 2.3**. As the salinity of an aqueous phase increases, the solubility of an ionic surfactant decreases. Therefore, salinity has a strong influence on phase behavior. At relatively low salinity, solutions in the multiphase region would divide into a water-external microemulsion and an excess oil phase, which is called Type II (-) phase environment. The slopes of tie lines are negative, as shown in **Fig. 2.3**. At relatively high salinity, an oil-external microemulsion and an excess, more dense, water phase exist in the system, which is called Type II (+) phase environment. In this phase environment, tie lines have positive slope. At intermediate salinity, the system separates into three phases: oil, microemulsion, and water phases. This type of phase environment is called Type III system. This three-phase environment is of particular interest, because interfacial tension with both water and oil are found to be very low. In UTCHEM, the phase behavior is modeled as a function of effective salinity with the formulation of binodal curve and tie lines using Hand's rule (Hand 1939).

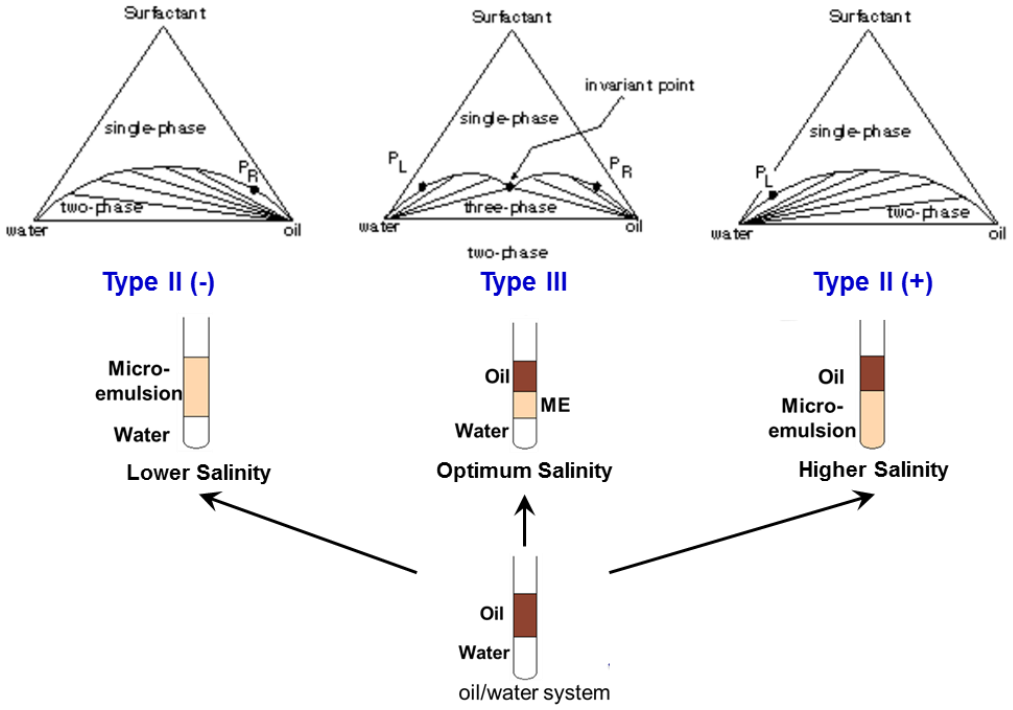

Fig. 2.3 Effect of salinity on microemulsion phase behavior

2.2.2 Interfacial Tension

In UTCHEM, two models based on Healy and Reed (1974) and Huh (1979) are used to calculate interfacial tension (IFT).

Based on Hirasaki's modification (Hirasaki 1981) of the Healy and Reed's model (Healy and Reed 1974), the interfacial between microemulsion and the excess water and oil phase (σ_{13}, σ_{23}) are calculated as follows:

$$\begin{cases} \log_{10}\sigma_{13} = \log_{10}F_l + G_{l2} + \dfrac{G_{l1}}{1+G_{l3}R_{l3}} & \text{for } R_{l3} \geq 1 \\ \log_{10}\sigma_{13} = \log_{10}F_l + (1-R_{l3})\log_{10}\sigma_{ow} + R_{l3}\left(G_{l2} + \dfrac{G_{l1}}{1+G_{l3}}\right) & \text{for } R_{l3} < 1 \end{cases} \quad \text{for } l = 1,\ 2 \quad \text{.....(2.4)}$$

where G_{l1}, G_{l2} and G_{l3} are input parameters; and R_{l3} is the solubilization ratio (C_{l3}/C_{33}).

F_l is a correction factor introduced by Hirasaki to ensure IFT at the plait point is zero.

$$F_l = \frac{1 - \exp\left(-\sqrt{\sum_{\kappa=1}^{3}\left(C_{\kappa l} - C_{\kappa 3}\right)^2}\right)}{1 - \exp\left(-\sqrt{2}\right)} \qquad \text{for } l = 1,\ 2 \quad \text{.....(2.5)}$$

When surfactant is absent or surfactant concentration is below CMC, the interfacial tensions are equal to σ_{ow}.

In Chun-Huh's equation, the interfacial tension is a function of solubilization ratio and described as:

$$\sigma_{l3} = \frac{c}{R_{l3}^2} \qquad \text{for } l = 1, \text{ or } 2 \quad \text{.....(2.6)}$$

where c is typically equal to 0.3. Hirasaki's correction factor F_l is introduced to modify Huh's equation, so that IFT reduces to water-oil IFT (σ_{ow}) when surfactant concentration is near zero. After modification by Hairasaki's correction factor, the interfacial tension is calculated as follows:

$$\sigma_{l3} = \sigma_{ow} \exp\left(-\alpha R_{l3}\right) + \frac{cF_l}{R_{l3}^2}\left[1 - \exp\left(-\alpha R_{l3}^3\right)\right] \qquad \text{for } l = 1 \text{ or } 2 \quad \text{.....(2.7)}$$

where α is a constant and usually equals to 10.

2.2.3 Trapping Number

Another important mechanism that UTCHEM captures is the mobilization of trapped organic phase as interfacial tension reduces. Two separate dimensionless groups – bond number and capillary number, are often used to describe the trapping and mobilization of

a nonwetting phase. The bond number is to represent (gravity / capillary) forces, and is defined as follows:

$$N_{Bl} = \frac{kg\left(\rho_l - \rho_{l'}\right)}{\sigma_{ll'}} \quad \text{for } l = 1, ..., n_p \text{ .....(2.8)}$$

Capillary number is to represent (viscous / capillary) forces, and is defined as follows:

$$N_{cl} = \frac{\left| -\vec{k} \cdot \vec{\nabla} \Phi_{l'} \right|}{\sigma_{ll'}} \quad \text{for } l = 1, ..., n_p \text{ .....(2.9)}$$

where l and l' are the displaced and displacing fluids respectively; and the gradient of flow potential is calculated as $\nabla \Phi_{l'} = \nabla P_{l'} - \rho_{l'} g \nabla h$.

In UTCHEM, a newly developed dimensionless number – trapping number, is introduced to model the combined effect of viscous and buoyancy forces. For one-dimensional vertical flow, the trapping number can be defined by directly adding viscous and buoyancy forces together as $N_{Tl} = \left| N_{cl} + N_{Bl} \right|$. For two-dimensional flow, trapping number is defined as follows:

$$N_{Tl} = \sqrt{N_{cl}^2 + 2 N_{cl} N_{Bl} \sin\theta + N_{Bl}^2} \quad \text{for } l = 1, ..., n_p \text{ .....(2.10)}$$

where θ is the angle between the local flow vector and the horizontal (counter clockwise). Jin (1995) gave the derivation of trapping number in three-dimensional, heterogeneous, anisotropic porous media.

With the definition of trapping number, residual saturation's dependence on interfacial tension is calculated as a function of trapping number as:

$$S_{lr} = \min\left(S_l, S_{lr}^{high} + \frac{S_{lr}^{low} - S_{lr}^{high}}{1 + T_l N_{T_l}} \right) \quad \text{for } l = 1,..., n_p \quad \text{.....(2.11)}$$

where T_l, capillary desaturation curve parameter, is a positive input parameter from the experimental observation based on the relationship between residual saturation and trapping number. S_{lr}^{low} and S_{lr}^{high} are the input residual saturation for each phase at low and high trapping numbers.

Due to detrapping, the endpoints and exponents of relative permeability curves change with residual saturation at high trapping numbers. Delshad et al. (1986) proposed the formulations where the endpoints and exponents in relative permeability functions are calculated as a linear interpolation between the input values at low and high trapping numbers ($k_{rl}^{o\,low}$, $k_{rl}^{o\,high}$, n_l^{low}, n_l^{high}).

$$k_{rl}^{o} = k_{rl}^{o\,low} + \frac{S_{lr}^{low} - S_{lr}}{S_{lr}^{low} - S_{lr}^{high}}\left(k_{rl}^{o\,high} - k_{rl}^{o\,low}\right) \quad \text{for } l = 1,..., n_p$$
$$n_l = n_l^{low} + \frac{S_{lr}^{low} - S_{lr}}{S_{lr}^{low} - S_{lr}^{high}}\left(n_l^{high} - n_l^{low}\right) \quad \text{for } l = 1,..., n_p \quad \text{.....(2.12)}$$

2.2.4 Adsorption

Surfactant and polymer adsorption is another important mechanism since it leads to consumption and retardation of injected surfactant and polymer. In UTCHEM, Langmuir isotherm is used to model adsorption. The adsorbed concentration of surfactant (κ = 3) or polymer (κ = 4) is calculated as:

$$\hat{C}_\kappa = \min\left(\tilde{C}_\kappa, \frac{a_\kappa\left(\tilde{C}_\kappa - \hat{C}_\kappa\right)}{1 + b_\kappa\left(\tilde{C}_\kappa - \hat{C}_\kappa\right)} \right) \quad \text{for } \kappa = 3 \text{ or } 4$$
$$a_3 = \left(a_{31} + a_{32} C_{SE}\right) k^{-0.5} \quad \text{for surfactant} \quad \text{.....(2.13)}$$
$$a_4 = \left(a_{41} + a_{42} C_{SEP}\right) k^{-0.5} \quad \text{for polymer}$$

where C_{SE} is effective salinity; a_{31}, a_{32}, and b_3 are determined by matching laboratory surfactant adsorption data; C_{SEP} is effective salinity for polymer calculated as $C_{SEP} = \frac{C_{51} + (\beta_P - 1)C_{61}}{C_{11}}$; a_{41}, a_{42}, and b_4 are determined by matching laboratory surfactant adsorption data.

From above description, we can see that as a general chemical flood simulator, UTCHEM can accurately account for effects of phase behavior, interfacial tension, capillary desaturation, adsorption, etc. It will generalize our model calibration process by incorporating UTCHEM into the workflow as a forward simulator.

2.3 Summary

In this chapter, we proposed the assisted history matching workflow using Genetic Algorithm (GA) to calibrate uncertain parameters associated with dynamic history data. Objective function is defined as a weighted average of misfits between observed data and simulated values. First, design of experiments is used to randomly sample between key parameters identified from sensitivity analysis for initialization of population. Then, response surface is used to construct proxy model, which can filter out models whose objective function is higher than defined threshold, and avoid unnecessary simulation. During history matching process, models are selected according to fitness, and populations are evolved by GA operators (crossover and mutation).

Chemical flooding simulator UTCHEM is coupled during the inverse process. It can simulate multi-phase, multi-component compositional model, considering complex phase behavior, chemical and physical transformations in heterogeneous porous media. It will largely generalize the model calibration workflow by incorporating UTCHEM as the forward simulator.

CHAPTER III
MULTI-STAGE MODEL CALIBRATION IN ALKALINE-SURFACTANT-POLYMER FLOODING

In this chapter we present an approach to calibrate model in multiple stages that can efficiently reduce uncertainties in alkaline-surfactant-polymer (ASP) flooding. First, uncertain parameters regarding capillary desaturation, relative permeability, and adsorption are studied and their effects on reservoir behavior and well response are evaluated respectively for further model calibration. Then, in our pilot application, based on the sensitivity analysis results, dominating reservoir parameters are identified and then calibrated to match field performance in the first stage; afterwards, less dominating chemical-flooding-related parameters are calibrated to match well response in the second stage. Comparison between history matching results show that multi-stage model calibration outperforms single-stage model calibration. The proposed multi-stage history matching workflow is demonstrated by an Alkaline-Surfactant-Polymer flooding synthetic case.

3.1 Introduction

3.1.1 Overview of ASP Flooding

Chemical enhanced oil recovery (EOR) methods have been widely used in recent years as the global demand for energy grows. One main reason is the increasing oil price relative to the chemicals. **Fig. 3.1** shows price of crude oil, surfactant and polymer from year 1995 and year 2014. The price of surfactant and polymer roughly stays in the range \$1/lb - \$3/lb, while the price of crude oil increased from \$18/bbl in year 1995 to \$100/bbl in year 2014. (Anderson et al. 2006; Henthorne et al. 2014; U.S. Energy Information Administration 2014; Wu et al. 1996). Another reason is that chemical EOR

has an advantage over steam and miscible gas flooding since it does not need extra expensive pipelines and compression or recycling. The infrastructure used in chemical flooding can be simply derived from waterflooding, which is available in thousands of mature oil fields. Alkaline-surfactant-polymer is a common enhanced oil recovery method. The main objective of ASP flooding is to recover the remaining oil after waterflooding by mobilizing trapped oil in porous media due to capillary forces. Usually a solution of alkali, surfactant and polymer is injected in the same slug, which not only makes use of each component's advantage, but also the synergy among three components to effectively displace the remaining oil.

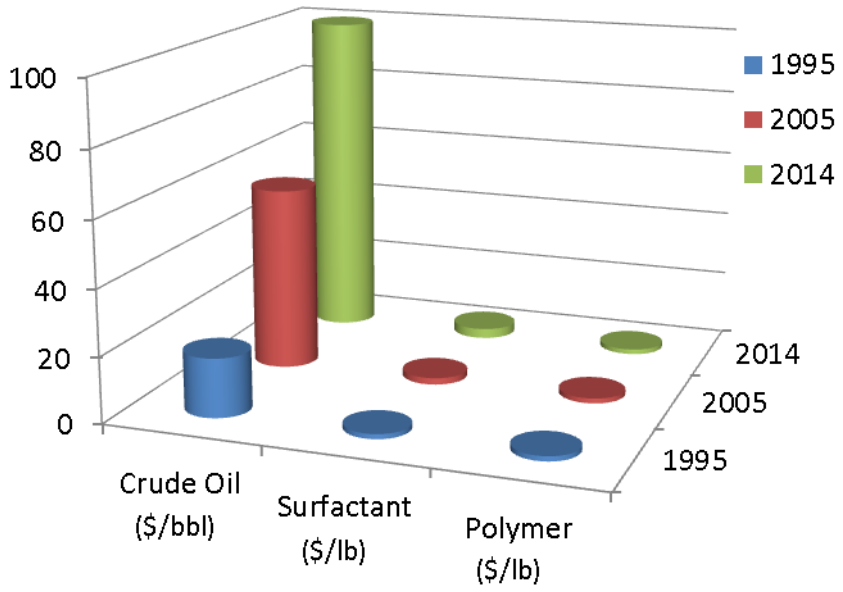

Fig. 3.1 Historical crude oil and chemical price

Surfactant is a term to describe surface active agent, which lowers the energy barrier between two immiscible phases. A surfactant molecule consists of two parts: hydrophilic part and hydrophobic part. The hydrophilic part is soluble in water, while the hydrophobic part is soluble in oil. When surfactant is injected in an oil/water system,

surfactant molecules will accumulate at the oil-water interface, with hydrophobic portion existing in oil and hydrophilic portion existing in water. In this way, it reduces the energy between the two immiscible phases. As the surfactant concentration increases, the molecules start to associate and form aggregates, which are called micelles. The concentration at which micelles are formed is called critical micelle concentration (CMC) (**Fig. 3.2**). If the surfactant concentration increases above CMC, it will only increase the micelle concentration. The hydrophobic interior of the micelles formed in aqueous solution is capable of solubilizing large amounts of oil under the right conditions. Conversely, the hydrophilic interior of the micelles formed in hydrocarbon solvent can solubilize water. Thus, the addition of surfactant at a concentration above CMC can significantly increase the solubility between oil and water which originally have little solubility for each other. This phenomenon results in lowering the interfacial tension (IFT) between two phases.

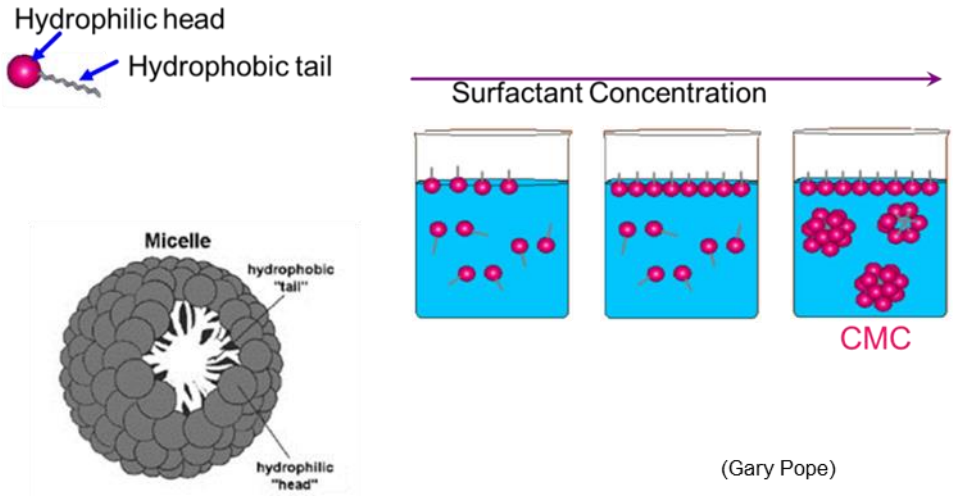

Fig. 3.2 Definition, structure and formation of micelle

The IFT between aqueous surfactant solution and hydrocarbon phase is a function of salinity, surfactant concentration, surfactant type, and temperature, etc. The effect of IFT

on recovery during the displacement process is shown in **Fig. 3.3**, where residual oil is correlated as a function of capillary number. The capillary number, N_c, is defined as

$$N_c = \frac{u\mu}{\sigma} \quad \text{.....(3.1)}$$

where μ is the viscosity of the displacing fluid, u is the displacing velocity, and σ is the interfacial tension between the displacing fluid and the displaced fluid. It is known that interfacial tension is about 10 to 30 dynes/cm in a typical waterflooding. A significant reduction in residual oil saturation can be achieved as IFT reduces down to 10^{-3} dynes/cm.

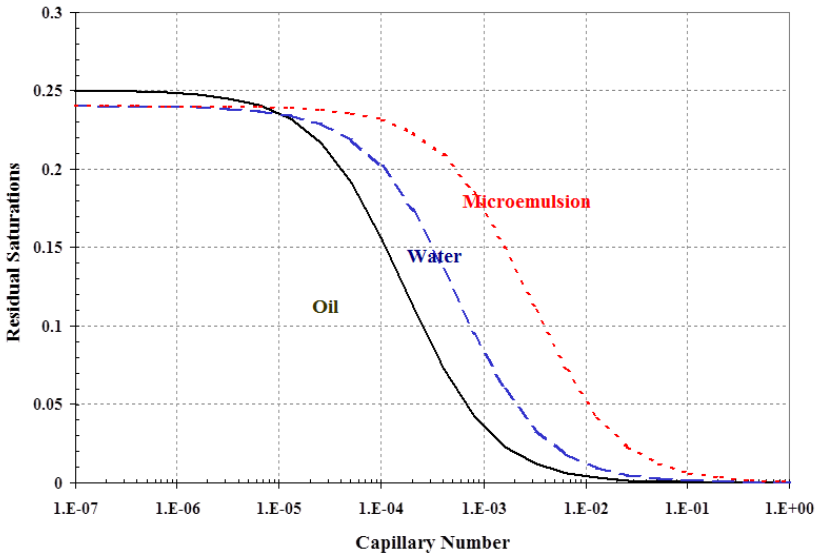

Fig. 3.3 Residual saturation as a function of capillary number

During the displacement, surfactant loss can happen during ASP slug injection by precipitation, adsorption, etc. These mechanisms will cause surfactant retention in the

porous medium, and damage on the chemical composition, and eventually decrease the displacement efficiency.

The role of polymer in ASP slug as a mobility control agent is to improve displacement and volumetric sweep efficiency by increasing the viscosity. During the displacement, both adsorption onto rock surfaces and trapping in small pores can cause the retention of polymer in porous media.

The primary objective of alkaline is the formation of in-situ surfactant (also called soap) generated by the chemical reaction between alkali and acid component in the crude oil, to reduce the interfacial tension, which, in turn, reduces the requirement of surfactant injection in ASP slug. Another major use of alkaline is that it can reduce the surfactant adsorption. Under the high pH values brought by addition of the alkaline chemicals, the rock surfaces will get negative charge, which repels the anionic sulfonate.

Above favorable features make ASP flooding very attractive for enhance oil recovery. Olsen et al. (1990) once compared different chemical EOR processes by the coreflood experiments on fresh Upper Edwards reservoir core. The oil recoveries of alkaline-surfactant-polymer, alkaline-polymer, and polymer are 45.3%, 10.0%, and 11.6% respectively, which shows that ASP slug achieves much higher recovery result than alkaline-polymer, or polymer solution. Sheng (2013) summarized the field performance used in 21 ASP field-scale applications worldwide. The average incremental recovery is 21.8% OOIP, and the average decreases in water cut due to ASP injection is 18% OOIP.

3.1.2 Overview of Model Calibration in ASP Flooding

There are not many literatures about history matching ASP flooding, and most of the documented results are regarding single surfactant or polymer flooding. Up to now, most of history matching in ASP flooding is done manually in a trial and error way or based on largely simplified ASP modeling. Abu-shiekah et al. (2013) applied adjoint method to history match gridblock permeability and porosity for full field polymer flooding using a

Shell proprietary reservoir simulator. The advantage of adjoint method is that it can calculate the sensitivity between data mismatch and parameters in one forward simulation. Mantilla and Srinivasan (2011) used Bayesian inversion algorithm to integrate production data, such as well pressures and water cut. UTCHEM was used to run forward simulation. Their work focused on incorporating geologic uncertainty as prior information to control polymer flooding process. Delaplace et al. (2013) investigated uncertain parameters like porosity and absolute permeability of geological units, rock compressibility, relative permeability curves, and value of polymer adsorption, with their influence on flow rates, water cut, and polymer breakthrough time, and successfully history matched polymer flooding pilot in the Pelican Lake heavy oil field in Canada. Karpan et al. (2011) demonstrated the history matching results based on their proposed effective modeling for ASP flooding. However, their work emphasized on modeling ASP flooding by considering adsorption, interfacial tension, desaturation, etc. The history matching was accomplished manually.

3.1.3 Problem Description

After summarizing the literatures about modeling and history matching of chemical flooding, we can see that currently there is no systematic method to calibrate model and integrate production data for ASP flooding. The methods documented for history matching single surfactant or polymer flooding also have restrictions if applied to ASP flooding. For example, if adjoint method is used, the sensitivity calculation would become extremely complicated in ASP flooding due to numerous parameters and complex physical and chemical behavior. Therefore, it is of great significance and necessity to develop a systematic, general and powerful procedure for model calibration in ASP flooding, which can achieve: 1) thorough forward modeling considering mechanisms such as complex phase behavior, chemical and physical transformations, etc.; 2) general model calibration over not only static reservoir parameters but also

parameters from ASP experiments; 3) universal application in ASP coreflooding, pilot case, and field case. The above three goals are the objectives of my work.

In this chapter, a general workflow is introduced for multi-stage assisted history matching using evolutionary algorithm. The outline of this chapter is as follows. First, we will discuss the methodology and software for model calibration and forward simulation, and explore the general workflow for multi-stage history matching in ASP flooding. Next, we will conduct sensitivity analysis through a 3D ASP pilot synthetic case to identify key parameters and study how they influence reservoir behavior and well response. The results of this study are crucial for applying multi-stage history matching workflow. At last, the multi-stage history matching workflow will be illustrated step by step through its application to this ASP case.

3.2 Multi-Stage Model Calibration

The history matching methodology we used in this part of work is Genetic Algorithm (GA) explained in previous chapter. Experimental design and response surface methodologies with evolutionary algorithm are used to calibrate parameters and history match production data. First, a set of key parameters is selected by sensitivity analysis. The evolution is initialized from a set of randomly generated potential individuals using Latin Hypercube Sampling with respect to key parameters. Chemical flooding simulator UTCHEM is used to run simulations so that the objective function for each individual is evaluated. The objective functions with respect to selected key parameters are used to generate a response surface proxy using experimental design and response surface methodology. The proxy model is constructed to filter the model whose objective function is higher than the unacceptable threshold without running the actual simulation. In each generation, the objective function of each individual in the population is evaluated with proxy check. Individuals are randomly selected from current population and modified via GA operators (selection, crossover, mutation) to generate a new

population for next iteration. The iteration stops when the maximum number of generations has been reached or a satisfactory solution has been achieved.

After we have studied the methodology and tool for model calibration and forward simulation, another important portion of the research is to explore a general structured workflow so that adjustments over uncertainties follow systematic and logical sequence. Williams et al. (1998) once proposed a structured approach in which adjustments follow the sequence from global, flow units, then local properties when conducting traditional manual history matching. Cheng et al. (2008) and Yin et al. (2010) followed the similar principles to apply assisted probabilistic history matching. Sensitivity analysis was given special consideration to identify key parameters and their ranges for global properties, regional properties and local properties respectively. Then hierarchical history matching was carried out based on the results from sensitivity studies. In the first stage of history matching, global properties such as reservoir pressure and total fluid rates were matched by adjusting corresponding key parameters. In the following stages of history matching, continued with calibrated parameters from last stage, new influential parameters were introduced to match less global, more local properties.

For chemical flooding, especially ASP flooding, numerous uncertainties are involved to affect to-be-matched properties through affecting relative permeability, adsorption, etc. Besides, what is different from previous history matching applications is that the relationship between to-be-matched properties is not only global-local and field-individual well from stratigraphic aspect, but also hierarchy based on level of dominance. Therefore, it is essential to first apply sensitivity study to specify the dominant and subordinate properties and their corresponding key parameters. A workflow for multi-stage model calibration is shown in **Fig. 3.4**.

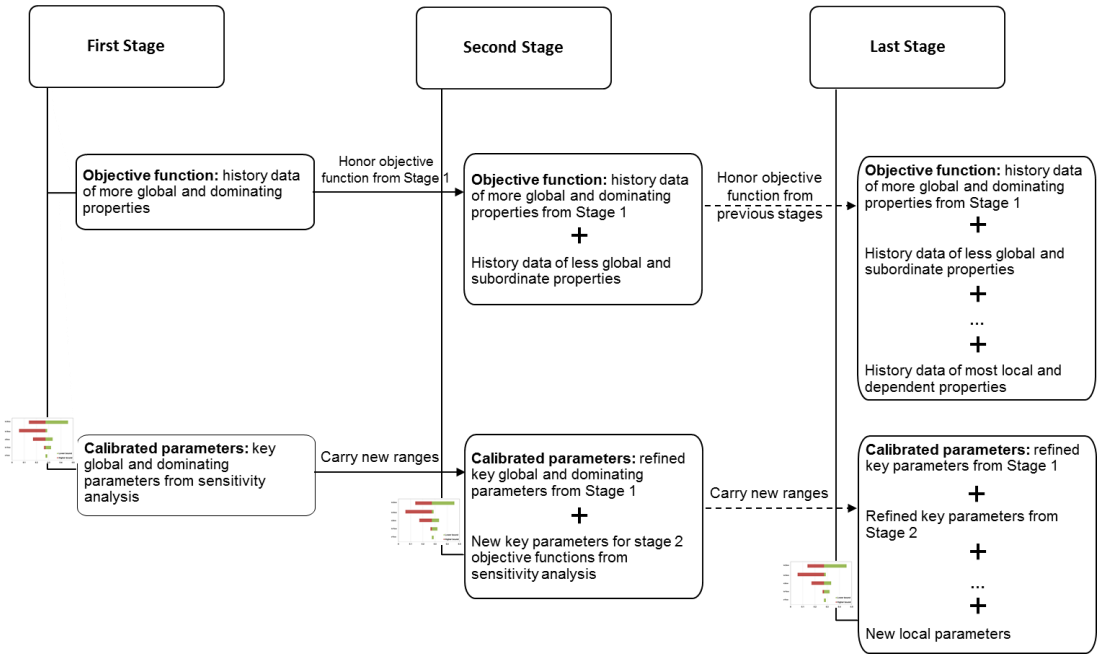

Fig. 3.4 Flowchart of multi-stage history matching

The workflow starts with all possible uncertain parameters and ranges considering empirical observations. In order to improve the quality and efficiency of the history matching process, it is not recommended to calibrate all parameters at once. First of all, sensitivity analysis is conducted to not only explore the dominant-subordinate relationship between objective functions, but also to identify key parameters over each objective function. Based on the results from sensitivity study, the first stage should focus on history matching observed data of global and dominant properties by adjusting their corresponding key parameters. Common observed data to be matched at this stage is pressure drop in coreflooding, cumulative oil recovery, etc. The refined ranges of the key parameters for first stage are carried over to the next stage. In the second stage, less global and less dominant properties, such as oil cut, chloride concentration, etc., are history matched by adjusting their related key parameters together with parameters carried over from previous stage, while honoring objective functions from the first stage. Stages can be added as necessary based on practical situation of different cases, during

which the same approach from the first stage to the second stage should be followed. In last stage, the most local and dependent properties are usually matched, such as surfactant and/or polymer concentration from each producer, by adjusting new local parameters together with refined parameters from all previous stages.

In the next section, we will illustrate the workflow through a synthetic example of ASP flooding pilot case. The outline of this pilot application is as follows. First, the background and simulation model are described. Then sensitivity analysis is carried out to study important parameters in ASP flooding and investigate how all possible uncertain parameters affect objective functions, and eventually identify key parameters. Based on the results from sensitivity study, the proposed workflow is applied to do multi-stage model calibration. Finally, history matching results multi-stage model calibration are compared with results under single-stage model calibration.

3.3 Pilot Application of ASP Flooding

3.3.1 Model Description

The pilot area is 492 ft × 492 ft × 157.5 ft with heterogeneous permeability within each layer (**Fig. 3.5**). Five-spot pattern is applied (as shown in **Fig. 3.6**) to flood this area with water injection for the first 122 days, followed by ASP solution for about 150 days, and then polymer for the last 300 days. A three dimensional model is built to simulate the flooding process in the pilot area using UTCHEM. The dimension of the grids is 15×15×36, with wells perforated throughout the whole vertical layers. Other major input parameters in the simulation model are given in **Table 3.1**.

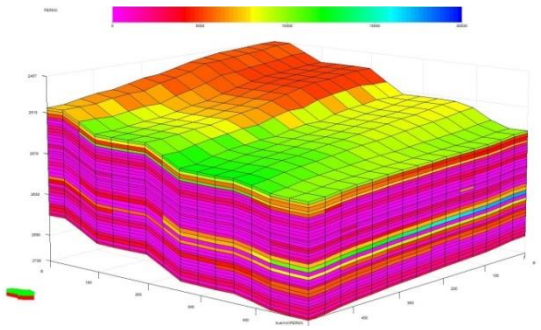

Fig. 3.5 Permeability distribution

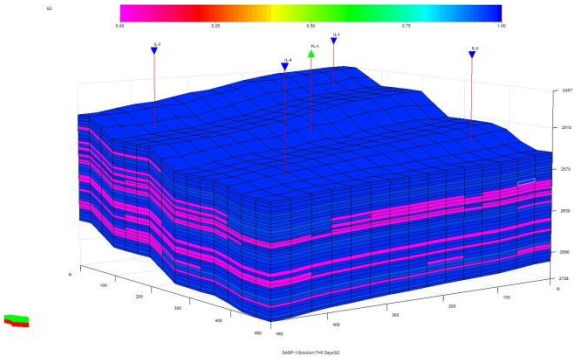

Fig. 3.6 Initial oil saturation in five-spot pattern

Fig. 3.7 shows the observed data from the producer in the reference model. In **Fig. 3.7**(a), oil cut decreases during the waterflooding, and then increases significantly during ASP flooding. During the polymer injection afterwards, a large amount of microemulsion is produced, and oil cut drops to zero. **Fig. 3.7**(b) gives the cumulative injected surfactant and cumulative produced surfactant, the drop between which refers to surfactant consumption and adsorption. So it is with polymer in **Fig. 3.7**(c).

In this model, surfactant adsorption and polymer adsorption are simulated using Langmuir Isotherm, and interfacial tension reduction is simulated by Chun-Huh's equation in UTCHEM. **Fig. 3.8** shows at 366 days how interfacial tension reduces along the direction flooded from one injector to the producer in the center. Meanwhile, **Fig. 3.8** also shows that as interfacial tension reduces, the effective salinity of the system along the same displacement direction resides in Type III phase environment, which is our favorable region.

Table 3.1 Major input parameters in the simulation model

Initial reservoir pressure	1436 psia
Depth	2632 ft
Constant initial brine salinity	0.1323 meq/ml
Initial divalent cation concentration of brine	0.03391 meq/ml
Lower effective salinity limit for Type III phase region	0.55 meq/ml
Upper effective salinity limit for Type III phase region	1.1meq/ml
Crude acid number	0.50 mg KOH/g
Water viscosity	0.48 cp
Oil viscosity	17 cp

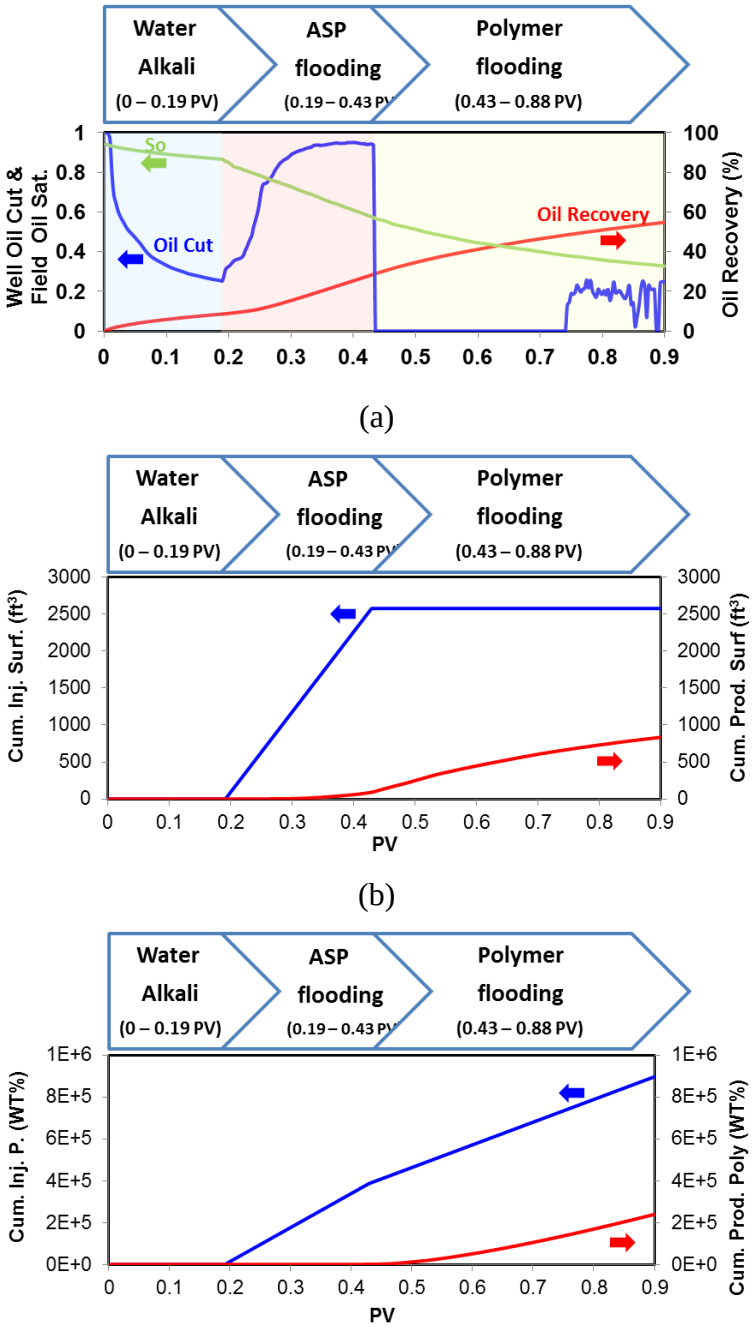

Fig. 3.7 Observed data in the reference model.

(a) oil cut and oil recovery, (b) cumulative injected surfactant and cumulative produced surfactant, and (c) cumulative injected polymer and cumulative produced polymer

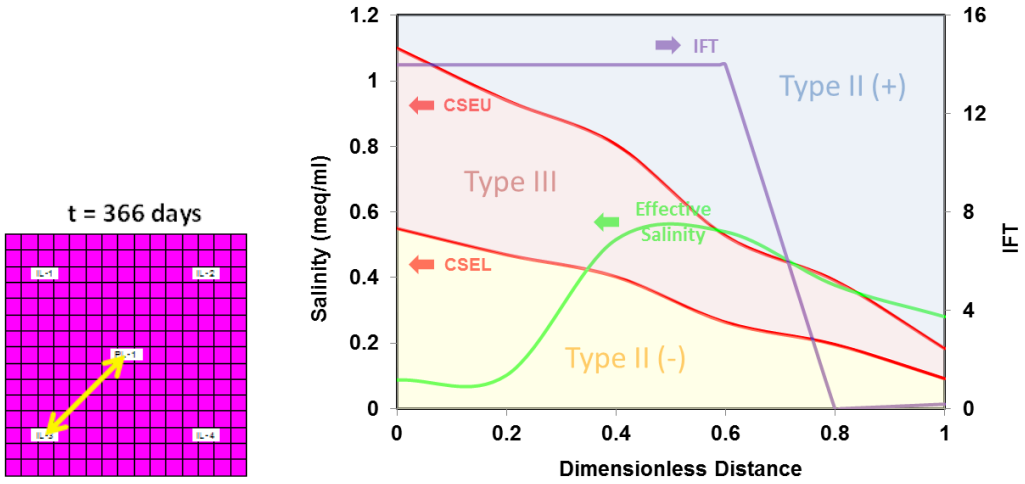

Fig. 3.8 IFT reduction along the flooding direction at time of 366 days

Capillary desaturation is modeled using **Eq. 3.9**, in which capillary desaturation curve parameter T_l is determined based on experimental observation. **Fig. 3.9** shows how residual oil and water saturation reduces as a function of trapping number due to detrapping. Correspondingly, the endpoint and exponent of relative permeability curve for each phase change with trapping number as they are a function of residual saturation (**Fig. 3.10**)(Delshad et al. 1986).

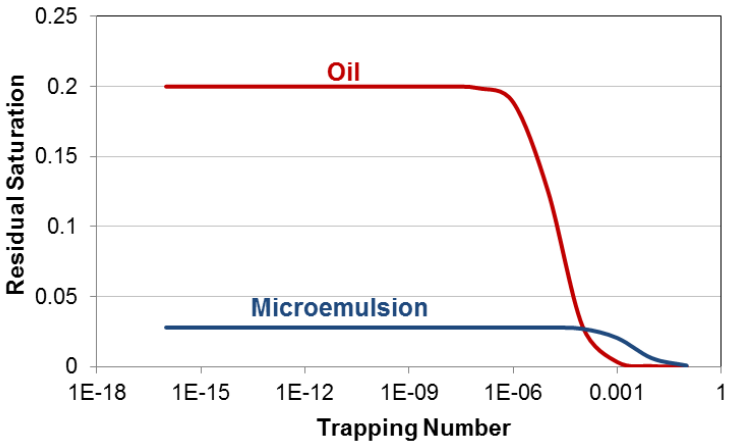

Fig. 3.9 Residual saturation as a function of trapping number

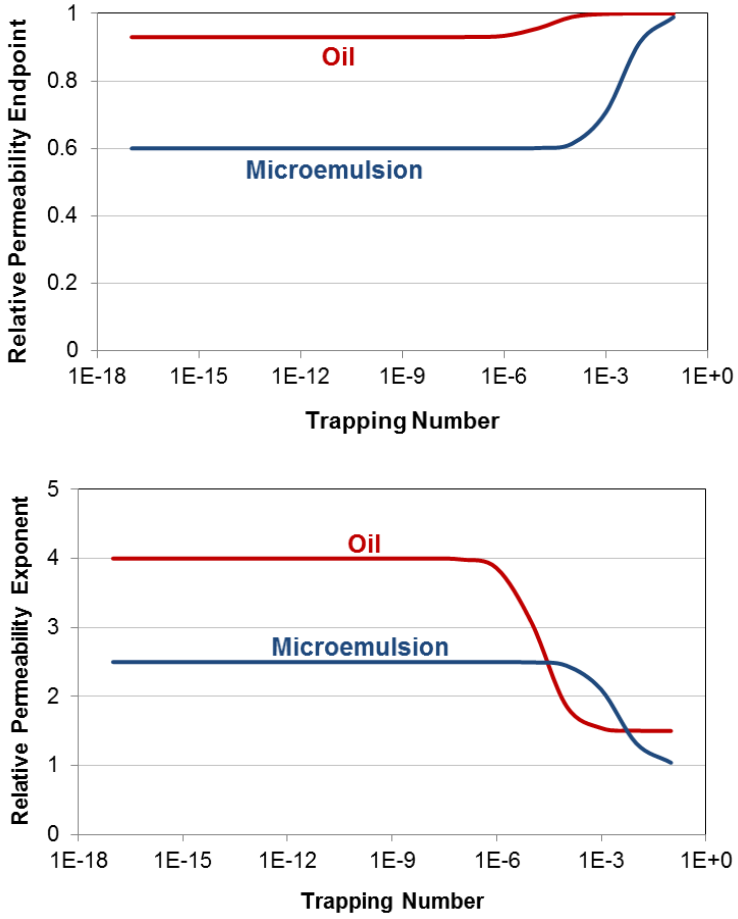

Fig. 3.10 Relative permeability endpoint and exponent change with trapping number

3.3.2 Sensitivity Analysis

Before history matching, it is essential to study important parameters in ASP flooding and find the hierarchical structure among objective functions and key parameters for each objective function. Sensitivity analysis can provide as a useful tool to screen out not influential parameters and prepare for further model calibration. In this case, parameters such as capillary desaturation curve (CDC) parameters, adsorption parameters are firstly studied; afterwards, sensitivity analysis of all possible 11 parameters regarding relative permeability, surfactant adsorption and polymer adsorption was performed over to-be-matched objective functions. The objective functions studied are changes for oil cut,

chloride concentration history, surfactant concentration history and polymer concentration history. The range for each uncertain parameter is collected from empirical observations and summarized in **Table 3.2**.

3.3.2.1 Capillary Desaturation Curve (CDC) parameters

During the process of lowering interfacial tension (IFT), one of the most important physical relation is capillary desaturation curve (CDC), which defines the relationship between residual saturation and trapping number. Trapping number is defined as a dimensionless number combine the effect of viscous and buoyancy forces, as introduced in Chapter 2.2. The correlation between residual phase saturation and trapping number was derived based on experimental results for n-decane from Delshad (1990)'s work (**Eq. 3.9**). Since the correlation for CDC is unknown, the results presented in Delshad (1990) are used in the model, in which, capillary desaturation curve parameters for water (T_1), oil (T_2) and microemulsion (T_3) are T_1 = 1865, T_2 = 59074, and T_3 = 364, respectively. To study the impact of CDC parameters on residual saturation, a range is assigned to CDC parameters for each phase, as listed in **Table 3.2**. **Fig. 3.11** shows the residual saturation reduction caused by different CDC parameters for each phase. For small trapping number, based on **Eq. 3.9**, residual saturation basically equals to S_{lr}^{low} (residual saturation at low trapping number). For large trapping number, change of CDC parameters in magnitude order will cause large difference in residual saturation for each phase.

Usually, CDC parameters should be determined by experimental data. Since no specific experiments were carried out for this ASP flooding case, CDC parameters in the model will continue to adopt the results from Delshad (1990). During history matching, we will not calibrate CDC parameters in this case.

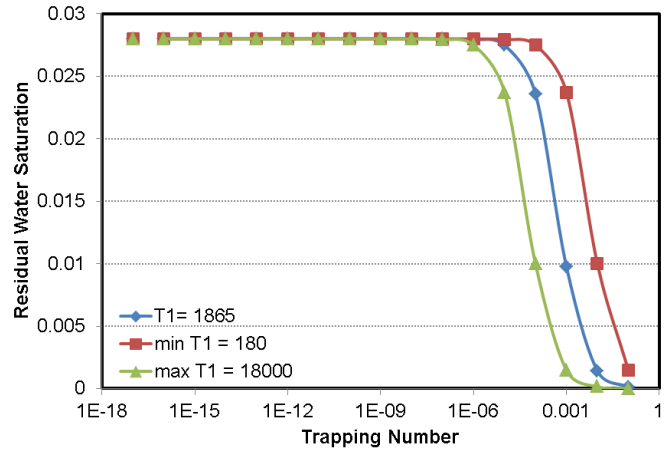

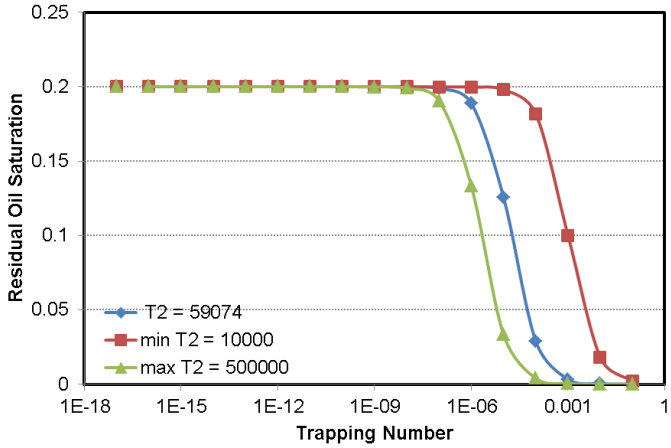

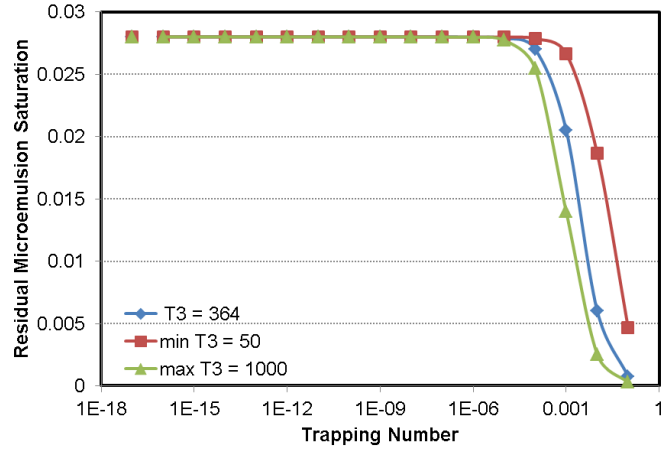

Fig. 3.11 Residual saturation vs. trapping number under different CDC parameters

3.3.2.2 Adsorption parameters

Surfactant and polymer adsorption is modeled by Langmuir Isotherm (**Eq. 3.11**), in which a_{31}, a_{32} and b_3 are parameters to be calibrated for surfactant adsorption, and a_{41}, a_{42}, and b_4 for polymer adsorption. **Fig. 3.12** and **Fig. 3.13** show the change of adsorbed surfactant and adsorbed polymer after assigning a range of each parameter. It can be seen that a_{32} and a_{42} do not influence adsorbed surfactant and polymer. The effect of adsorption parameters on to-be-matched objective functions is evaluated by tornado charts with other parameters afterwards.

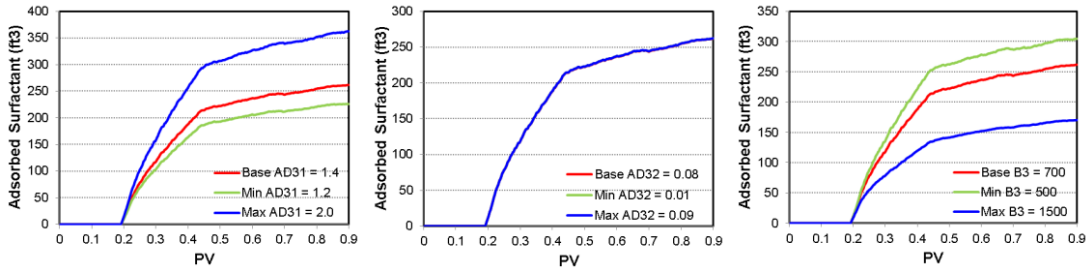

Fig. 3.12 Adsorbed surfactant under different surfactant adsorption parameters

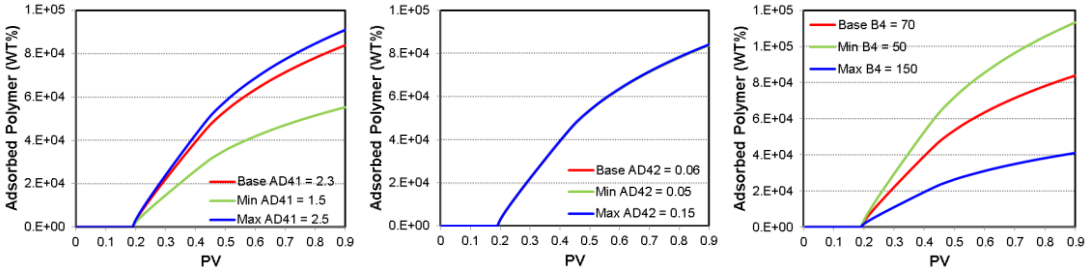

Fig. 3.13 Adsorbed polymer under different polymer adsorption parameters

3.3.2.3 Tornado charts

To evaluate the relative impact of relative permeability parameters and adsorption parameters on each objective function, tornado charts are plotted by perturbing each parameter from the base model to the lower or upper extreme values, as shown in **Fig. 3.14**. It can be seen that for all four objective functions, endpoints for oil phase and microemulsion phase at low trapping number are the most influential parameters. For oil cut and chloride concentration history, the situations are similar that most of parameters for relative permeability have much more impact than surfactant and polymer adsorption parameters. For surfactant concentration history and polymer concentration history, adsorption parameters have growing influence, but still not as much as the heavy-hitters from relative permeability. This means that oil cut and chloride concentration should be matched through calibrations over relative permeability parameters in a more global and dominating stage; calibrations over adsorption parameters to match surfactant and polymer concentration belong to a more local and subordinate stage.

Table 3.2 Uncertain parameters and their ranges in sensitivity analysis

	Uncertainty	Reference	Base	Low	High	Description
Relative Permeability	kr1low	0.6	0.3	0.1	0.7	Endpoint for water phase at low trapping number
	kr2low	0.93	0.5	0.1	1.0	Endpoint for oil phase at low trapping number
	kr3low	0.6	0.3	0.1	1.0	Endpoint for microemulsion phase at low trapping number
	e1low	2.5	5	2	6	Exponent for water phase at low trapping number
	e3low	2.5	5	1	7	Exponent for microemulsion phase at low trapping number
Surfactant Adsorption	ad31	1.7	1.4	1.2	2.0	Surfactant adsorption parameters
	ad32	0.05	0.08	0.01	0.09	
	b3	1000	700	500	1500	
Polymer Adsorption	ad41	2.0	2.3	1.5	2.5	Polymer adsorption parameters
	ad42	0.1	0.06	0.05	0.15	
	b4	100	70	50	150	

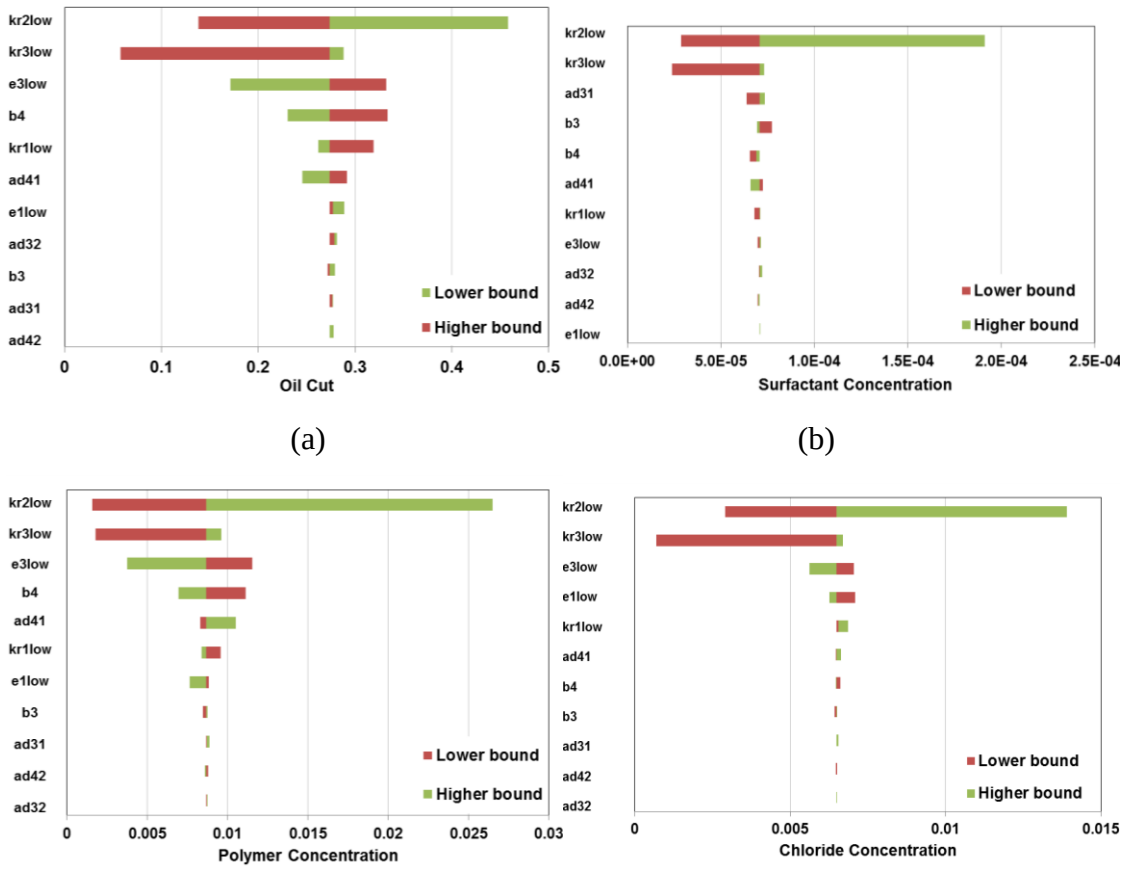

Fig. 3.14 Tornado charts for sensitivity analysis.

(a) oil cut, (b) surfactant concentration, (c) polymer concentration, and (d) chloride concentration

3.3.3 First Stage of Model Calibration

The sensitivity studies in the previous section not only help to determine the hierarchical structure among multiple objective functions, but also find the key parameters for each objective function. Based on the sensitivity analysis results, a two-stage workflow of model calibration is set up for the pilot case as shown in **Fig. 3.15**. In the first stage, history data of global and dominating properties is matched, which are oil cut and chloride concentration. Endpoints and exponents of relative permeability for each phase are possible parameters regarding oil cut and chloride concentration. Sensitivity analysis is applied to rank these possible parameters with realistic ranges. The results are shown by the tornado chart in **Fig. 3.16**. It can be seen that the endpoint of relative permeability for oil and microemulsion phase are the most sensitive parameters. In our first-stage workflow, we kept all five uncertain parameters to go through history matching.

Fig. 3.17 gives the history matching results for oil cut and chloride concentration, from which we can see that there is a good agreement between updated models obtained and observed data. In **Fig. 3.18**, we have also shown the distribution of calibrated parameters before and after history matching. For comparisons, the calibrated parameters in the reference model are exhibited as black markers. We can see that the uncertainties in most of the relative permeability parameters are largely reduced.

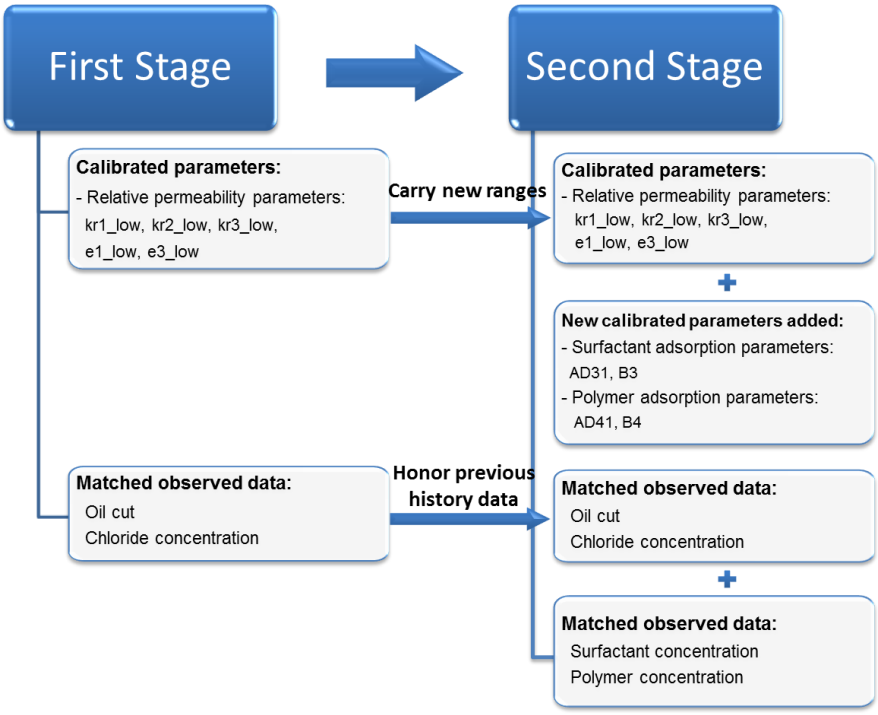

Fig. 3.15 Two-stage workflow of model calibration in ASP synthetic case

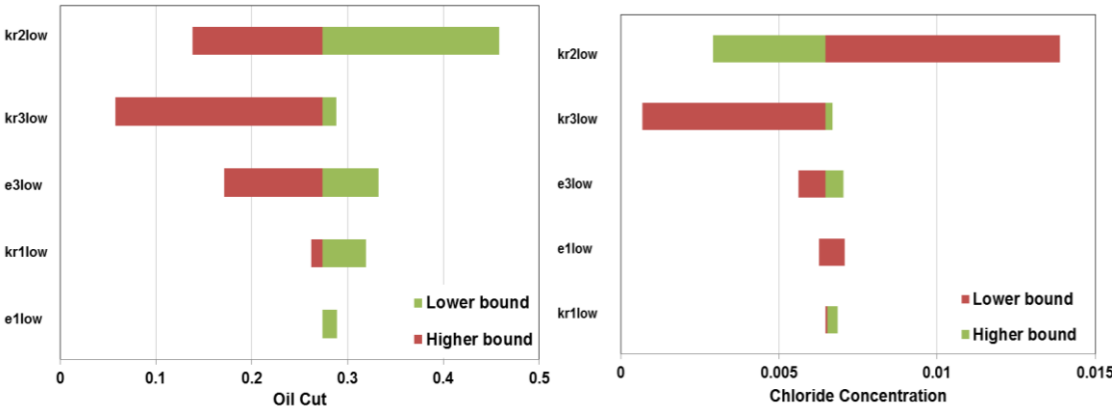

(a) (b)

Fig. 3.16 Sensitivity for stage one parameters and objectives

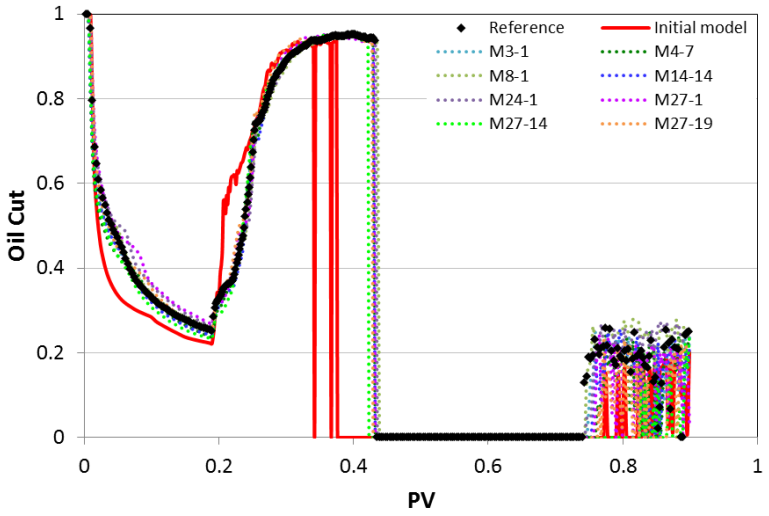

(a)

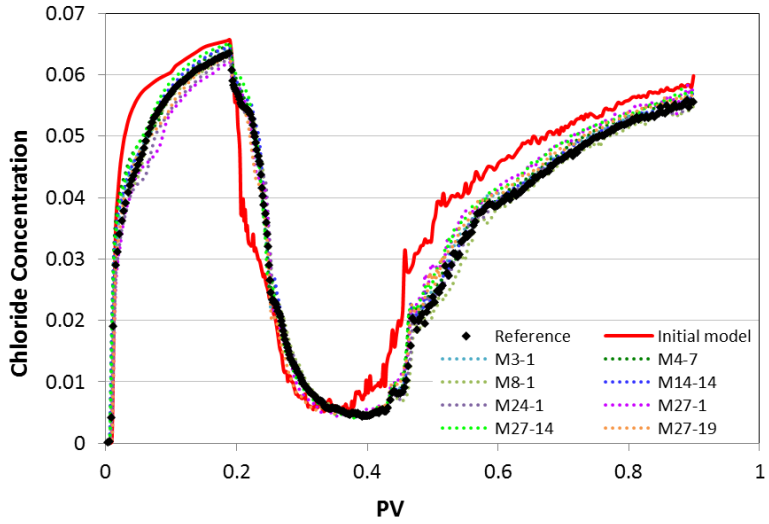

(b)

Fig. 3.17 History matching results for first stage.

(a) oil cut, and (b) chloride concentration

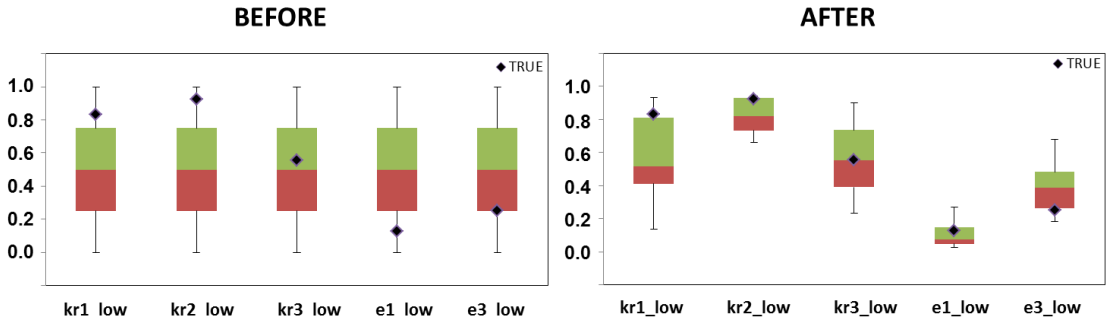

Fig. 3.18 Uncertainty analysis of models before and after first stage calibration

3.3.4 Second Stage of Model Calibration

For the second stage of model calibration, calibrated parameters from first stage, as globally dominating parameters, will be carried over with refined ranges. In addition, local and subordinate parameters, such as surfactant and polymer adsorption parameters, will also be included for calibration. In this stage, we will match surfactant and polymer concentration from the producer while honoring the observed data from first stage (oil cut and chloride concentration) at the same time. Sensitivity analysis of surfactant and polymer adsorption parameters is conducted before history matching to screen out insensitive parameters. **Fig. 3.19** displays the results of sensitivity analysis by tornado charts, from which we can see that parameters like ad32 and ad42 are not sensitive for further history matching.

Fig. 3.20 gives the history matching results for oil cut, chloride concentration, surfactant and polymer concentration. For oil cut and chloride concentration, since they have already got good match from stage one, the match results are not significantly improved. For surfactant and polymer concentration, a good agreement between updated models and observed data is reached. Again we use boxplot to compare the distribution of calibrated parameters before and after second stage model calibration, as shown in **Fig. 3.21**. Before second stage model calibration, the distribution of relative permeability parameters is carried over directly from first stage, and the adsorption parameters show

normal distribution. After second stage model calibration, the distribution of all uncertain parameters is more narrowed and approached to reference model, which means the uncertainties are all largely reduced.

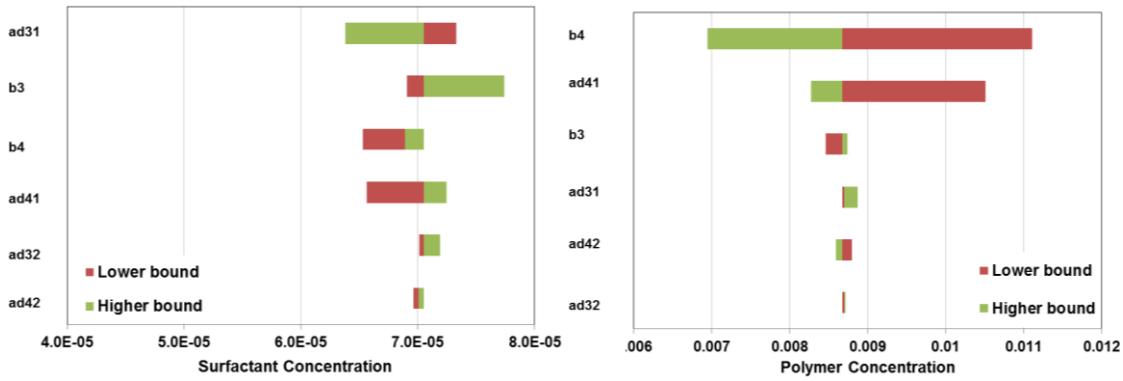

(a) (b)

Fig. 3.19 Sensitivity for stage two parameters and objectives

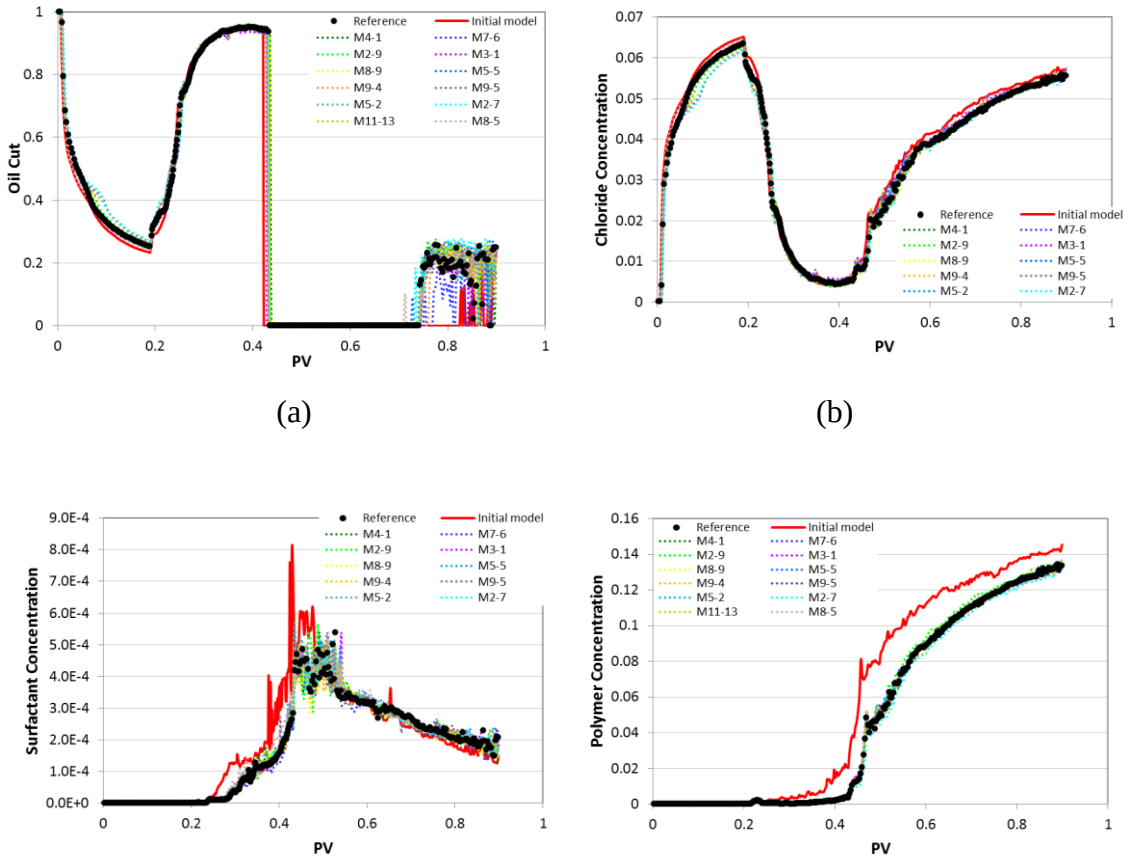

Fig. 3.20 History matching results for second stage.

(a) oil cut, (b) chloride concentration, (c) surfactant concentration, and (d) polymer concentration

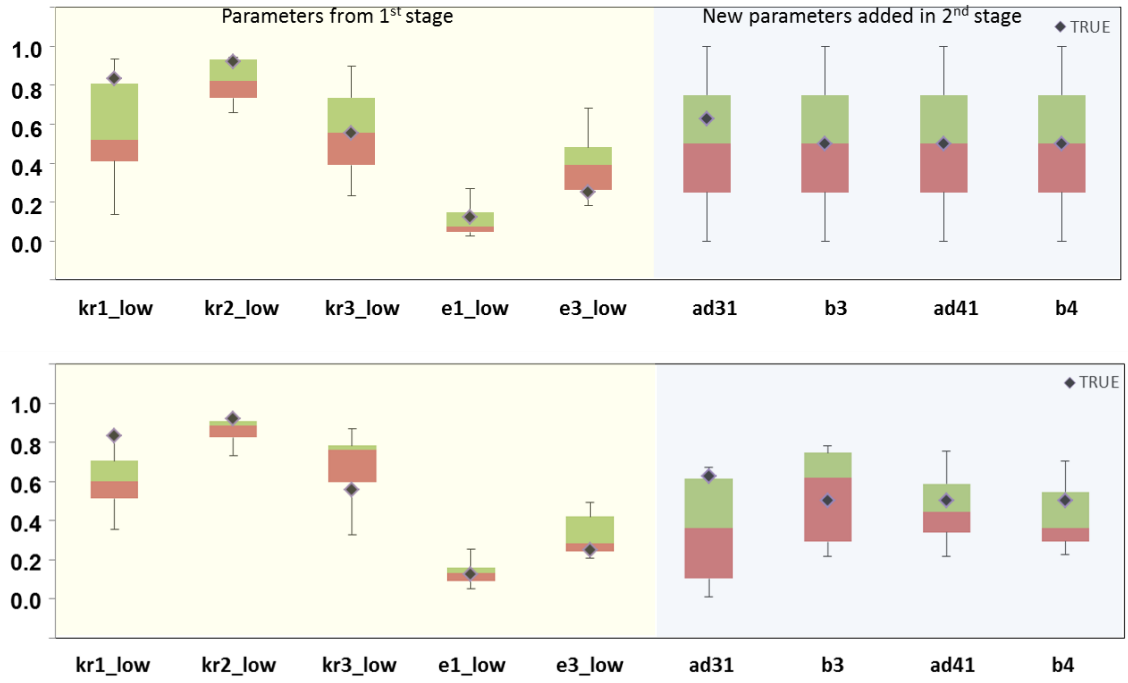

Fig. 3.21 Uncertainty analysis of models before and after second stage calibration

3.3.5 Comparison between Multi-Stage Workflow and Single-stage Workflow

We conducted another test to do history match all objectives by adjusting all uncertain parameters together, so that multi-stage workflow and single-stage workflow can be compared. Under the same range as multi-stage workflow, parameters are calibrated to also match the same objectives. The history matching results for oil cut, chloride concentration, surfactant concentration and polymer concentration are basically acceptable, but not as good as using multi-stage workflow (**Fig. 3.22**). Most importantly, in terms of parameter calibration, the ranges of uncertainties such as kr1_low, kr3_low, e1_low, and ad41 in single-stage workflow are not reduced as well as in multi-stage workflow (**Fig. 3.23**). This experiment proves that multi-stage workflow outperforms single-stage workflow for problems with large amounts of uncertain parameters and multiple objectives.

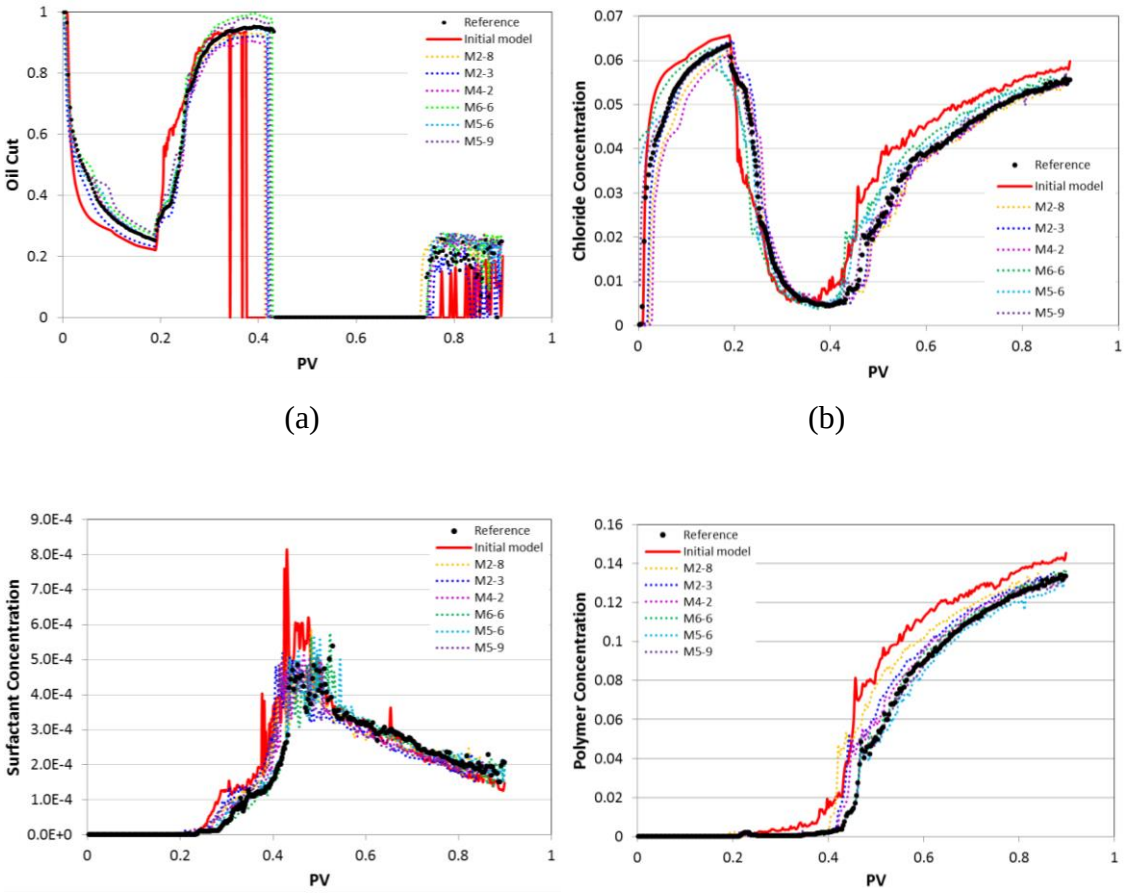

(a) (b)

(c) (d)

Fig. 3.22 History matching results under single-stage workflow.
(a) oil cut, (b) chloride concentration, (c) surfactant concentration, and (d) polymer concentration

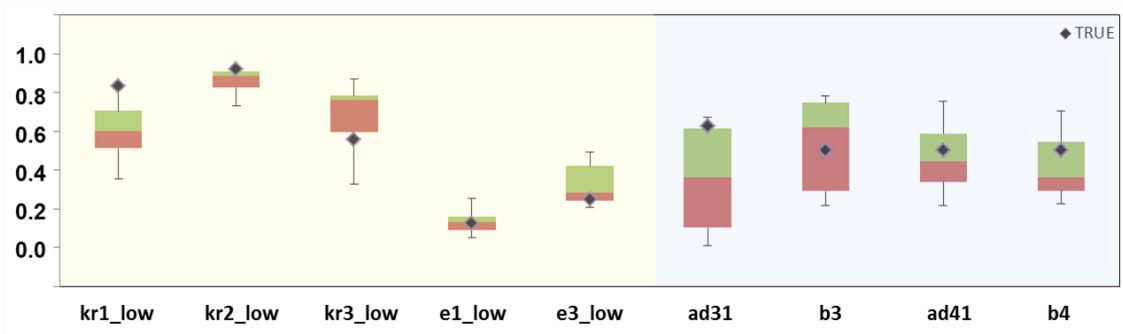

(a)

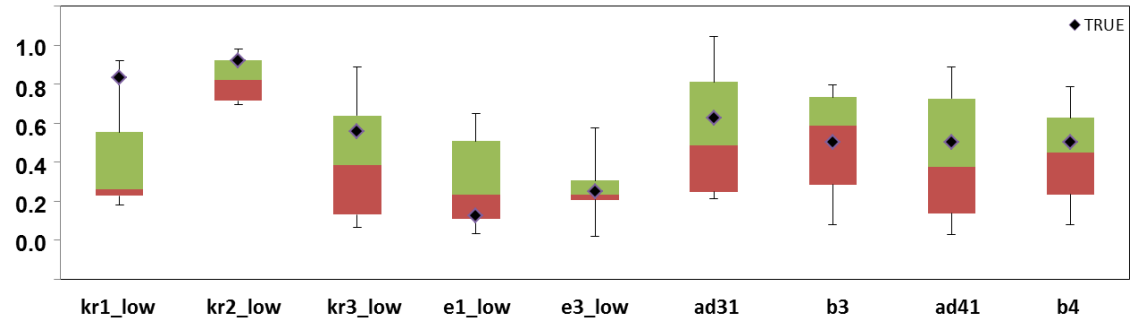

(b)

Fig. 3.23 Uncertainty analysis of calibrated models.
(a) multi-stage workflow, and (b) single-stage workflow

3.4 Summary and Conclusion

In this chapter, we proposed a multi-stage history matching workflow in alkaline-surfactant-polymer (ASP) flooding. First, physical mechanism inside ASP flooding is studied to find all possible uncertain parameters. Then sensitivity analysis is applied to identify key parameters and corresponding objective function for more global dominating level and for local subordinate level separately. Based on the sensitivity results, multi-stage history matching workflow is implemented in a synthetic ASP flooding case, and following conclusions are obtained:

- Genetic Algorithm proves to be powerful to find multiple solutions during history matching process. Chemical flood simulator UTCHEM is coupled as

forward simulator to capture ASP mechanism.

- According to the sensitivity results, relative permeability endpoints and exponents are the heavy hitters to calibrate to match oil cut and chloride concentration for stage one of the workflow.
- In stage two, adsorption parameters are adjusted to match surfactant concentration and polymer concentration from the producer. After two stages model calibration, the uncertainty has been largely reduced.
- A single-stage workflow is also applied to compare with the multi-stage workflow for history matching. Under single-stage workflow, all key parameters are calibrated together to match all objectives. The matching results are acceptable, however, the uncertainty of some parameters are not reduced as well as that under multi-stage workflow.

CHAPTER IV
MULTI-OBJECTIVE OPTIMIZATION WITH APPLICATION TO CHEMICAL FLOODING

In this chapter, we are going to use the evolutionary algorithm mentioned in Chapter II-Chapter III to optimize ASP flooding process. Usually there does not exist a feasible solution that minimizes all objective functions simultaneously such as oil production and chemical efficiency. Therefore, the concept of Pareto optimality is introduced to develop a workflow that can consider multiple conflicting objectives during the optimization of ASP flooding. The advantage of Pareto front is that it can find a representative set of optimal solutions and quantify the trade-offs in satisfying individual objectives. The proposed Pareto-based optimization approach is illustrated through a synthetic ASP flooding case, and also applied to a mixed-wet dolomite reservoir, to demonstrate its robustness and applicability to find optimal solutions. Additional economical criterion is considered to determine the optimum case selected from the Pareto front.

4.1 Introduction

4.1.1 Overview of Optimization of ASP Flooding

In the depleted and water flooded reservoirs, residual oil is trapped in the porous media by capillary forces, which can sometimes account for almost 70% of the original oil in place (Doscher and Wise 1976). Alkaline-surfactant-polymer (ASP) flooding, as an enhanced oil recovery method, has shown impressive effects on reducing residual oil saturation in laboratory scale and pilot scale by reducing interfacial tension and mobility ratio between oil and water phase. As reported (Clark et al. 1993; Demin et al. 1999; Meyers et al. 1992; Vargo et al. 1999), the oil recovery can reach over 60% of the original oil in place in some ASP pilot cases.

In the process of ASP flooding, surfactant is injected to create low interfacial tension between oil and water phases to reduce capillary forces, so that the trapped oil can be mobilized. The role of polymer in the ASP solution as a mobility control agent is to improve displacement and volumetric sweep efficiency by increasing the viscosity of the slug. The addition of alkaline can generate in-situ surfactant (also called soap) by the chemical reaction between alkali and acids in oil, to reduce interfacial tension, which, in turn, reduces the requirement of surfactant injection in the ASP slug. During the displacement, both surfactant and polymer can be adsorbed onto solid surfaces and trapped within small pores. However, the addition of alkaline can help mitigate surfactant adsorption since the high pH values in the system by alkaline would repel the anionic sulfonate.

Polymer flooding has been applied successfully in core, pilot, and field scale, whereas applications of surfactant/polymer or alkaline/surfactant/polymer flooding were limited to pilot scale or small field scale, due to requirement of large amounts of chemical products, high chemical costs, and lack of mature techniques. However, with the increasing crude oil price in recent years, SP or ASP flooding has been drawing the industry's attention. A successful application of SP or ASP flooding requires extensive design of flooding process, accurate reservoir and fluids characterizations and modeling, and comprehensive optimization to help make both technical and financial decisions.
Technically, the design and optimization of SP or ASP flooding process should follow three principles: active propagation of surfactant and polymer, less chemical adsorption, and improved sweep efficiency. To achieve these three goals, various parameters need to be investigated, such as different formulations of the chemicals on phase behavior and adsorption, reservoir and fluid data, the concentration of the ASP solution, slug size, and so on. If economical aspect is included, uncertain parameters such as chemical costs, oil price, tax, and discount rate should also be considered.

The systematic workflow to design and optimize SP or ASP flooding process is to bring SP or ASP flooding from the laboratory to the field, as shown in **Table 4.1**. Stoll et al. (2010) followed this process and applied to Petroleum Development Oman (PDO)'s

single-well pilot case from the design of ASP formulation to actual pattern-flood pilot in the field, so that the feasibility of the ASP project was evaluated and demonstrated for further large field-scale development. The process of design and optimization for SP/ASP flooding should be chosen from **Table 4.1** according to the practical situation, but basically follow the route from core scale, to pilot scale, and eventually to the field scale.

Previous works on the design and optimization of SP and ASP flooding are summarized in **Table 4.2**, in terms of parameters considered, objectives, optimization scale, whether formulation study, sensitivity study are investigated, optimization methods, etc. From this table, we can see that regarding SP or ASP flooding, previous works have mainly focused on designing formulations that can achieve minimum interfacial tension through experiments and empirical correlations. Some works used traditional approaches for optimization process, which are trial and error method or sensitivity analysis using numerical models at core and pilot scale. Very few works have addressed optimization of injection scheme using numerical optimization methods and achieve maximum field performance (such as oil recovery, displacement efficiency) in a field scale. Therefore, in this chapter, our work will focus on the optimization of SP or ASP flood process using numerical optimization method.

Table 4.1 Process of design and optimization for chemical flooding

Laboratory work	
• Chemical phase-behavior experiments	Identify a surfactant mixture type and its required concentration, alkali concentration, etc. to achieve very low interfacial tension
• Coreflood experiments	➢ Test formulation to prove its ability to mobilize residual oil ➢ Provide information about the adsorption characteristics of chemicals ➢ Study displacement stability of the polymer drive
• Model calibration	➢ Build numerical simulation model to represent the coreflood process ➢ Conduct history matching to validate model parameters
Piloting	
• Series of single-well chemical-tracer tests (SWCTs)	Predict injection pressures, liquid rates, and effluent concentrations for different pilot configurations
• Pattern-flood pilot	Verify the robustness of SP/ASP process: ➢ Subsurface-related uncertainties: stability of the chemicals, formation of an oil bank, susceptibility to reservoir heterogeneity, etc. ➢ Surface-related challenges: separation of oil from produced emulsion, logistics, etc
• Model calibration	➢ Build numerical simulation model of the pilot case ➢ Conduct history matching to reduce uncertainty
Field-scale application	
• Model calibration	➢ Build numerical simulation model of the field case ➢ Conduct history matching to reduce uncertainty
• Optimization	➢ Optimized variables: surfactant/polymer concentration, slug size, etc. ➢ Objectives: oil recovery, NPV, etc.

Table 4.2 Previous work on design and optimization of chemical flooding

Authors	Parameters	Objective function	Study scale	Formu-lation design	Simula-tion	Sensiti-vity study	Optimiza-tion method
Delshad et al. (1998)	Surfactant and polymer amounts, slug size, adsorption	Displacement efficiency, oil recovery	Core	No	Yes	Yes	No
Manrique et al. (2000)	Polymer thermal stability, phase behavior, IFT,	Oil recovery	Labora-tory, core	Yes	No	No	No
Hernandez et al. (2001)	Fluid interactions and compatibility, phase behavior, IFT, rock-fluid interactions, polymer rheology	Oil recovery	Labora-tory, core, pilot	Yes	Yes	No	No
Pandey et al. (2012)	IFT, cation exchange, adsorption, capillary end effect, gravity effect	Displacement efficiency, oil recovery	Labora-tory, core, pilot, field	Yes	Yes	Yes	No
Bazin et al. (2010)	Phase behavior, solubility, adsorption, surfactant positioning	Robust formulation	Labora-tory, core	Yes	Yes	No	No
Buijse et al. (2010)	Phase behavior, surfactant solubility, polymer rheology and viscosity, polymer filtration	Displacement efficiency	Labora-tory, core	Yes	No	No	No
Dang et al. (2011)	Heterogeneity, surfactant and polymer concentration, injection pressure, injection rate	Oil recovery	Field	No	Yes	Yes	No
Jain et al. (2012)	CMC, IFT, phase behavior, chemical solubility and stability	Displacement efficiency, oil recovery	Core, pilot	Yes	Yes	No	No

Table 4.2 Continued

Authors	Parameters	Objective function	Study scale	Formu-lation design	Simula-tion	Sensiti-vity study	Optimization method
Zhang et al. (2012)	Phase behavior, IFT, core tests for surfactant concentration and adsorption	Displacement efficiency, oil recovery	Labora-tory, core	Yes	No	No	No
Luo et al. (2013)	IFT, polymer rheology, comparisons among P, SP, and ASP	Displacement efficiency, oil recovery	Labora-tory, core	Yes	No	No	No
Wu et al. (1996)	Polymer concentration, permeability, kv/kh, oil price, discount rate, operating cost, surfactant and polymer cost	Oil recovery, NPV	Field	No	Yes	Yes	Monte Carlo
Zerpa et al. (2004)	Slug size and concentration of chemical agents	Oil recovery	Field	No	Yes	No	Weighted average of surrogates by polynomial regression /krigging
Anderson et al. (2006)	Surfactant concentration, slug size, mass of polymer, salinity	Oil recovery, chemical efficiency	Pilot	No	Yes	Yes	No
Zerpa et al. (2007)	Injection rates, slug size, and initial time	Oil recovery, displacement efficiency	Pilot	No	Yes	No	Experimental design, response surface
Rai et al. (2009)	Dimensionless permeability, heterogeneity, dip and top depth of the reservoir, grid resolution	Oil recovery	Field	No	Yes	Yes	Dimensionless group, response surface

4.1.2 Problem Description

From **Table 4.2**, we can see that numerical optimization methods, such as Monte Carlo simulation, Experimental Design, Response Surface, have been implemented to optimize SP or ASP flood process. In Wu et al. (1996) 's work, Monte Carlo simulation technique carried out a large amount of project evaluations with multiple input variables sampled from certain probability distributions in random combinations. Monte Carlo simulation was able to assess the risk in the optimum SP flooding design. However, it requires massive forward simulations, so that it is only suitable for small cases. Zerpa et al. (2004) generated samples using Latin Hypercube Samplings and constructed surrogate models by weighted average of polynomial Regression and Krigging. The optimum design was selected based on evaluations of surrogate-based optimal solutions. This method was also limited to the case with large scale of numerical simulations. In this proposed method, the advantage of using multiple surrogate models was not clearly addressed. Zerpa et al. (2007) constructed 81 designs by D-optimal design of experiments and represented sampled pairs of input variables and output measurements by fitting into a quadratic response surface model. According to the sensitivity study, since oil recovery has more effect on reservoir recovery factor than displacement efficiency does, the case with higher oil recovery was chosen as the optimum design. This proposed methodology for ASP flooding process is problem-specific and case-specific. Changes of cases, variables, and objectives require a completely new fitting process. Also, the significance of two performance measures on oil recovery is under-estimated by simply comparing the values between two optimal cases. In terms of objective functions, most of the work only considers oil recovery. Even chemical efficiency is included, the strategy is to choose the optimal case with less chemical used with more oil produced manually. However, the relationship between oil recovery and chemical efficiency is overlooked.

Based on the investigation of previously applied numerical optimization methods, several critical issues exist in the optimization process of SP or ASP flooding: 1) more general approach to handle different cases and different problems; 2) multiple objective

functions to be considered simultaneously, such as oil production, chemical efficiency, etc.; 3) more elaborate representation of relationship between multiple objective functions. These above three issues would be the objectives of the work in this chapter.

In this chapter, a Pareto-based optimization approach is proposed to solve the multi-objection problems, especially conflicting objectives in SP/ASP flooding. Based on the definition of dominance, the concept of Pareto optimality was introduced to generate a set of Pareto optimal solutions which serve as a good representation of the trade-off relationship between conflicting objectives. The Pareto optimal solutions were searched using Non-dominated Sorting Genetic Algorithm (NSGA-II), which evaluate each population by dominance relationship instead of fitness values in ordinary single objective genetic algorithm. This proposed approach is implemented for a 3D synthetic example and a 3D field-scale application.

4.2 Methodology

4.2.1 Traditional Multi-Objective Optimization

Successful implementation of SP or ASP flooding in pilot scale and field scale requires optimization of injection scheme (such as surfactant/polymer concentration, slug size, etc.), to eventually maximize oil recovery and minimize consumed chemicals at the same time. This makes the optimization of SP or ASP flooding process a problem with multiple, conflicting objectives.

Optimization problems with multiple, conflicting objectives are often solved by aggregating the objectives (f_i) into a scalar function with weighting factor (w_i) applied, which simplifies the multi-objective problem to a single-objective problem, as shown in **Eq. 4.1**. This approach is called scalarization (weighted-sum) method.

$$f = \min \sum_{i=1}^{n} w_i f_i(\mathbf{x})$$
$$\sum_{i=1}^{n} w_i = 1,\ w_i > 0 \qquad \text{.....(4.1)}$$

Due to its simplicity, the weighted-sum approach is widely used. However, it shows limitation when each objective is in different scale units. In addition, appropriate weight for each objective can be challenging to identify. Park et al. examined the influence of the weight factor on the optimization results. These limitations make weighted-sum approach less favorable for multi-objective optimization problem.

To overcome these limitations, Pareto-based approach takes advantage of the dominance relation to assign ranks instead of fitness values and explores a set of optimal solutions which can represent the trade-off relation between the conflicting objectives.

4.2.2 Pareto-Based Multi-Objective Optimization

4.2.2.1 Multi-objective optimization problem definition

A multi-objective optimization problem is an optimization problem that involves *n* objective functions with *m* decision variables (uncertainty parameters). In mathematical terms, a multi-objective optimization problem can be formulated as

$$\min \quad \mathbf{y} = \left(f_1(\mathbf{x}),\ f_2(\mathbf{x}), \ldots,\ f_n(\mathbf{x})\right) \in \mathbf{Y}$$
$$\text{s.t.} \quad \mathbf{x} = \left(x_1, x_2, \ldots, x_m\right) \in \mathbf{X}$$

where **x** is called a decision vector or a feasible solution, **X** is the feasible set of decision vector, also called the parameter space, as denoted in **Fig. 4.1**; **y** is called the objective vector, **Y** is called the feasible set of objective vector or the objective space, as denoted in **Fig. 4.1**. In multi-objective optimization, there does not usually exist a feasible solution that minimizes all objective functions simultaneously. In other words,

individual objectives can be conflicting. Therefore, *Pareto optimal solutions* are preferred to a single solution; that is, decision vectors cannot be improved in any objective without causing degradation in at least one other objective. Mathematically, a feasible solution $\mathbf{a} \in \mathbf{X}$ is said to Pareto *dominate* another solution $\mathbf{b} \in \mathbf{X}$ if and only if two conditions are satisfied:

1. $f_i(\mathbf{a}) \leq f_i(\mathbf{b})$ for all indices $i \in \{1,2,\cdots,n\}$
2. $f_j(\mathbf{a}) < f_j(\mathbf{b})$ for at least one index $j \in \{1,2,\cdots,n\}$

And the decision vector **a** and its corresponding objective vector is called Pareto optimal when there is no other solution that dominates it. At the same time, the set of Pareto optimal objective vectors is often called the *Pareto front*.

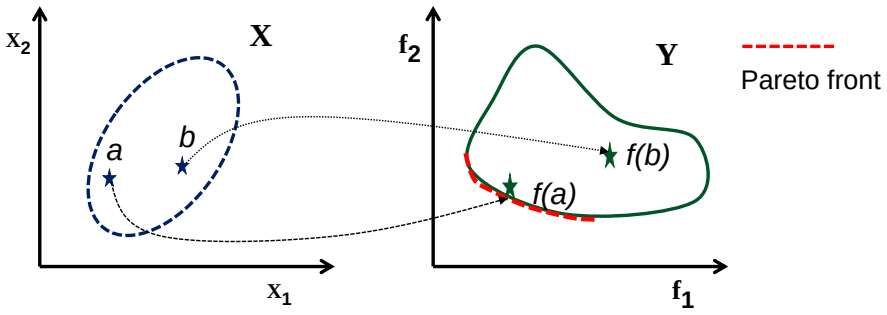

Fig. 4.1 Mapping for multiobjectives from parameter space into objective space (Park 2012)

Note that without additional subjective preference information, all Pareto optimal solutions are considered equally good, and therefore vectors cannot be ordered completely. The goal of Pareto front based optimization is to find a representative set of optimal solutions and quantify the trade-offs in satisfying individual objectives, and ultimately finding a single solution that is subject to additional criterion such as human

preferences, weighted compromise etc. Variation of the criterion can result in different single solutions, as shown in **Fig. 4.2**.

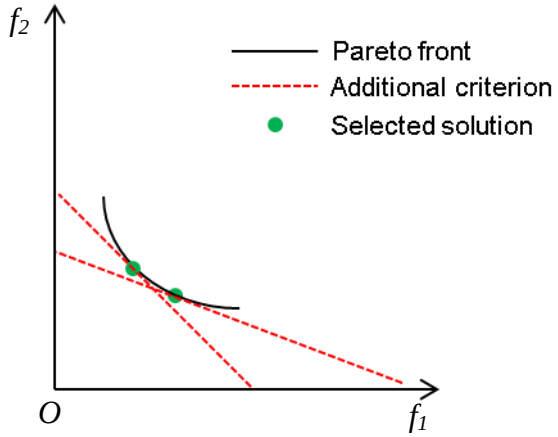

Fig. 4.2 Post processing of Pareto front solutions

4.2.2.2 Multi-objective Optimization Algorithms

In order to optimize multi-objective problems without compromising conflicts, most classical search approaches are not sufficient for several major reasons (Schulze-Riegert et al. 2007):

a. Most methods can find multiple solutions in a single run, therefore requiring them to run as many times as the number of desired Pareto front solutions.
b. Multiple applications of these methods cannot guarantee that a diversified Pareto front will be found especially for problems with multiple optimal solutions. Deterministic methods like perturbation methods, gradient or sensitivity based methods typically strongly rely on initial solutions, and are often are trapped by local optima.
c. Most of them cannot handle discrete decision variables.

In contrast, recently Pareto-based evolutionary approaches have been drawing more and more attention to handle multi-objective optimization problems in petroleum engineering.

Schulze-Riegert et al. (2007) first applied multi-objective optimization techniques to reservoir simulation and utilized the Strength Pareto Evolutionary Algorithm (SPEA) to implement history matching. Han et al. (2010) successfully applied Multi-Objective Evolutionary Algorithm to history matching a waterflooding project. Hajizadeh et al. (2011) proposed differential evolution for multi-objective optimization using Pareto ranking (DEMOPR) and coupled the algorithm with Bayesian uncertainty quantification framework for history matching and uncertainty quantification. Park et al. (2013) used Pareto-based multi-objective evolutionary algorithm (MOEA) to conduct history matching with Grid Connectivity-based Transformation (GCT).

Generating the Pareto set can be computationally expensive and sophisticated due to the complexity of the underlying problem. Two key issues to addresses are: how to accomplish fitness assignment and selection, and how to maintain population diversity. In order to resolve these issues, various evolutionary algorithms were proposed in literature including Niched Pareto Genetic Algorithm (Horn 1993), Strength Pareto Evolutionary Algorithm (SPGA) (Schulze-Riegert et al. 2007), and Non-dominated Sorting Genetic Algorithm (NSGA-II) (Park et al. 2013). In our study, NSGA-II will be used to explore a set of optimal solutions and Pareto-based multi-objective method will be utilized to optimize SP or ASP flooding process. A typical workflow for NSGA-II is described in the following figure (**Fig. 4.3**).

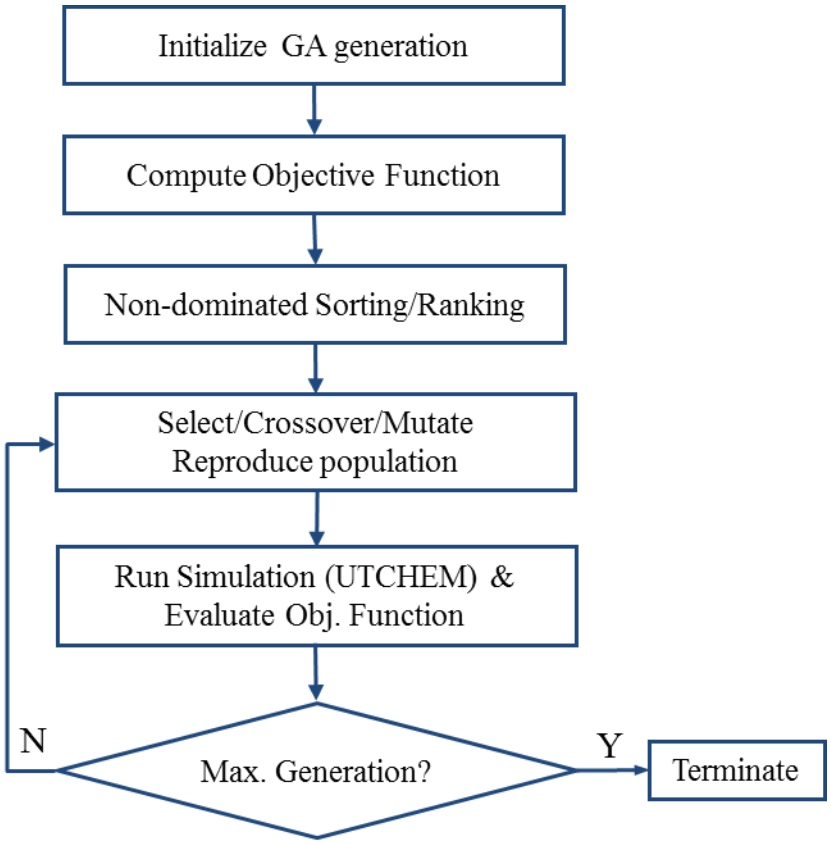

Fig. 4.3 Non-dominated sorting genetic algorithm (NSGA-II) workflow

The workflow is similar to the genetic algorithm in the previous chapter in that it uses typical genetic reproduction operations (crossover, mutation). The key difference for workflow in **Fig. 4.3** is in the way the selection operator works. The selection process of a single objective and weighted multi-objective problem is according to fitness evaluation of solution models. The smaller the single or weighted objective value is, the larger the fitness is assigned to a solution model. Then the selection procedure picks the parent models to reproduce offspring using crossover and mutation. As mentioned previously, the most common selection method is to use the ratio of each model's fitness to the total fitness of all population in the same generation. However, this selection is subjective for multi-objective problems since the objective value and fitness function of each model depends on the way of weighing objectives.

On the contrary, the selection algorithm in the NSGA-II uses non-dominated ranking instead of calculating fitness function of weighted objective. In order to illustrate the algorithm, supposed we have a two-objective problem (m=2, f_1, f_2) to optimize. The models are evaluated and mapped in the objective space as shown in **Fig. 4.1**. We sort the population based on Pareto dominance concept mentioned previously and assign a rank to individual model according to its non-dominance. Specifically, for solutions of a given population of size n: $\mathbf{x}_1$, $\mathbf{x}_2$, .., $\mathbf{x}_n$, a simplified sorting algorithm is as follows:

```
for i = 1, n
        rank(x_i) ← 1
for i = 1, n
        for j = i+1,n
                if f1(x_i)<f1(x_j) and f2(x_i)<f2(x_j)
                        rank(x_j) ← rank(x_j) + 1
sort(x_1,x_2,…,x_n) based on ranks
for i = 2,n
        if ran(x_i) > rank(x_i-1) + 1
```

In the next section, we will illustrate this workflow by the application to an ASP flooding synthetic case. The outline of the application is as follows: first, the simulation model for ASP flooding synthetic case is described and sensitivity study is carried out based on the simulation model to identify the parameters and objectives to optimize. Based on the results from sensitivity study, the workflow is implemented to optimize ASP flooding process with multiple conflicting objectives. Finally, following the optimization results, optimal scheme is discussed and selected with the consideration of economical constraint.

4.2.3 Illustration of the Approach: A Synthetic Example

In this part, we will illustrate our procedure using a synthetic example, which is a three-dimensional reservoir consisting of 15×15×3 grid blocks, with four injectors and one producer. The permeability distribution is shown in **Fig. 4.4**. This field goes through waterflooding for 122 days (about 1 PV), and then ASP flooding, followed by a polymer drive. **Fig. 4.5** gives the oil saturation distribution after the waterflooding. The goal is to optimize the ASP flooding process by optimizing parameters such as surfactant concentration, polymer concentration and slug size to maximize oil production with minimum usage of chemicals.

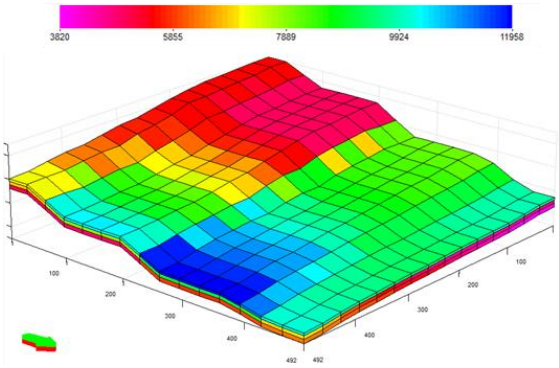

Fig. 4.4 Permeability distribution

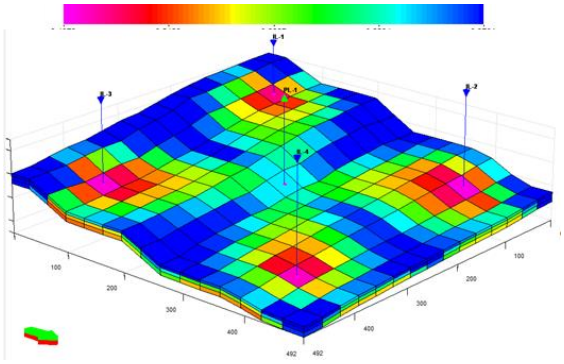

Fig. 4.5 Oil saturation after waterflooding

To formulate the objectives mathematically, incremental oil production is defined as the difference of oil production with ASP solution injection and without ASP solution injection, as shown in **Eq. 4.2**.

$$\Delta N_p = N_p(\text{with ASP}) - N_p(\text{without ASP}) \quad \text{.....(4.2)}$$

The chemical efficiency is defined as the amount of chemicals required to get 1 STB of oil gain, which is called utility factor (UF). For ASP flooding, the total utility factor is the sum of logarithm of utility factor for each chemical, as shown in **Eq. 4.3**. High chemical efficiency means small total utility factor.

$$\begin{aligned} \text{UF\_surf} &= \frac{\text{Surfactant required, volume fraction}}{\text{1STB of incremental oil production}} \\ \text{UF\_poly} &= \frac{\text{Polymer required, weight percentage}}{\text{1STB of incremental oil production}} \\ \text{UF\_total} &= \log(\text{UF\_surf}) + \log(\text{UF\_poly}) \end{aligned} \quad \text{.....(4.3)}$$

With objectives defined, sensitivity analysis is conducted to study the effects of uncertain parameters on each objective and the relationship between the two objectives.

Table 4.3 summarizes the range for each parameter and the two objectives considered. **Fig. 4.6** shows the incremental oil production and chemical utility factor under different surfactant concentration, polymer concentration, and slug size. We can see that within given range of each parameter, incremental oil production and chemical utility factor are conflicting objectives, which makes the optimization example a multi-objective problem with conflicting objectives.

Table 4.3 Parameters and objectives for optimization of chemical flooding

Parameters	
Surfactant concentration range, volume fraction	0.02 – 0.1
Polymer Concentration range, weight percentage	0.2 – 1
Slug Size range, days	154 - 354
Objectives	
Incremental Oil Production, bbl	
Chemical Utility Factor	

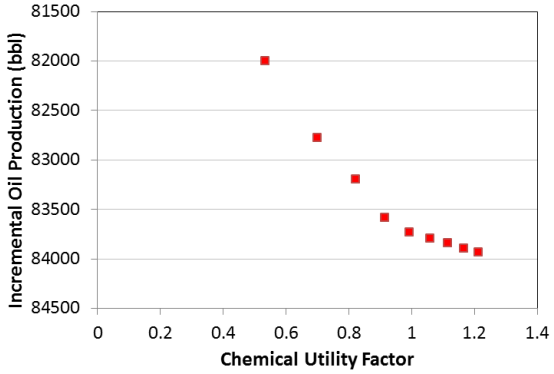

(a)

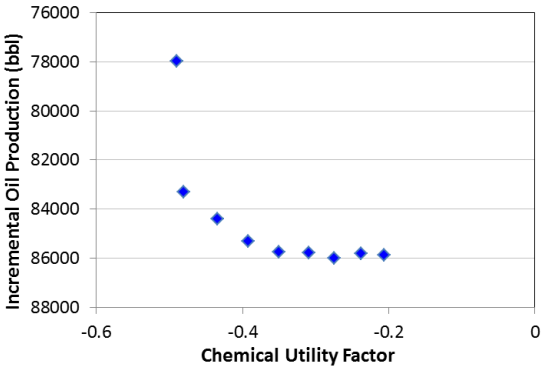

(b)

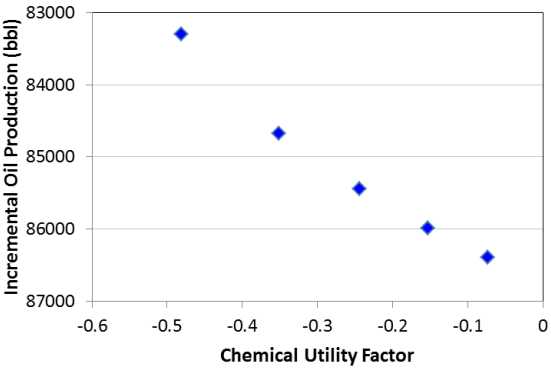

(c)

Fig. 4.6 Sensitivity of each parameter.

(a) different surfactant concentration, (b) polymer concentration, and (c) slug size

To solve this problem, our proposed workflow is implemented and the results are displayed in **Fig. 4.7**. Firstly, initial population is generated by Latin Hypercube Sampling, and mapped to objective space, as shown in **Fig. 4.7**(a). Then non-dominated sorting genetic algorithm is used to selectively keep the low rank member, which results in moving all the population to the front. The optimal condition is reached when all members of the population become rank one, which implies all the members of the population approach close to the Pareto front, as shown in **Fig. 4.7**(b).

Within the Pareto front is a set of optimal solutions that represent the compromised trade-off relationship between conflicting objectives. It can serve as a decision tool to determine the optimal case given certain constraint, which is usually economical constraint.

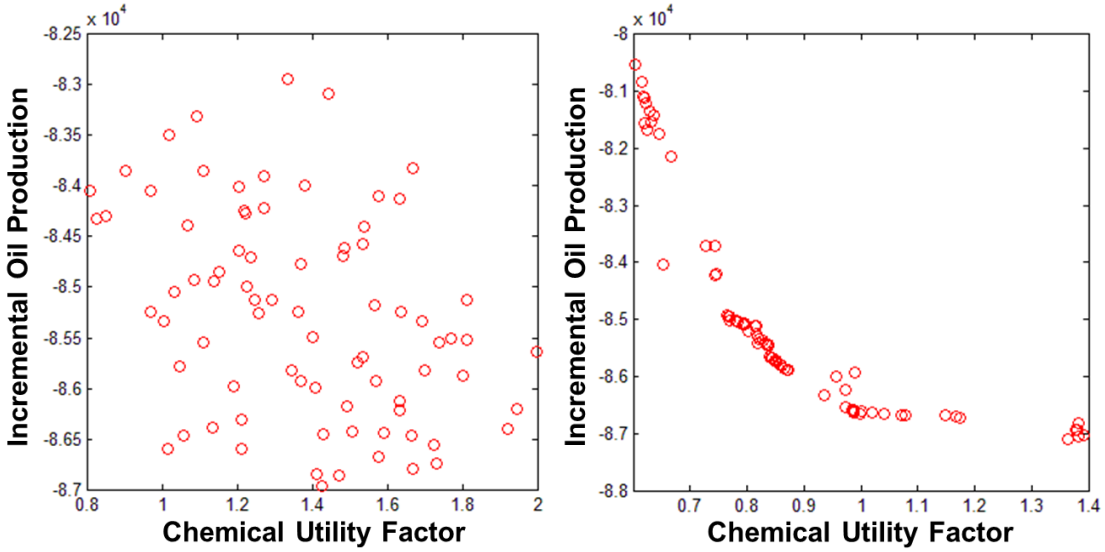

(a) (b)

Fig. 4.7 Optimization results.

(a) objective distribution of initial population, (b) pareto front after 10 generations

4.3 Field Scale Application: Optimization of Surfactant - Polymer Flooding in a Mixed-Wet Dolomite Reservoir

In this section, we apply the proposed method of optimization to a mixed-wet reservoir to demonstrate its applicability for optimization under multiple conflicting objectives. First, the field background and simulation model are described. Sensitivity of uncertain parameters is investigated regarding two objectives (incremental oil production and chemical efficiency), not only to study the effect of parameters on each objective, but also to find out the conflicting relationship between the two objectives. Then the proposed Pareto-based multi-objective optimization approach is applied to generate a set of optimal solutions to represent the trade-off relation between conflicting objectives. Finally, economical factor is introduced as an additional constraint to help choose the optimal solution.

4.3.1 Field Background and Simulation Model Description

The mixed-wet reservoir we studied in this section is from a Grayburg dolomite reservoir in the Permian Basin. The reservoir depth is 400 ft and thickness is 100 ft. The main reservoir properties are listed in **Table 4.4**. The relative permeability is modeled based on Corey functions, in which the residual saturation, relative permeability endpoints and exponents are obtained from laboratory data. **Table 4.5** also lists the reservoir fluid properties from the field operator.

The simulation model built by UTCHEM is a quarter of a 40-acre five-spot pattern with one injector and one producer. The heterogeneous permeability distribution, as shown in **Fig. 4.8**(a), was provided by the field operator based on well log data and geological model.

The physical property data used in the model such as surfactant phase behavior, surfactant adsorption, and polymer viscosity were obtained from reported literature (Levitt et al. 2006), in which experiments were conducted to design the formulation and

determine the optimum salinity and solubilization ratio using reservoir crude, formation brine and surfactant solutions. Experimental coreflooding was also performed to measure the surfactant and polymer flooding performance.

The initial oil saturation is shown in **Fig. 4.8**(b). The reservoir has gone through a long history of waterflooding. The water cut has reached up to about 98% in 2006, and it was not economically practical. Therefore, surfactant-polymer solution was designed and optimized to improve oil recovery. In the model, the waterflooding is first simulated to obtain the oil saturation and pressure distribution after waterflooding.

Table 4.4 Reservoir and simulation model properties

Model dimensions	700 ft × 800 ft ×99.1 ft
Porosity	Min = 0.06 Max = 0.273 Average = 0.16
Permeability	Min = 4.4 mD Max = 870 mD Average = 156 mD kv/kh = 0.05
Residual saturation	Water = 0.3 Oil = 0.42
Corey type relative permeability endpoint	Water = 0.4 Oil = 0.6
Corey type relative permeability exponent	Water = 2 Oil = 2
Simulated model pore volume	1.610 MMbbl
Simulated post waterflood saturation (Average)	Water = 0.53 Oil = 0.47
Simulated post waterflood oil in place	0.75 MMbbl
Simulated post waterflood pressure (Average)	755 psi

Table 4.5 Fluid properties

Density	Oil = 31 °API (0.87 g/ml)
Viscosity	Water = 0.72 cp Oil = 5 cp
Brine composition	Overall = 1 meq/mL Ca^{2+} = 2066 ppm Mg^{2+} = 539 ppm Na^{+} = 20533 ppm SO_4^{2-} = 4540 ppm CI^{-} = 32637 ppm

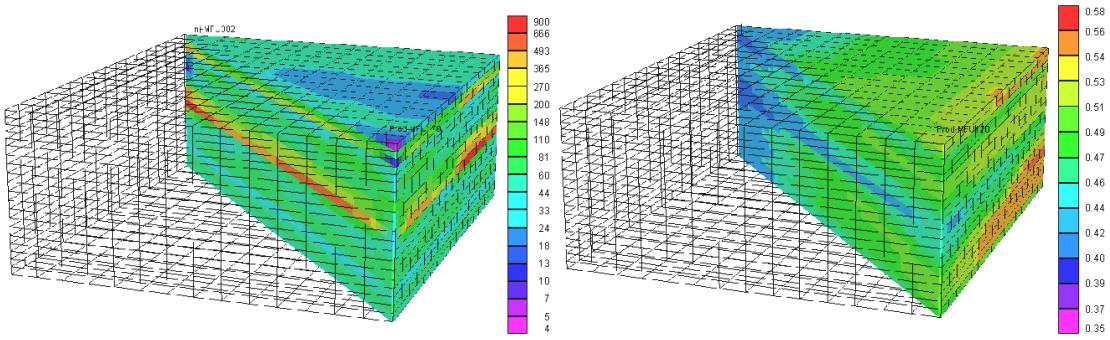

(a) (b)

Fig. 4.8 Simulation model.

(a) Permeability distribution, (b) initial oil saturation

Anderson et al. (2006) optimized surfactant and polymer flooding in this reservoir mainly by sensitivity analysis. Appropriate ranges were assigned to design variables (surfactant concentration, polymer concentration, and slug size) to evaluate their effect on cumulative oil recovery and chemical efficiency. In addition, parameters such as surfactant adsorption, polymer adsorption, vertical to horizontal permeability ratio, average permeability and the dependence of the oil saturation on capillary number were

also studied. An optimum case was chosen based on the observations of sensitivity results. On the basis of their results, we will focus more on the trade-off relation between oil production and chemical efficiency in our work.

4.3.2 Optimization Results

To optimize SP flooding process in this reservoir, we followed Anderson's work to adjust design variables (surfactant concentration, polymer concentration, and slug size) to maximize oil recovery and minimize chemical usage at the same time. First, sensitivity cases are run to study the effects of design variables on each objective. The ranges of the variables are summarized in **Table 4.6**. **Fig. 4.9** shows the sensitivity results for different surfactant concentration, polymer concentration, and slug size. We can see that within the given range, incremental oil production and total utility factor are two conflicting objectives in this problem.

Our proposed approach is applied and the results are shown in **Fig. 4.10**. The initial population is generated by Latin Hypercube Sampling to cover the whole variable space, and the objective of each member of population is mapped in **Fig. 4.10**(a). After five generations of evolution, the Pareto front is well formed to represent the trade-off between two objectives (**Fig. 4.10**(b)).

Table 4.6 The range of each design variable in sensitivity study

Parameters	
Surfactant concentration, volume fraction	0.02 – 0.01
Polymer Concentration, weight percentage	0.05 - 0.5
Slug Size, PV	0.3 – 0.5

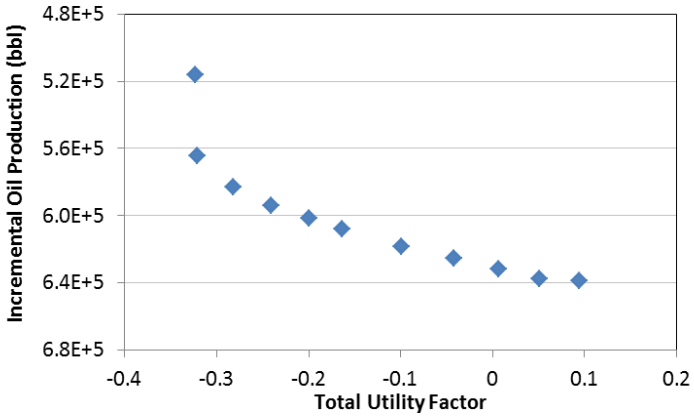

(a)

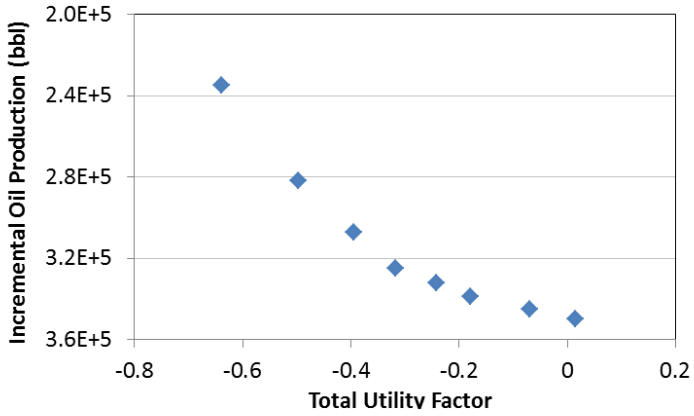

(b)

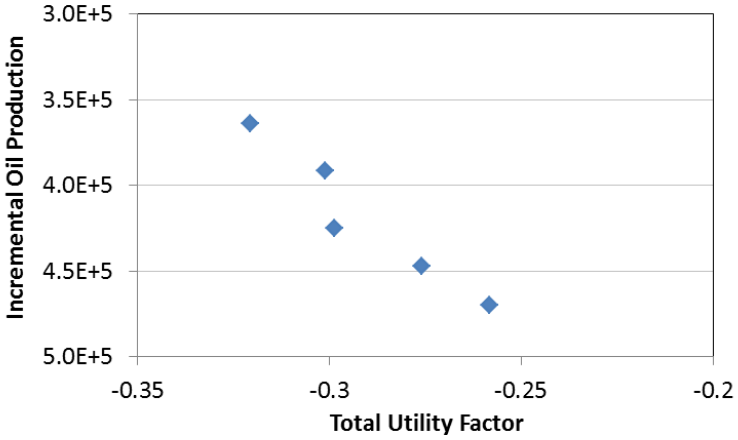

(c)

Fig. 4.9 Sensitivity of each parameter in the field case.

(a) different surfactant concentration, (b) polymer concentration, and (c) slug size

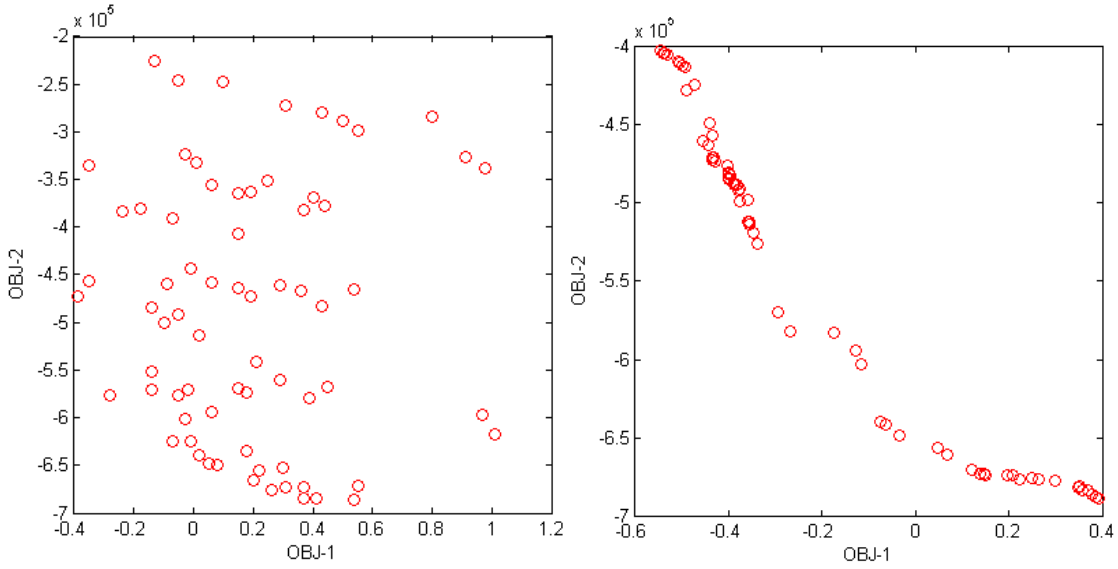

(a) (b)

Fig. 4.10 Optimization results.

(a) objective distribution of initial population, (b) pareto front after 5 generation

Along Pareto front, MSE algorithm (**Fig. 4.11**) is used to select optimal solutions, which are considered as a compromise between production increase and chemical usage. As shown in **Fig. 4.12**, after applying the MSE algorithm, models with minimal errors are chosen as the optimal solutions (circled by purple). To study the distribution of control variables along the Pareto front, we choose six models with minimal utility factor (circled by green), six models with maximal incremental oil production (circled by blue), and five comparable models in the middle (circled by orange).

Histogram (**Fig. 4.13**) is plotted to show the distribution of control variables (surfactant concentration, polymer concentration, and slug size) for different groups of models in **Fig. 4.12**, and **Table 4.7** summarizes the distribution of control variables. For models with minimal utility factor, surfactant and polymer concentration stays in the lower range; for models with maximal incremental oil production, surfactant and polymer concentration centralizes in the higher range; while for optimal models, surfactant and polymer concentration distributes in the middle. The distribution of slug

size for the four groups of models is scattered and doesn't follow the order as surfactant and polymer concentration. This means surfactant and polymer concentration are sensitive variables, while slug size is a less sensitive variable.

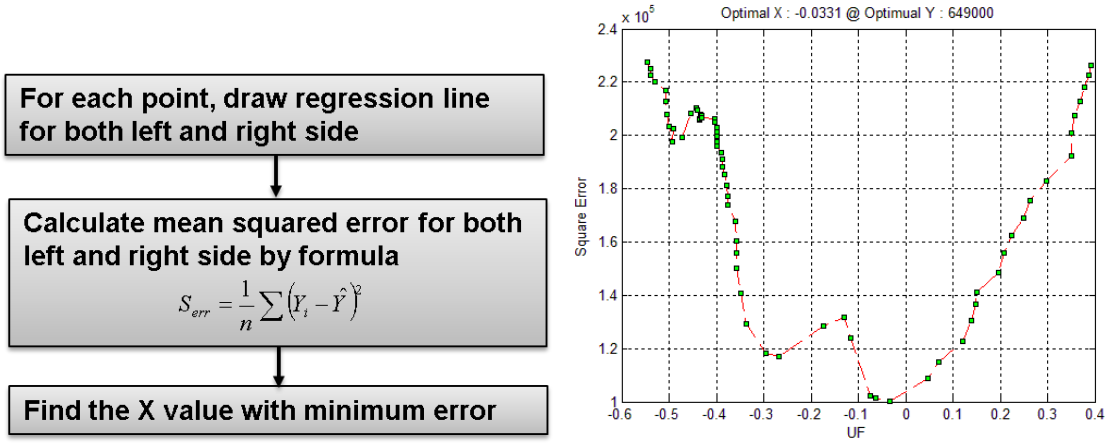

Fig. 4.11 MSE algorithm

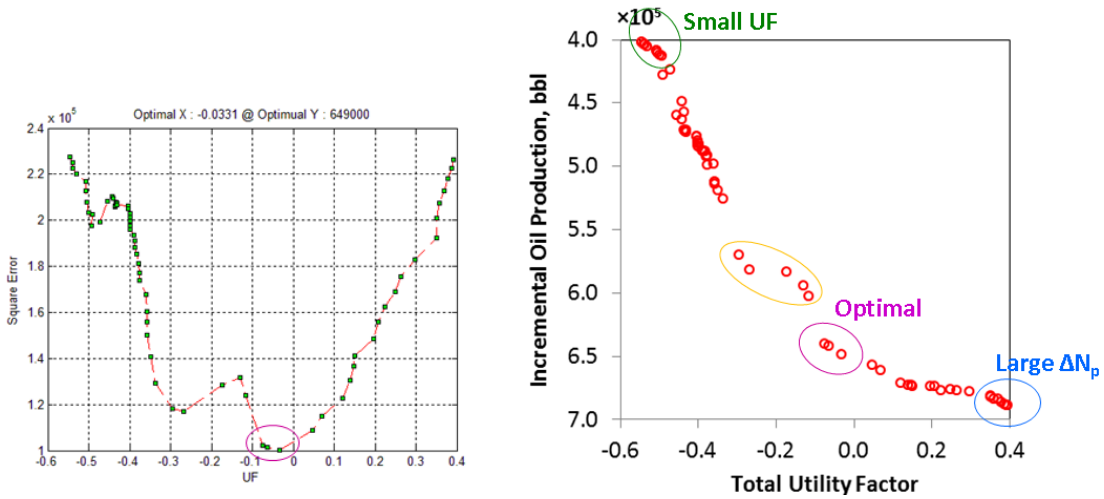

Fig. 4.12 Classification of Pareto front models

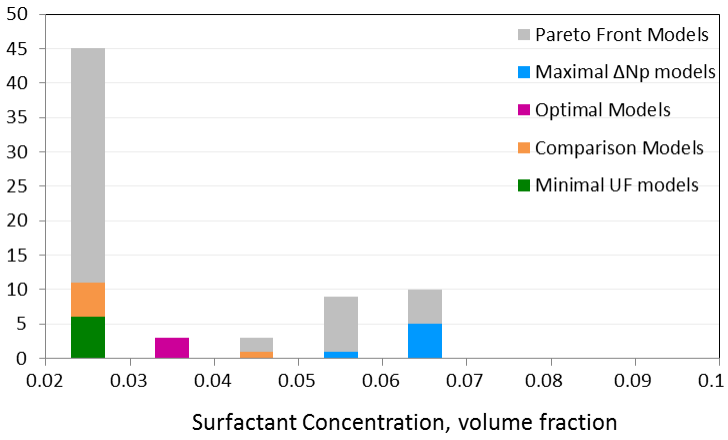

(a)

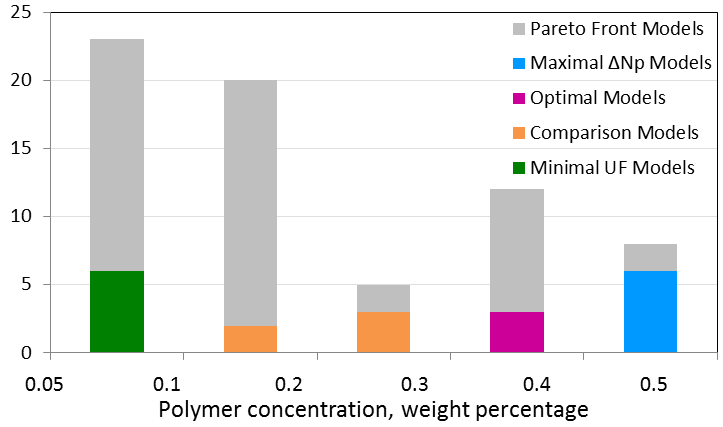

(b)

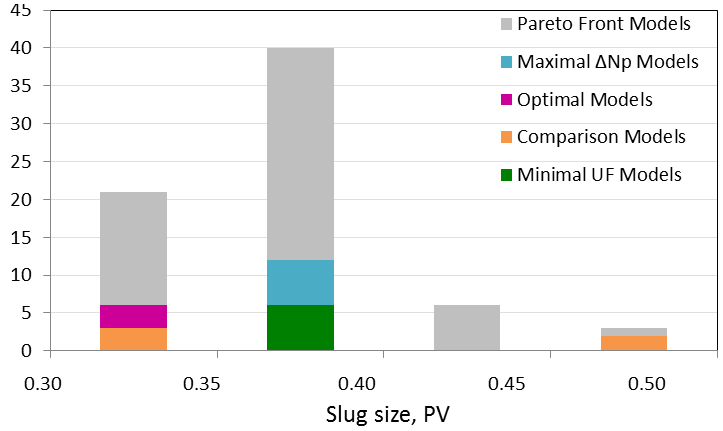

(c)

Fig. 4.13 Histogram of control variables.

(a) surfactant concentration, (b) polymer concentration, and (c) slug size

Table 4.7 Summary of control variable distribution

	C_{surf}	C_{poly}	Slug Size
Minimal UF models	0.02~0.03	0.05~0.1	0.35~0.40
Comparison models	scatter in between	scatter in between	scatter
Optimal models	0.03~0.04	0.3~0.4	0.30~0.35
Maximal ΔNp models	0.05~0.07	0.4~0.5	0.35~0.40

To examine the oil production and chemical usage under different groups of models, we compared the cumulative oil production, cumulative injected surfactant and cumulative injected polymer from chosen models: one with minimum utility factor, one with maximum incremental oil production, and one optimal model. From results in **Fig. 4.14**, we can see that, the model with maximum incremental oil production produces only 3% more oil than the optimal case; however, it requires 47% more surfactant and 61% more polymer than the optimal case. The model with minimum utility factor does require 44% less surfactant and polymer than the optimal case; however, it also produces 24% less oil.

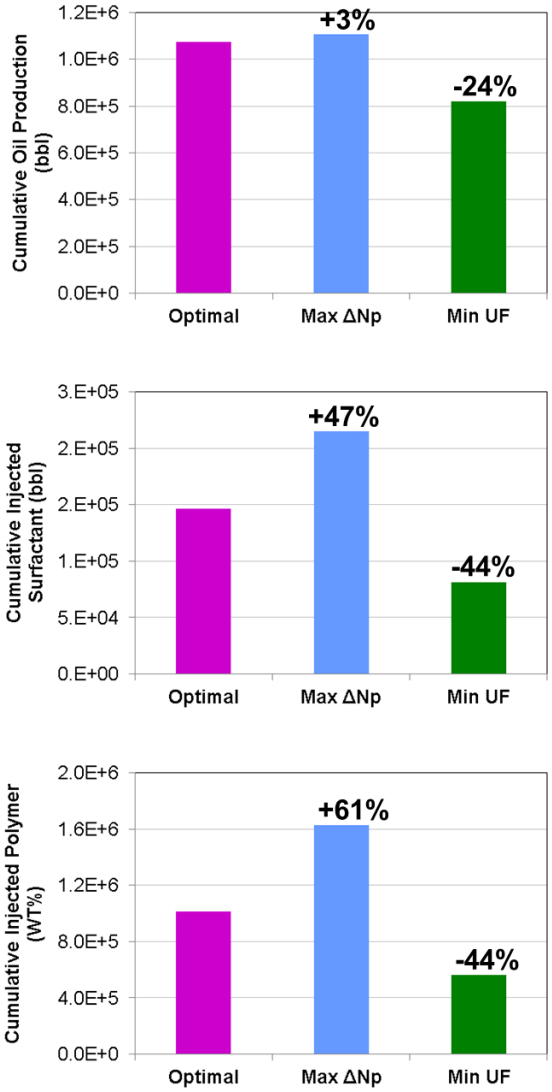

Fig. 4.14 Comparison between three cases

4.4 Summary and Conclusion

In this chapter, a Pareto-based optimization approach is presented to tackle multiple conflicting objectives in chemical flooding. Currently, most of the optimization applications in chemical flooding focus on the design of the formulation of chemical solution. Limited works have been done to optimize the injection process by numerical methods, such as sensitivity analysis, experimental design, and response surface, etc., in

which either oil recovery or chemical usage is considered. The goal of optimization in chemical flooding is to maximize oil recovery and minimize chemical usage at the same time, which makes it a multi-objective problem with conflicting objectives. To solve this problem, we introduced the concept of Pareto optimality to represent the trade-off relationship between conflicting objectives. The major findings are as follows:

- Traditional multi-objective optimization method has limitations when objectives are in different scales and have different units. It is also challenging to determine the appropriate weight for each objective.
- Non-dominated Sorting Genetic Algorithm (NSGA-II) is successfully used to search for multiple Pareto optimal solutions that can represent the trade-off relationship between conflicting objectives.
- For chemical flooding, parameters such as surfactant concentration, polymer concentration and slug size are usually optimized to maximize oil production and minimize chemical usage.
- The proposed approach showed its robustness and practical feasibility through the applications of ASP flooding in a synthetic pilot case and SP flooding in a mixed-wet dolomite reservoir. Application results show that slug size is a less sensitive variable compared with surfactant and polymer concentration.

CHAPTER V
CONCLUSIONS AND RECOMMENDATIONS

In this work, we have presented the applicability of stochastic methods for reservoir management in chemical EOR. The goal of reservoir management is to maximize oil and gas recovery, which is based on a thorough understanding of static properties and dynamic behavior of the field. History matching is the essential process to develop reliable reservoir model and integrate historical dynamic production data. Based on the reservoir model built from history matching, reservoir performance can be optimized by adjusting injection design.

First, we presented the workflow of history matching using Genetic Algorithm. to calibrate uncertain parameters associated with the dynamic history data. Objective function is defined as a weighted average of misfits between observed data and simulated values. Design of experiments is used to randomly sample key parameters identified from sensitivity analysis for initialization of model parameter of population. Then, response surface is used to construct proxy models, which can filter out models whose objective function is higher than a pre-defined threshold, and avoid unnecessary simulation. During history matching process, models are selected according to fitness, and populations are evolved by GA operators (crossover and mutation).

Next, we presented an approach to calibrate model in multiple stages that can efficiently reduce large amounts of uncertain parameters in alkaline-surfactant-polymer (ASP) flooding. Each stage of model calibration will follow a hierarchical order of field scale, and then individual well scale, with consideration of behaviors brought by ASP flooding, such as surfactant/polymer adsorption and phase behavior. The application in an ASP synthetic pilot case proves the robustness of the proposed approach. The comparison with single-stage history matching workflow showed that multi-stage history matching can deliver better history matching results and effectively reduce the uncertainty of large numbers of parameters.

We also extended the evolutionary workflows used in Chapter II-Chapter III for multi-objective optimization via introducing the concept of Pareto optimality. Pareto front method is proposed to handle conflicting objective functions such as oil production and chemical efficiency instead of traditional weighted sum method in optimizing ASP flooding. A field application demonstrated the improved workflow.

5.1 Conclusions

Some specific conclusions can be made from this work.

First, chemical flooding simulator UTCHEM is coupled with inverse modeling process for history matching and optimization. It can simulate multi-phase, multi-component compositional model, considering complex phase behavior, chemical and physical transformations in heterogeneous porous media. This work will largely generalize the model calibration workflow by incorporating UTCHEM as forward simulator.

Next, some conclusions about the proposed multi-stage history matching approach for chemical flooding are summarized in the following:

- Sensitivity study is crucial to identify key parameters and corresponding objective function for more global dominating level and for local subordinate level separately.
- Genetic Algorithm proved to be a powerful tool to find multiple solutions during history matching process. Chemical flood simulator UTCHEM is coupled as forward simulator to capture ASP mechanisms.
- According to the sensitivity analysis results, relative permeability endpoints and exponents are the heavy hitters to calibrate to match oil cut and chloride concentration history for the first stage of the workflow.
- In the second stage, adsorption parameters are adjusted to match surfactant concentration history and polymer concentration history from the producer. For the example cases, after two stages model calibration, the uncertainty has been

significantly reduced.

- A single-stage workflow is also applied to compare with the multi-stage workflow for history matching. Under single-stage workflow, all key parameters are calibrated together to match all objectives. The matching results are acceptable, however, the uncertainty of some parameters are not reduced as well as that under multi-stage workflow.

Some conclusions from the Pareto-based multi-objective optimization in chemical flooding are as follows:

- The goal of optimization in chemical flooding is to maximize oil recovery and minimize chemical usage at the same time, which makes it a multi-objective problem with conflicting objectives. To solve this problem, the concept of Pareto optimality is introduced to represent the trade-off relationship between conflicting objectives.
- Traditional multi-objective optimization method has limitations when objectives are in different scales and have different units. It is also challenging to determine the appropriate weight for each objective.
- Non-dominated Sorting Genetic Algorithm (NSGA-II) is successfully used to search for multiple Pareto optimal solutions that can represent the trade-off relationship between conflicting objectives.
- For chemical flooding, parameters such as surfactant concentration, polymer concentration and slug size are usually optimized to maximize oil production and minimize chemical usage.
- The proposed approach showed its robustness and practical feasibility through the applications of ASP flooding in a synthetic pilot case and SP flooding in a mixed-wet dolomite reservoir. To ultimately find a single optimum solution, additional criterion such as human preferences, economical factors are required.

5.2 Recommendations and Future Work

In our study, based on the specific problems in unconventional reservoirs and chemical EOR, genetic algorithm is used to establish workflows to accomplish model calibration and data integration in Chapter II and Chapter III. In Chapter IV, genetic algorithm is extended to search for Pareto optimal solutions. Some recommendations are made below for the implementation of genetic algorithm and future work:

- Genetic algorithm can take uncertainty of large amounts of reservoir parameters into account. Larger numbers of variables require larger population set for GA parameters. In addition, during the calibration, uniform crossover is used to introduce diversity to the population, the rate of which can be adjusted from 0.1% to 1% based on similarity of generated populations. The sensitivity of GA parameters on final results can be a meaningful area of future research.
- Genetic algorithm has been proved to be powerful to include all types of data to do history matching. However, the applications in chemical flooding shows that for better history matching results and calibration of the uncertain parameters, a better way is to analyze the influence levels of different data types first, and then integrate in multiple stages based on their levels of dominance hierarchy.
- Pareto-based evolutionary algorithm has been successfully applied to the optimization problem with few objectives (less than five). Larger number of objectives may cause problems such as increased dimension of Pareto front, unapparent Pareto front due to too much compromise among objectives, stagnation of search process, increased computational cost, etc. For optimization problem involving large numbers of objectives, special attention needs to be paid to satisfy these objectives at the same time and apply additional criterion to choose optimum solution.

REFERENCES

Abu-shiekah, I.M., Al-Kindi, Z.Y., and Douma, S.G. 2013. Full Field History Matching for Chemical Flooding with the Adjoint Method. Paper presented at the SPE Kuwait Oil and Gas Show and Conference, Kuwait City, Kuwait, 8-10 October.

Anderson, G.A., Delshad, M., Brown King, C.L. et al. 2006. Optimization of Chemical Flooding in a Mixed-Wet Dolomite Reservoir. Paper presented at the SPE/DOE Symposium on Improved Oil Recovery, Tulsa, Oklahoma, USA, 22-26 April.

Bazan, L.W., Larkin, S.D., Lattibeaudiere, M.G. et al. 2010. Improving Production in the Eagle Ford Shale with Fracture Modeling, Increased Fracture Conductivity, and Optimized Stage and Cluster Spacing Along the Horizontal Wellbore. Paper presented at the Tight Gas Completions Conference, San Antonio, Texas, USA, 2-3 November.

Bazin, B., Morvan, M., Douarche, F. et al. 2010. An Integrated Workflow for Chemical Eor Pilot Design. Paper presented at the SPE Improved Oil Recovery Symposium, Tulsa, Oklahoma, USA, 24-28 April.

Bhuyan, D., Lake, L.W., and Pope, G.A. 1990. Mathematical Modeling of High-Ph Chemical Flooding. *SPE Reservoir Engineering* **5** (02): 213-220.

Bissell, R., Killough, J.E., and Sharma, Y. 1992. Reservoir History Matching Using the Method of Gradients on a Workstation. Paper presented at the European Petroleum Computer Conference, Stavanger, Norway, 24-27 May.

Buijse, M.A., Prelicz, R.M., Barnes, J.R. et al. 2010. Application of Internal Olefin Sulfonates and Other Surfactants to Eor. Part 2: The Design and Execution of an Asp Field Test. Paper presented at the SPE Improved Oil Recovery Symposium, Tulsa, Oklahoma, USA, 24-28 April.

Cheng, H., Datta-Gupta, A., and He, Z. 2005. A Comparison of Travel-Time and Amplitude Matching for Field-Scale Production Data Integration: Sensitivity,

Non-Linearity and Practical Implications. Paper presented at the SPE Annual Technical Conference and Exhibition, Denver, Colorado, USA, 5-8 October.

Cheng, H., Dehghani, K., and Billiter, T.C. 2008. A Structured Approach for Probabilistic-Assisted History Matching Using Evolutionary Algorithms: Tengiz Field Applications. Paper presented at the SPE Annual Technical Conference and Exhibition, Denver, Colorado, USA, 21-24 September.

Cheng, H., Wen, X.-H., Milliken, W.J. et al. 2004. Field Experiences with Assisted and Automatic History Matching Using Streamline Models. Paper presented at the SPE Annual Technical Conference and Exhibition, Houston, Texas, USA, 26-29 September.

Cipolla, C.L. and Lolon, E. 2009a. Modeling Well Performance in Shale-Gas Reservoirs. Paper presented at the SPE/EAGE Reservoir Characterization and Simulation Conference, Abu Dhabi, UAE, 19-21 October.

Cipolla, C.L. and Lolon, E. 2009b. Reservoir Modeling and Production Evaluation in Shale-Gas Reservoirs. Paper presented at the International Petroleum Technology Conference, Doha, Qatar, 7-9 December.

Clark, S.R., Pitts, M.J., and Smith, S.M. 1993. Design and Application of an Alkaline-Surfactant-Polymer Recovery System to the West Kiehl Field. *SPE Advanced Technology Series* **1** (01): 172-179.

Dang, C.T.Q., Chen, Z., Nguyen, N.T.B. et al. 2011. Successful Story of Development and Optimization for Surfactant-Polymer Flooding in a Geologically Complex Reservoir. Paper presented at the SPE Enhanced Oil Recovery Conference, Kuala Lumpur, Malaysia, 19-21 July.

Datta-Gupta, A. 1985. Three Dimensional Simulation of Chemical Flooding. Master of Science, The University of Texas at Austin.

Datta-Gupta, A., Kulkarni, K.N., Yoon, S., Vasco, D.W. 2001. Streamlines, Ray Tracing and Production Tomography: Generalization to Compressible Flow. *Petroleum Geoscience* **7** (S): 75-86.

Delaplace, P., Delamaide, E., Roggero, F. et al. 2013. History Matching of a Successful Polymer Flood Pilot in the Pelican Lake Heavy Oil Field (Canada). Paper presented at the SPE Annual Technical Conference and Exhibition, New Orleans, Louisiana, USA, 30 September-2 October.

Delshad, M. 1990. Trapping of Micellar Fluids in Berea Sandstone. Doctor of Philosophy, The University of Texas at Austin.

Delshad, M., Bhuyan, D., Pope, G.A. et al. 1986. Effect of Capillary Number on the Residual Saturation of a Three-Phase Micellar Solution. Paper presented at the SPE Enhanced Oil Recovery Symposium, Tulsa, Oklahoma, USA, 20-23 April.

Delshad, M., Han, W., Pope, G.A. et al. 1998. Alkaline/Surfactant/Polymer Flood Predictions for the Karamay Oil Field. Paper presented at the SPE/DOE Improved Oil Recovery Symposium, Tulsa, Oklahoma, USA, 19-22 April.

Delshad, M., Pope, G.A., and Sepehrnoori, K. 1995. A Compositional Simulator for Modeling Surfactant Enhanced Aquifer Remediation, 1 Formulation. *Journal of Contaminant Hydrology* **23**: 303-327.

Demin, W., Jiecheng, C., Junzheng, W. et al. 1999. Summary of Asp Pilots in Daqing Oil Field. Paper presented at the SPE Asia Pacific Improved Oil Recovery Conference, Kuala Lumpur, Malaysia, 25-26 October.

Doscher, T.M. and Wise, F.A. 1976. Enhanced Crude Oil Recovery Potential-an Estimate. *Journal of Petroleum Technology* **28** (5): 575-585.

Duong, A.N. 2010. An Unconventional Rate Decline Approach for Tight and Fracture-Dominated Gas Wells. Paper presented at the Canadian Unconventional Resources and International Petroleum Conference, Calgary, Alberta, Canada, 19-21 October.

Fan, L., Martin, R.B., Thompson, J.W. et al. 2011. An Integrated Approach for Understanding Oil and Gas Reserves Potential in Eagle Ford Shale Formation. Paper presented at the Canadian Unconventional Resources Conference, Alberta, Canada, 15-17 November.

Fan, L., Thompson, J.W., and Robinson, J.R. 2010. Understanding Gas Production Mechanism and Effectiveness of Well Stimulation in the Haynesville Shale through Reservoir Simulation. Paper presented at the Canadian Unconventional Resources and International Petroleum Conference, Calgary, Alberta, Canada, 19-21 October.

Galassi, M., Davis, J., Theiler, J., Gough, B., Jungman, G. et al. 2009. *Gnu Scientific Library Reference Manual*: UK: Network Theory Ltd. . Original edition.

Gill, P.E., Murray, W., Wright, M.H. 1981. *Practical Optimization*: Academic Press. Original edition.

Hajizadeh, Y., Christie, M.A., and Demyanov, V. 2011. Towards Multiobjective History Matching: Faster Convergence and Uncertainty Quantification. Paper presented at the SPE Reservoir Simulation Symposium, The Woodlands, Texas, USA, 21-23 February.

Han, Y., Park, C., and Kang, J.M. 2010. Estimation of Future Production Performance Based on Multi-Objective History Matching in a Waterflooding Project. Paper presented at the SPE EUROPEC/EAGE Annual Conference and Exhibition, Barcelona, Spain, 14-17 June.

Hand, D.B. 1939. Dineric Distribution: I. The Distribution of a Consolute Liquid between Two Immiscible Liquies. *Journal of Physics and Chem.* **34**: 1961-2000.

Healy, R.N. and Reed, R.L. 1974. Physsicochemical Aspects of Microemulsion Flooding. *Society of Petroleum Engineers Journal* **14** (05): 491-501.

Henthorne, L., Pope, G.A., Weerasooriya, U. et al. 2014. Impact of Water Softening on Chemical Enhanced Oil Recovery Project Economics. Paper presented at the SPE Improved Oil Recovery Symposium, Tulsa, Oklahoma, USA, 12-16 April.

Hernandez, C., Chacon, L.J., Lorenzo, A. et al. 2001. Asp System Design for an Offshore Application in the La Salina Field, Lake Maracaibo. Paper presented at the SPE Latin American and Caribbean Petroleum Engineering Conference, Buenos Aires, Argentina, 25-28 March.

Hirasaki, G.J. 1981. Application of the Theory of Multicomponent, Multiphase Displacement to Three-Component, Two-Phase Surfactant Flooding. *Society of Petroleum Engineers Journal* **21** (02): 191-204.

Hohl, D., Jimenez, E., and Datta-Gupta, A. 2006. Field Experiences with History Matching an Offshore Turbiditic Reservoir Using Inverse Modeling. Paper presented at the SPE Annual Technical Conference and Exhibition, San Antonio, Texas, USA, 24-27 September.

Holland, J.H. 1992. Genetic Algorithms. *Scientific American* **267** (1): 44-50.

Horn, J., Nafpliotis, N. 1993. *Multiobjective Optimization Using the Niched Pareto Genetic Algorithm*: Illinois Genetic Algorithms Laboratory. Original edition.

Huh, C. 1979. Interfacial Tensions and Solubilizing Ability of a Microemulsion Phase That Coexists with Oil and Brine. *Journal of Colloid Interface Science* **71**: 408-426.

Jain, A.K., Dhawan, A.K., and Misra, T.R. 2012. Asp Flood Pilot in Jhalora (K-Iv), India - a Case Study. Paper presented at the SPE Oil and Gas India Conference and Exhibition, Mumbai, India, 28-30 March.

Jin, M. 1995. A Study of Nonaqueous Phase Liquid Characterization and Surfactant Remediation. Doctor of Philosophy, The University of Texas at Austin.

Johnson, N.L., Currie, S.M., Ilk, D. et al. 2009. A Simple Methodology for Direct Estimation of Gas-in-Place and Reserves Using Rate-Time Data. Paper presented at the SPE Rocky Mountain Petroleum Technology Conference, Denver, Colorado, USA, 14-16 April.

Karpan, V., Farajzadeh, R., Zarubinska, M. et al. 2011. Selecting the "Right" Asp Model by History Matching Coreflood Experiments. Paper presented at the SPE Enhanced Oil Recovery Conference, Kuala Lumpur, Malaysia, 19-21 July.

Kirkpatrick, S., Gelatt, C.D., Jr, Vecchi, M.P. 1983. Optimization by Simulated Annealing. *Science* **220** (4598): 671-680.

Levitt, D., Jackson, A., Heinson, C. et al. 2006. Identification and Evaluation of High-Performance Eor Surfactants. *SPE Reservoir Evaluation & Engineering* **12** (02): 243-253.

Lun, L., Dunn, P.A., Stern, D. et al. 2012. A Procedure for Integrating Geologic Concepts into History Matching. Paper presented at the SPE Annual Technical Conference and Exhibition, San Antonio, Texas, USA, 8-10 October.

Luo, P., Wu, Y., and Huang, S.-S.S. 2013. Optimized Surfactant-Polymer Flooding for Western Canadian Heavy Oils. Paper presented at the SPE Heavy Oil Conference-Canada, Calgary, Alberta, Canada, 11-13 June.

Ma, X., Al-Harbi, M., Datta-Gupta, A. et al. 2006. A Multistage Sampling Method for Rapid Quantification of Uncertainty in History Matching Geological Models. Paper presented at the SPE Annual Technical Conference and Exhibition, San Antonio, Texas, USA, 24-27 September.

Manrique, E., De Carvajal, G., Anselmi, L. et al. 2000. Alkali / Surfactant / Polymer at Vla 6/9/21 Field in Maracaibo Lake: Experimental Results and Pilot Project Design. Paper presented at the SPE/DOE Improved Oil Recovery Symposium, Tulsa, Oklahoma, USA, 3-5 April.

Mantilla, C.A. and Srinivasan, S. 2011. Feedback Control of Polymer Flooding Process Considering Geologic Uncertainty. Paper presented at the SPE Reservoir Simulation Symposium, The Woodlands, Texas, USA, 21-23 February.

McCormick, G.P., Tapia, R.A. 1972. The Gradient Projection Method under Mild Differentiability Conditions. *SLAM Journal on Control* **10** (1): 93-98.

Meyers, J.J., Pitts, M.J., and Wyatt, K. 1992. Alkaline-Surfactant-Polymer Flood of the West Kiehl, Minnelusa Unit. Paper presented at the SPE/DOE Enhanced Oil Recovery Symposium, Tulsa, Oklahoma, USA, 22-24 April.

Nelson, R.C. and Pope, G.A. 1978. Phase Relationships in Chemical Flooding. *Society of Petroleum Engineers Journal* **18** (05): 325-338.

Olsen, D.K., Hicks, M.D., Hurd, B.G. et al. 1990. Design of a Novel Flooding System for an Oil-Wet Central Texas Carbonate Reservoir. Paper presented at the

SPE/DOE Enhanced Oil Recovery Symposium, Tulsa, Oklahoma, USA, 22-25 April.

Orangi, A., Nagarajan, N.R., Honarpour, M.M. et al. 2011. Unconventional Shale Oil and Gas-Condensate Reservoir Production, Impact of Rock, Fluid, and Hydraulic Fractures. Paper presented at the SPE Hydraulic Fracturing Technology Conference, The Woodlands, Texas, USA, 24-26 January.

Ouenes, A. and Bhagavan, S. 1994. Application of Simulated Annealing and Other Global Optimization Methods to Reservoir Description: Myths and Realities. Paper presented at the SPE Annual Technical Conference and Exhibition, New Orleans, Louisiana, USA, 25-28 September.

Pan, Y. and Horne, R.N. 1998. Improved Methods for Multivariate Optimization of Field Development Scheduling and Well Placement Design. Paper presented at the SPE Annual Technical Conference and Exhibition, New Orleans, Louisiana, USA, 27-30 September.

Pandey, A., Suresh Kumar, M., Jha, M.K. et al. 2012. Chemical Eor Pilot in Mangala Field: Results of Initial Polymer Flood Phase. Paper presented at the SPE Improved Oil Recovery Symposium, Tulsa, Oklahoma, USA, 14-18 April.

Park, H.-Y. 2012. A Hierarchical Multiscale Approach to History Matching and Optimization for Reservoir Management in Mature Fields. Doctor of Philosophy, Texas A&M University.

Park, H.-Y., Datta-Gupta, A., and King, M.J. 2013. Handling Conflicting Multiple Objectives Using Pareto-Based Evolutionary Algorithm for History Matching of Reservoir Performance. Paper presented at the SPE Reservoir Simulation Symposium, The Woodlands, Texas, USA, 18-20 February.

Pope, G.A. and Nelson, R.C. 1978. A Chemical Flooding Compositional Simulator. *Society of Petroleum Engineers Journal* **18** (05): 339 - 354.

Prouvost, L., Pope, G.A., and Rouse, B. 1985. Microemulsion Phase Behavior: A Thermodynamic Modeling of the Phase Partitioning of Amphiphilic Species. *Society of Petroleum Engineers Journal* **25** (5): 693-703.

Qassab, H., Pavlas, M.K.R., Afaleg, N. et al. 2003. Streamline-Based Production Data Integration under Realistic Field Conditions: Experience in a Giant Middle-Eastern Reservoir. Paper presented at the SPE Annual Technical Conference and Exhibition, Denver, Colorado, USA, 5-8 October.

Rai, K., Johns, R.T., Lake, L.W. et al. 2009. Oil-Recovery Predictions for Surfactant Polymer Flooding. Paper presented at the SPE Annual Technical Conference and Exhibition, New Orleans, Louisiana, USA, 4-7 October.

Rey, A., Ballin, P.R., Vitalis, C.F. et al. 2009. Assisted History Matching in an Offshore Turbidite Reservoir with Active Reservoir Management. Paper presented at the SPE Annual Technical Conference and Exhibition, New Orleans, Louisiana, USA, 4-7 October.

Rubin, B. 2010. Accurate Simulation of Non Darcy Flow in Stimulated Fractured Shale Reservoirs. Paper presented at the SPE Western Regional Meeting, Anaheim, California, USA, 27-29 May.

Sambridge, M. and Mosegaard, K. 2002. Monto Carlo Methods in Geophysical Inverse Problems. *Reviews of Geophysics* **40** (3): 1009.

Scheidt, C. and Caers, J. 2009. Uncertainty Quantification in Reservoir Performance Using Distances and Kernel Methods--Application to a West Africa Deepwater Turbidite Reservoir. *Society of Petroleum Engineers Journal* **14** (04): 680-692.

Schulze-Riegert, R.W., Axmann, J.K., Haase, O. et al. 2002. Evolutionary Algorithms Applied to History Matching of Complex Reservoirs. *SPE Reservoir Evaluation & Engineering* **5** (02): 163-173.

Schulze-Riegert, R.W., Krosche, M., Fahimuddin, A. et al. 2007. Multi-Objective Optimization with Application to Model Validation and Uncertainty Quantification. Paper presented at the SPE Middle East Oil and Gas Show and Conference, Kingdom of Bahrain, 11-14 March.

Sheng, J.J. 2013. A Comprehensive Review of Alkaline-Surfactant-Polymer (Asp) Flooding. Paper presented at the SPE Western Regional & AAPG Pacific Section Meeting, Monterey, California, USA, 19-25 April.

Stoll, M., Al-Shureqi, H., Finol, J. et al. 2010. Alkaline-Surfactant-Polymer Flood: From the Laboratory to the Field. Paper presented at the SPE EOR Conference at Oil & Gas West Asia, Muscat, Oman, 11-13 April.

STREAMsim Technologies. 2012. Cluster Analysis by Metric Space Method. http://www.streamsim.com/technology/metric-space-methods-key-concepts.

Suzuki, S. and Caers, J.K. 2006. History Matching with an Uncertain Geological Scenario. Paper presented at the SPE Annual Technical Conference and Exhibition, San Antonio, Texas, USA, 24-27 September.

U.S. Energy Information Administration. 2011. Eagle Ford Shale Play, Western Gulf Basin, South Texas. http://www.eia.gov/oil_gas/rpd/shaleusa9.pdf.

U.S. Energy Information Administration. 2014. Crude Oil Price. http://www.eia.gov.

Valko, P.P. 2009. Assigning Value to Stimulation in the Barnett Shale: A Simultaneous Analysis of 7000 Plus Production Hystories and Well Completion Records. Paper presented at the SPE Hydraulic Fracturing Technology Conference, The Woodlands, Texas, USA, 19-21 January.

Vargo, J., Turner, J., Vergnani, B. et al. 1999. Alkaline-Surfactant-Polymer Flooding of the Cambridge Minnelusa Field. Paper presented at the SPE Rocky Mountain Regional Meeting, Gillette, Wyoming, USA, 15-18 May.

Wang, B., Lake, L.W., and Pope, G.A. 1981. Development and Application of a Streamline Micellar/Polymer Simulator. Paper presented at the SPE Annual Technical Conference and Exhibition, San Antonio, Texas, USA, 4-7 October.

Wang, J. and Liu, Y. 2011. Well Performance Modeling of Eagle Ford Shale Oil Reservoirs. Paper presented at the North American Unconventional Gas Conference and Exhibition, The Woodlands, Texas, USA, 14-16 June.

White, C.D. and Royer, S.A. 2003. Experimental Design as a Framework for Reservoir Studies. Paper presented at the SPE Reservoir Simulation Symposium, Houston, Texas, USA, 3-5 February.

Williams, G.J.J., Mansfield, M., MacDonald, D.G. et al. 2004. Top-Down Reservoir Modelling. Paper presented at the SPE Annual Technical Conference and Exhibition, Houston, Texas, USA, 26-29 September.

Williams, M.A., Keating, J.F., and Barghouty, M.F. 1998. The Stratigraphic Method: A Structured Approach to History Matching Complex Simulation Models. *SPE Reservoir Evaluation & Engineering* **1** (02): 169-176.

Winsor, P.A. 1954. Solvent Properties of Amphiphilic Compounds. *Angewandte Chemie* **68** (15): 504.

Wu, W., Vaskas, A., Delshad, M. et al. 1996. Design and Optimization of Low-Cost Chemical Flooding. Paper presented at the SPE/DOE Improved Oil Recovery Symposium, Tulsa, Oklahoma, USA, 21-24 April.

Yeten, B., Castellini, A., Guyaguler, B. et al. 2005. A Comparison Study on Experimental Design and Response Surface Methodologies. Paper presented at the SPE Reservoir Simulation Symposium, The Woodlands, Texas, USA, 31 January-2 Feburary.

Yeten, B., Durlofsky, L.J., and Aziz, K. 2002. Optimization of Nonconventional Well Type, Location and Trajectory. Paper presented at the SPE Annual Technical Conference and Exhibition, San Antonio, Texas, USA, 29 September-2 October.

Yilmaz, O., Nur, A., and Nolen-Hoeksema, R. 1991. *Pore Pressure Profiles in Fractured and Compliant Rooks*. Society of Petroleum Engineers.

Yin, J. 2011. A Hierarchical History Matching Method and Its Applications. Doctor of Phylosophy, Texas A&M University.

Yin, J., Park, H.-Y., Datta-Gupta, A. et al. 2010. A Hierarchical Streamline-Assisted History Matching Approach with Global and Local Parameter Updates. Paper presented at the SPE Western Regional Meeting, Anaheim, California, USA, 27-29 May.

Yin, J., Xie, J., Datta-Gupta, A. et al. 2011. Improved Characterization and Performance Assessment of Shale Gas Wells by Integrating Stimulated Reservoir Volume and

Production Data. Paper presented at the SPE Eastern Regional Meeting, Columbus, Ohio, USA, 17-19 August.

Zerpa, L.E., Queipo, N.V., Pintos, S. et al. 2004. An Optimization Methodology of Alkaline-Surfactant-Polymer Flooding Processes Using Field Scale Numerical Simulation and Multiple Surrogates. Paper presented at the SPE/DOE Symposium on Improved Oil Recovery, Tulsa, Oklahoma, USA, 17-21 April.

Zerpa, L.E., Queipo, N.V., Pintos, S. et al. 2007. An Efficient Response Surface Approach for the Optimization of Asp Flooding Processes: Asp Pilot Project Ll-03 Reservoir. Paper presented at the Latin American & Caribbean Petroleum Engineering Conference, Buenos Aires, Argentina, 15-18 April.

Zhang, J., Ravikiran, R., Freiberg, D. et al. 2012. Asp Formulation Design for Heavy Oil. Paper presented at the SPE Improved Oil Recovery Symposium, Tulsa, Oklahoma, USA, 14-18 April.

APPENDIX

UNCERTAINTY ANALYSIS AND ASSISTED HISTORY MATCHING WORKFLOW IN SHALE OIL RESERVOIRS*

For newly developed shale oil reservoirs, it is a challenging task to arrive at reasonable long-term production forecasts due to both large uncertainties associated with reservoir parameters and short production history. Assisted history matching plays an important role in integrating key uncertainties in order to arrive at a calibrated production prediction.

We present two workflows to utilize stochastic history matching method to a horizontal well in Eagle Ford shale oil reservoir. First, we discuss the impact of reservoir properties, hydraulic fractures, microfracs, phase behavior and rock characteristics on production behavior using sensitivity analysis. Next, we use the key uncertainties to calibrate the model against historical data using genetic algorithms. Three different geo-models were considered in all cases. However, in one workflow, they were evolved separately while in another one, they were evolved as a group. Production forecasting based on updated models from both workflows were categorized into several groups using cluster analysis. Then, the suggested workflows were compared according to their advantages and limitations. The results indicated that for workflow I, without providing accurate ranges of uncertainties, updated models for certain geo-model could not be found during evolution. For workflow II, reasonable probability must be provided; otherwise good model for certain geo-model may be ignored because the results are largely constrained by less-probable geo-models. For unconventional reservoirs with very short limited static and dynamic data, our proposed workflows are very flexible in

* Part of this chapter is reprinted with permission from "Uncertainty Analysis and Assisted History Matching Workflow in Shale Oil Reservoirs" by Zheng Zhang, M. Reza Fassihi, 2013. Paper 1581398 presented at SPE Unconventional Resources Technology Conference, Denver, USA, 12-14 Aug. Copyright 2013 by Unconventional Resources Technology Conference.

capturing key uncertainties and, thus, can be applied flexibly as an important tool for long-term production forecasting or for identifying key areas for further data acquisition.

A.1 Introduction

The Eagle Ford shale has become one of the most resourceful unconventional plays recently. The play extends from the Texas border with Mexico to the borders of Gonzales and Burleson Counties in the east and covers an area of approximately 11 million acres. **Fig. A.1** shows the Eagle Ford extension. This figure also shows three distinct maturation windows, gas, condensate and oil. Production data from different locations indicate different GOR patterns associated with these windows (U.S. Energy Information Administration 2011). Total organic carbon (TOC) in the Eagle Ford formation ranges from 1-7%. This formation is sandwiched between Buda limestone at the bottom and Austin chalk on top.

To efficiently and economically develop shale oil reservoirs, it is essential to be able to predict the range of expected recoveries based on different geology settings, completion strategies and operating parameters. However, uncertainties around shale rock and fluid characterization, mapping of fractured zones, behavior of rock and fluids under dynamic conditions and adequacy of conventional simulators for unconventional resource plays make this task difficult. Also, calibration of reservoir models by matching historical data has been effectively used for conventional reservoirs in order to arrive at ranges for production forecasting. However, the short duration of production at Eagle Ford makes the long-term forecasting a challenge.

In the past few years, many investigators have contributed to our current understanding of the impact of different parameters on reservoir response and well performance. Numerical simulation modeling is considered superior to the use of analytical or decline based methods for well modeling and reservoir forecasting (Cipolla and Lolon 2009a, 2009b; Fan et al. 2010; Rubin 2010). Bazan et al. (2010) used a first-order discrete fracture network (DFN) model to predict fracture geometry in the Eagle

Ford shale. Using the results of microseismic and fracture models along with production logging data, they history matched the production data from 2 wells in order to arrive at fracture and reservoir parameters. Wang and Liu (2011) used a simplified dual porosity simulation model to represent fractures. Their results were comparable to more rigorous fine-grid discrete fracture modeling method. They showed that natural fractures around hydraulic fractures had the biggest impact on well performance. Orangi et al. (2011) conducted a detailed compositional simulation of shale oil and gas condensate performance using a discrete fracture model. They observed that PVT and rock properties are very critical for unconventional reservoir performance prediction. Fan et al. (2011) used a dual-porosity model to simulate natural fractures in the Eagle Ford matrix. The latter was found to be the top production driver for horizontal wells.

To predict ultimate recoveries and propose development strategies, model calibration or history matching is one of the most common and effective ways. Previously history matching applications for the Eagle Ford Shale oil reservoirs (Bazan et al. 2010; Wang and Liu 2011) have been done by mainly adjusting fracture/completion parameters to match rates and bottom-hole pressure in a manual and deterministic way. Those deterministic methods usually result in a unique history-matched model and the uncertainty in geological parameters, rock/fluid behavior, etc. is not fully considered during the calibration. Global search techniques such as genetic algorithm have been known to be powerful to find multiple solutions. Also as a derivative-free method, genetic algorithm is effective for unconventional reservoirs in which uncertain parameters are highly coupled or the structure of the solution is not well understood. Cheng et al. (2008) established a workflow for probabilistic assisted history matching using genetic algorithm and demonstrated this workflow successfully in Tengiz field. Yin et al. (2011) used GA to calibrate static parameters such as fracture conductivity, fracture half length, matrix permeability and geo-mechanical /compaction parameters to match the dynamic data from shale gas wells. They included SRV as an additional constraint in their history matching effort in order to reduce uncertainty in other

reservoir parameters. Their results indicated that the permeability inside fracture and enhanced perm region and their compaction factors are key history matching parameters.

Besides the adjustment on various static parameters, many people have paid attention to the investigations of introducing geologic concepts during history matching recently. A single initial geological model may not be representative to start with for model calibration, and uncertainty that characterizes different geological scenarios should also be considered. Lun et al. (2012) evaluated the impact of uncertain geologic features on reservoir performance and obtained history-matched models by experimental design. Suzuki and Caers (2006) characterized each geological scenario by a training image, so that each geological realization can be stochastically generated using geo-statistical algorithms. History matching was then performed by stochastic search defining the parameter space using distance metric method. Their method provided a way to include reservoir structure as a parameter for history matching. Yin et al. (2010) proposed a global and local approach, in which they first calibrated parameters which quantified reservoir energy and flow in a global level, followed by local calibration to match well-by-well response.

In this part, we present two workflows, both of which can achieve three goals. First, key parameters for shale oil reservoirs are identified and calibrated to integrate dynamic production data. Second, multiple geological scenarios are introduced during model calibration. Third, the range of oil production in a long term is predicted based on updated models. These two workflows proposed work differently, and have their own advantages and requirements, which are illustrated by the application to a well in Eagle Ford reservoirs.

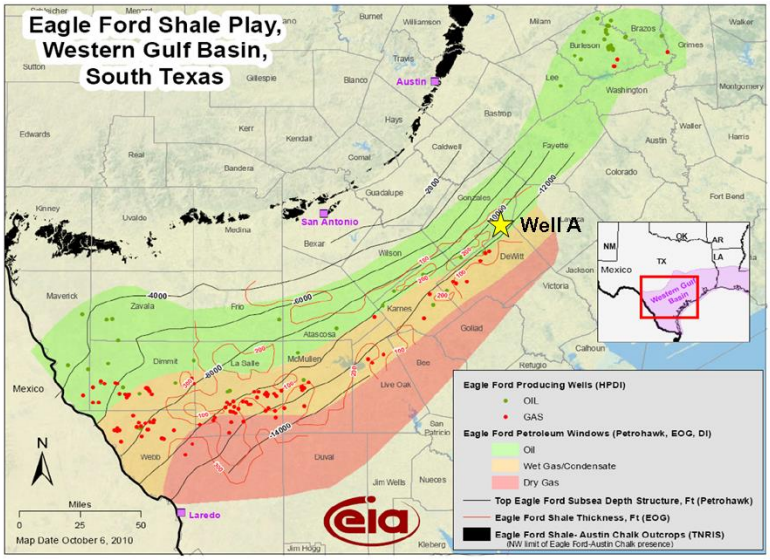

Fig. A.1 Eagle Ford map and the maturation windows (U.S. Energy Information Administration 2011)

A.2 Approach

Our goal here is to calibrate static parameters to integrate dynamic data, especially for unconventional reservoirs with limited static data and short dynamic data, and preserve geological realism at the same time, so that reliable long-term production can be forecast based on updated models. Two workflows are proposed to realize this goal.

In general, a set of geological scenarios are chosen considering different geological features. In our study, the reservoir properties that represent each geo-model are called realization parameters ($\boldsymbol{R_1}$, $\boldsymbol{R_2}$, …, $\boldsymbol{R_n}$). There are also many reservoir uncertainties that can affect reservoir response and well performance. The most influential uncertainties should first be identified via sensitivity analysis, and then calibrated during history matching, which we call experimental uncertainties ($\boldsymbol{E}$).

A.2.1 History Matching Methodology

In our study, experimental design and response surface methodologies with evolutionary algorithm are used to calibrate parameters and history match production data. The flow chart for assisted history matching using proxy and Genetic Algorithm (GA) is similar to the one used by Yin (2011) and is illustrated in **Fig. A.2**. A set of key parameters are selected by sensitivity analysis. The objective functions with respect to selected key parameters are used to generate a response surface proxy using experimental design and response surface methodology. The proxy model is constructed to filter the model whose objective function is higher than unacceptable threshold without running the actual simulation. The evolution is initialized from a set of randomly generated potential individuals. In each generation, the objective function of each individual in the population is evaluated with proxy check. Individuals are randomly selected from current population and modified via GA operators (selection, crossover, mutation) to generate a new population for next iteration. The iteration stops when the maximum number of generations has been reached or satisfactory solution has been achieved.

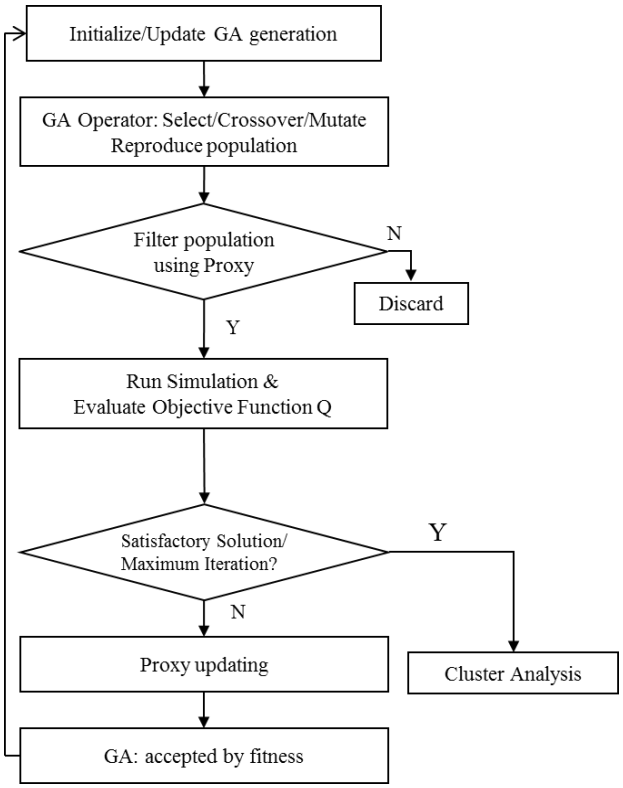

Fig. A.2 Flow chart for assisted history matching using proxy check and Genetic Algorithms (Yin 2011)

A.2.2 Cluster Analysis using Metric Space Method and Visualization by Multi-Dimensional Scaling (MDS)

Updated models are classified into discrete groups based on similarity of models, so that we can compare model properties between clusters and select models based on cluster. In our study we use metric space method to carry out cluster analysis. In metric space, a dissimilarity distance function is defined to measure the dissimilarity between pairs of reservoir models (**Fig. A.3 (a)**). The distance measures over all model pairs can form a distance matrix (**Fig. A.3 (b)**). To visualize this, we use multi-dimensional scaling (MDS), which can take the distance matrix, and translate the models into points in a

Euclidean space (Scheidt and Caers 2009). Therefore, in **Fig. A.3 (c)**, each point stands for a single reservoir model, and distance between two points is called similarity distance. Models close to each other are similar; models far from each other are dissimilar.

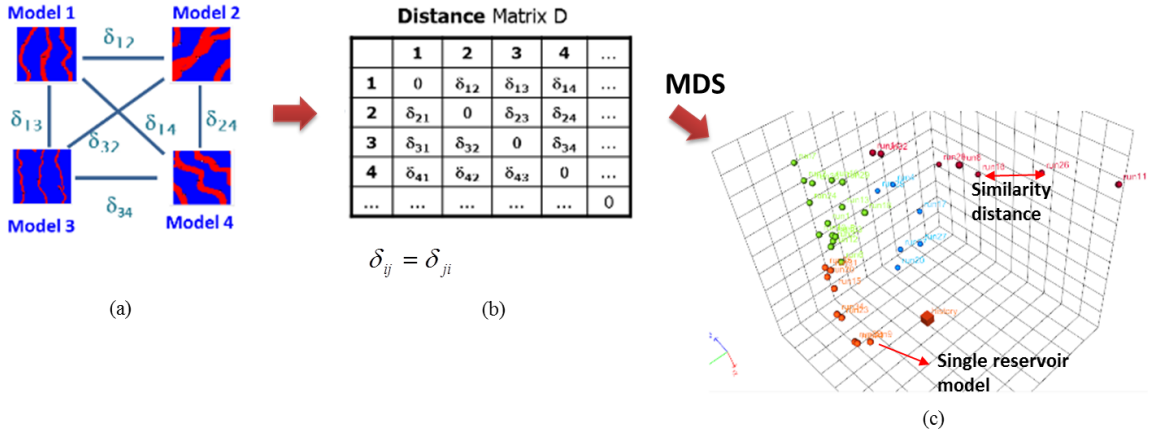

Fig. A.3 Cluster model similarity using metric space and visualize in MDS plot (STREAMsim Technologies 2012)

Above methodology is primarily used in our proposed workflows to perform assisted history matching and cluster analysis. In the following paragraphs, we will illustrate how to consider geological realism during data integration in different ways in two workflows.

A.2.3 Workflow I

Workflow I is demonstrated by the flow chart in **Fig. A.4**. Realization parameters are given a range as a superset covering realization parameters that represent each geo-model. Then realization parameters are calibrated together with experimental uncertainties from sensitivity analysis to go through assisted history matching. Since realization parameters are evolved during history matching, each geological scenario is

considered equally. Updated models are grouped and screened by cluster analysis based on model similarity, so that representative model for each geo-model can be selected for further production forecasting.

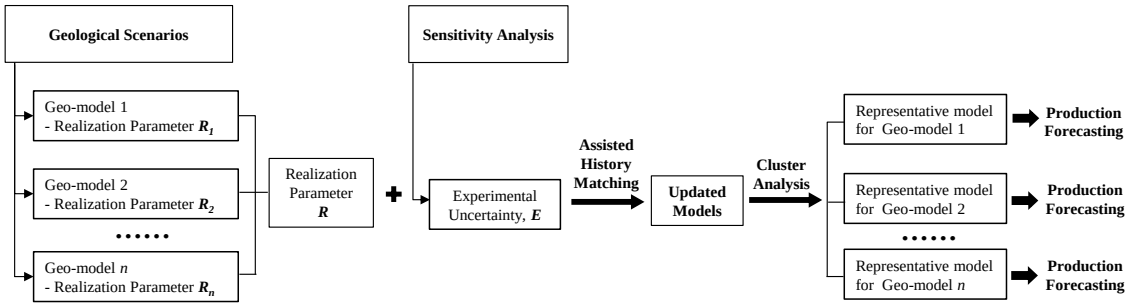

Fig. A.4 Flow chart of Workflow I

A.2.4 Workflow II

Fig. A.5 shows the flow chart of Workflow II. Each geological scenario is assigned with probability (W_1, W_2, …, W_n). Realization parameters for each geo-model will remain constant and only experimental uncertainty is evolved during data integration. Unlike Workflow I, under every generated potential solution (E_i), there will be n simulation runs with respect to n geo-models, which yield n sub-objective functions. The total objective function for current individual is evaluated by the weighted-average of sub-objective functions with the probability of each geo-model applied. Each updated model consists of n sub-models associated with geo-models. Therefore, cluster analysis and production forecasting will be performed for each geo-model separately.

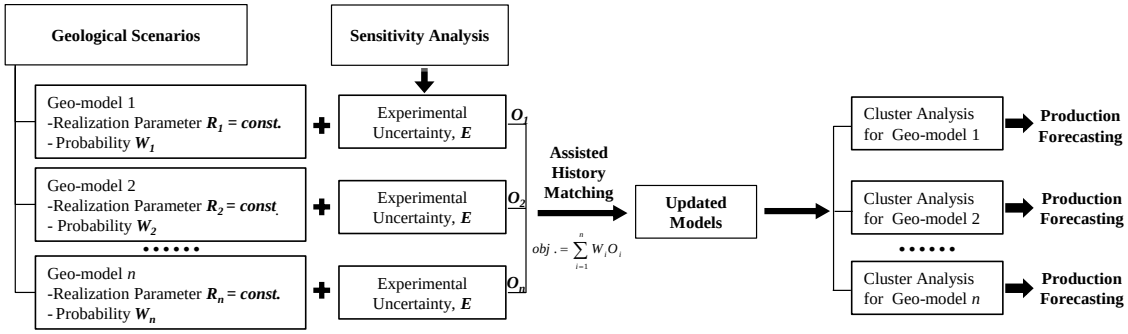

Fig.A.5 Flow chart of Workflow II

In next section, we will illustrate the two workflows with a real field case. The outline of this field application is as follows. First, the field background and simulation model is described. Next sensitivity analysis is used to study how certain uncertainties affect reservoir response and well performance, especially for shale oil reservoirs, and eventually identify key parameters. Then two workflows are applied to perform assisted history matching, followed by the comparison and discussion about two proposed workflows.

A.3 Field Application

A.3.1 Field Background

We chose well A in the Blackhawk area of the Eagle Ford for this study (**Fig. A.1**). The average permeability and porosity of the shale matrix were estimated at 500 nD and 9% respectively. Well A produces volatile oil with a GOR of approximately 3000 scf/stb. This is a "near-critical" fluid with significant changes in its properties such as viscosity, density and molar composition as it is produced.

The area around well A is over-pressured with a pressure/depth gradient of about 0.85 psia/ft. The initial reservoir pressure (10910 psia) is significantly higher than the bubble point pressure (4280 psia). It is expected that the reservoir pressure outside of the

stimulated rock volume will remain above the saturation point for most of the production life of the field. However, 2-phase flow is expected near fractures once the bottom-hole pressure goes below the saturation pressure. The historical production data (condensate and gas rates, flowing bottom-hole pressure) are presented in **Fig. A.6**.

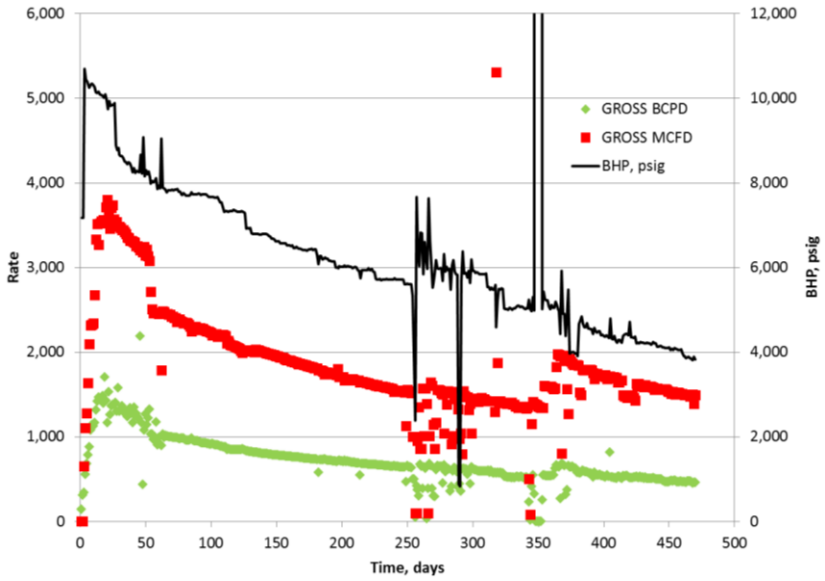

Fig. A.6: Historical Production data in Well A

Prior to carrying out any simulation, some diagnostic plots were generated in order to assess the importance of different flow regimes in the early phases of well production. An example of pressure-normalized rate (or productivity index) is shown in **Fig. A.7**. The corresponding ½ slope and unity slope lines are also shown on this graph. These data were used to arrive at approximate fracture half length. Notice that the deviation from linear flow occurs around 100 days. However, the compaction effect on shale permeability and fracture conductivity is expected to impact both the shape and the duration of these flow regimes.

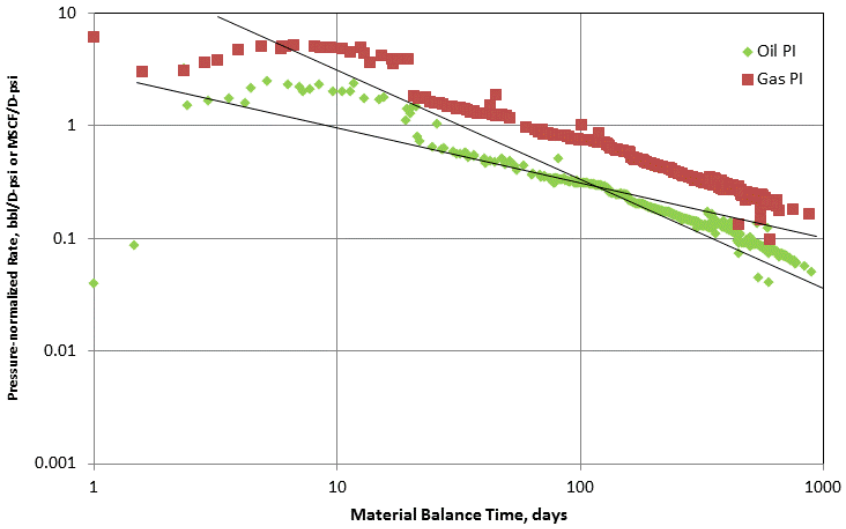

Fig. A.7 Diagnostic Plot for Well A

A.3.2 Decline Curve Analysis

Different decline curve analysis (DCA) methods have been proposed for forecasting production from shale reservoirs. These methods are generally based on correlations and do not have sound physical basis. However, their usage is widespread in the petroleum industry. We used the following DCA methods to do a quick forecast of the production before applying our physics-based numerical model.

- Power-Law Exponential (Johnson et al. 2009)
- Duong (Duong 2010)
- Stretched Exponential Production Decline (Valko 2009)
- Hyperbolic

The forecast oil production using the above-mentioned methods is shown in **Fig. A.8**. The estimated ultimate Recovery (EUR) in 30 years varied from 0.953 MMSTB (Power) to 2.3 MMSTB (Duong).

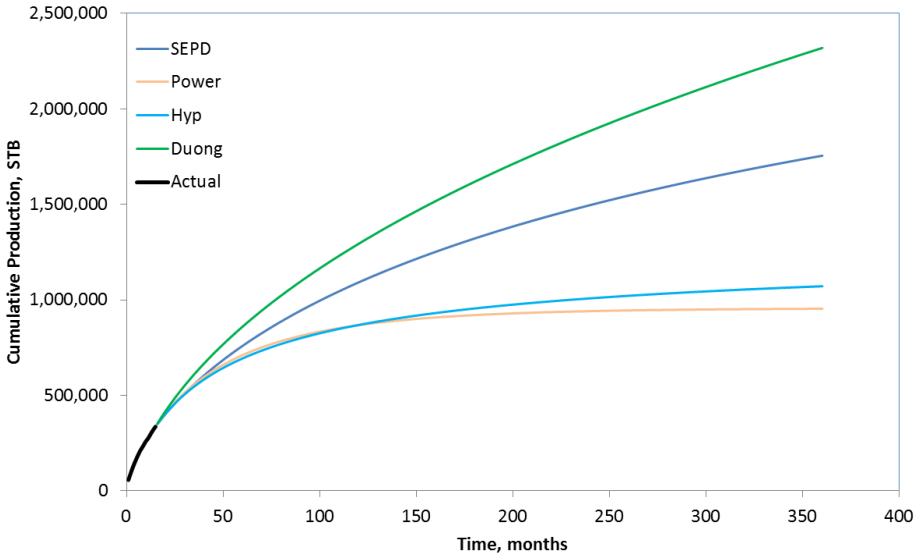

Fig. A.8 Production forecasting using DCA methods

A.3.3 Simulation Model Description

Well A is simulated using a single porosity - single permeability, compositional model. The reservoir model is 6667 ft long × 586 ft wide × 212 ft thick. This well covers 6268 ft in the lateral direction, and had undergone 19 fracture stages with 6 fracture clusters and 3 fractures per stage. We assumed equally spaced 57 hydraulic fractures perpendicular to the well orientation, as shown in **Fig. A.9(a)** and **(b)**. Fracture half-length and conductivity were estimated at 102 ft and 30 md-ft respectively.

There are totally 21780 grid cells in the model, with logarithmic local refined grids around each fracture, to better simulate the pressure and saturation changes around and between fractures. The dimension of coarse grids is 242×15×6, with wellbore on Layer 4. The dimension of refined grids for each fracture is 9×70×6. The middle refined grid represents the fracture as 219 ft long, 1 ft wide and 212 ft thick, so each fracture penetrates the whole pay thickness.

Matrix porosity and permeability are homogeneous within each layer. Fracture porosity is the same as matrix porosity in the base model. An enhanced permeability

region is introduced with 14 ft wide on each side of fractures with a permeability enhancement of 100 times rock permeability to represent natural fracture network and induced permeability enhancement around fractures. This model also considers rock compaction using transmissibility multipliers on both matrix and fracture during reservoir depletion. **Table A.1** lists some of the reservoir parameters used in the simulation model.

To reduce the run time, we used a symmetry element for a single fracture as shown in **Fig. 9(c)**. This resulted in reducing the simulation time from 3 hours for the whole model to only 15 minutes. The error introduced to cumulative oil production over 30 years was only 5.23% (mostly due to flow from matrix to wellbore directly).

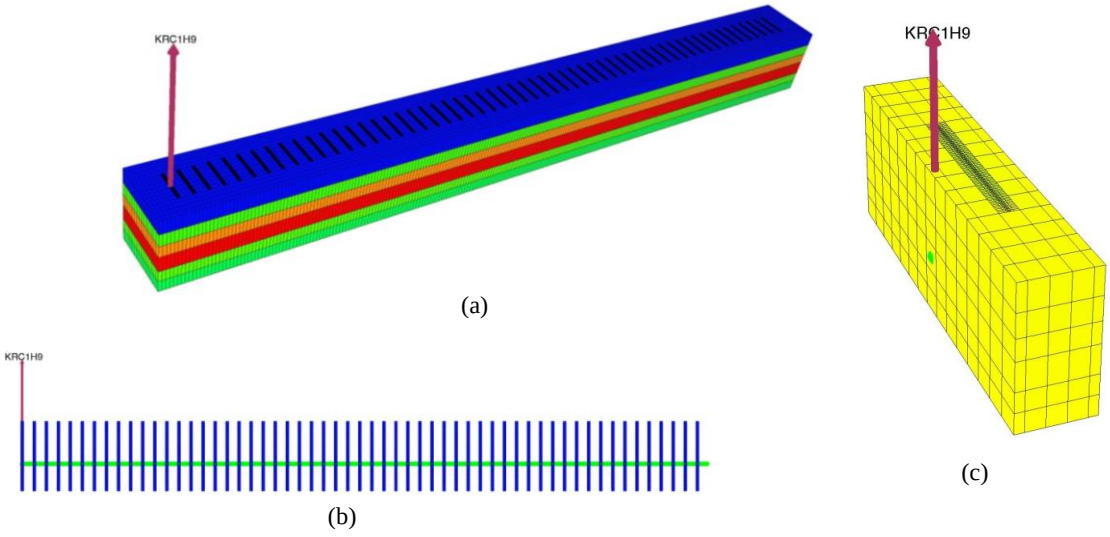

Fig. A.9 Simulation model description.

(a) Schematic diagram of simulation model, (b) Hydraulic fractures, and (c) Symmetry element model extracted from original model.

Table A.1 Reservoir parameters used in the model

Model area, acres	89	Bubble point pressure, psi	4242
Initial reservoir pressure, psia	10810	S_{wi}	0.13
Reservoir temperature, °F	316	S_{or}	0.25
Datum, ft	12745	S_{gc}	0.17
Gradient, psi/ft	0.85		

A.4 Sensitivity Analysis

To evaluate how various parameters affect reservoir response and well production performance, especially in shale oil reservoirs, sensitivity analysis was performed on selected 15 parameters including reservoir properties, hydraulic fractures, microfractures, phase behavior and rock characteristics. The uncertainty range for each parameter is shown in Table 3. The simulation was carried out for one year history (oil rate control), followed by 30 years prediction (oil rate control with 1300 psi BHP control as lower limit). The impact of some of the key variables on reservoir response is discussed in details below.

A.4.1 Matrix Permeability

Fig. A.10 presents the relationship between matrix permeability and porosity for Eagle Ford. Based on the average porosity in our model (9%), the range for matrix permeability is between 10 nD - 1000 nD. In the base case, the average matrix permeability is 550 nD. **Fig. A.11** shows the simulation results for these 3 cases. A low matrix permeability of 10 nD seems to be too low to provide a flow rate similar to the historical rate.

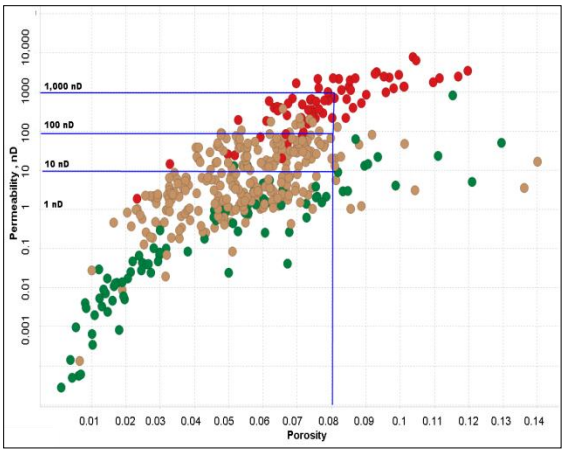

Fig. A.10 Relationship between k_m and porosity

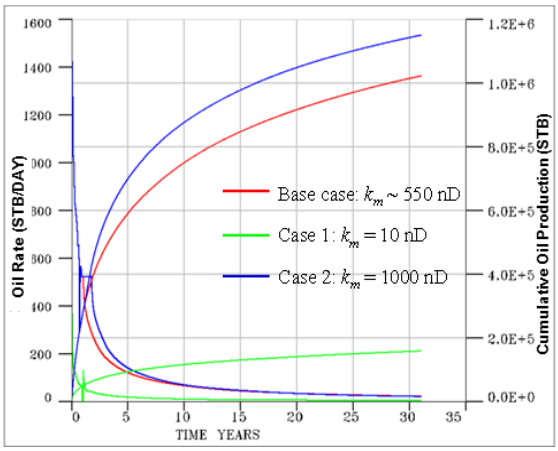

Fig. A.11 Oil rate and cum. oil production under different k_m

A.4.2 Permeability Change with Pressure and Rock Compaction

In the simulation model, rock compaction is modeled through reduction of permeability with depletion. In the base model, compaction was applied to both matrix and fracture. For sensitivity runs, matrix only compaction and fracture only compaction were also modeled. We followed Yilmaz et al. (1991) approach to account for permeability and

transmissibility reduction with pressure using a variable γ in the following equation (**Eq. A.1**):

$$k/k_i = e^{(\gamma(P-P_i))} \quad \text{.....(A.1)}$$

In our modeling, γ varied from 2E-4 to 7E-4 with the base case at 4E-4. **Fig. A.12** shows that for the high γ of 7E-4, oil rate dropped quickly due to low permeability at higher depletion.

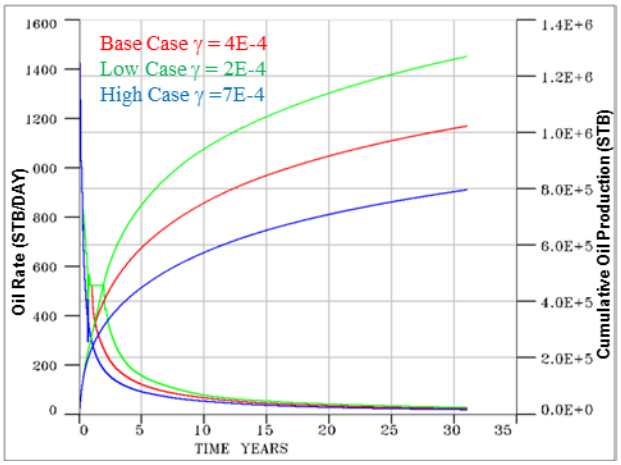

Fig. A.12 Oil rate and cum. oil production under different exponents in trans. vs. pressure

Fig. A.13-15 show pressure distribution, gas saturation buildup and condensate saturation buildup under each case vs. distance away from the fracture. When rock compaction is only applied on matrix, matrix permeability drops as pressure decreases, and fracture permeability remains the same. So the gas and condensate saturation builds up more quickly near fractures compared with the base case. Contrarily, when rock compaction is only applied on fracture, fracture permeability drops with pressure, and matrix permeability keeps the same. So the gas and condensate saturation would build up more quickly in the region away from fractures, compared to the base case.

Fig. A.16 shows the well production performance under different cases. Compaction only on fracture would deliver much higher oil rate, because permeability reduction on originally high fracture permeability would not have too much impact on the flow through fracture. However, permeability reduction on matrix permeability of 550 nD would largely restrict the flow from matrix. The case with no compaction delivers the highest oil rate after the reservoir average pressure drops below bubble point pressure. These results indicate the significant role of compaction in shale resource plays.

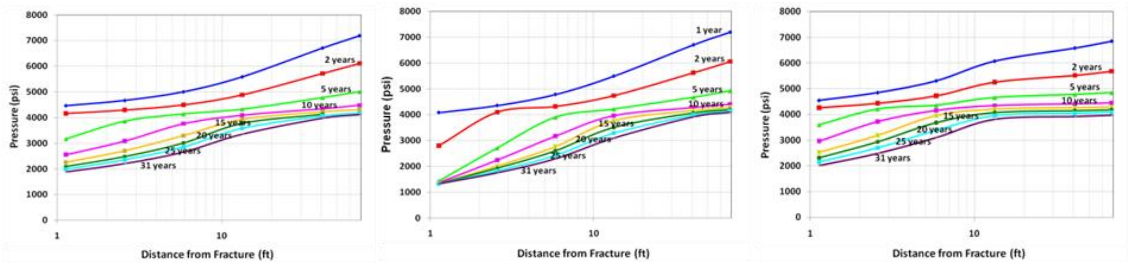

Fig. A.13 Pressure distribution vs. distance from fracture under three cases

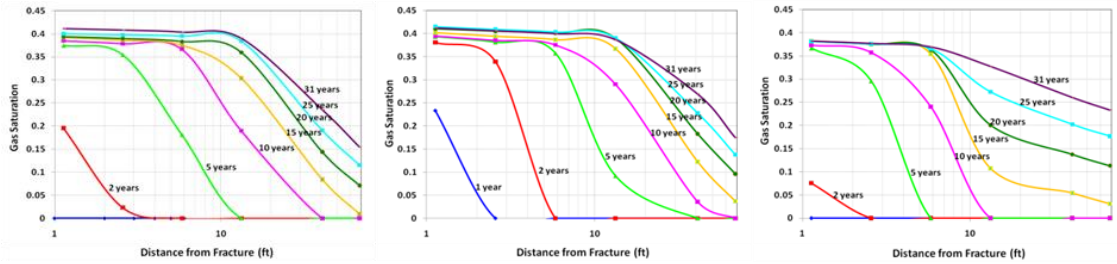

Fig. A.14 Gas saturation buildup vs. distance from fracture under three cases

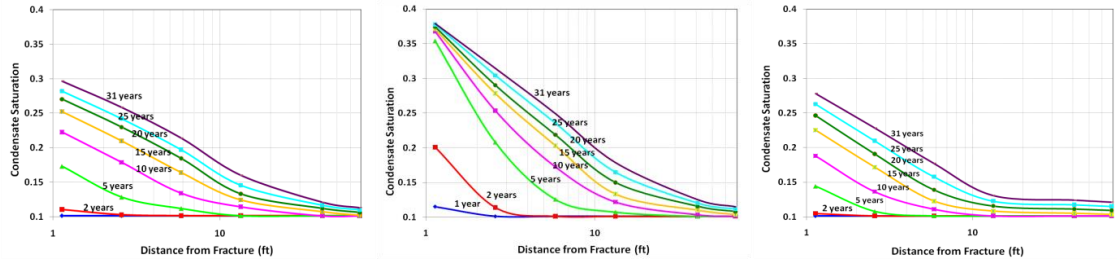

Fig. A.15 Condensate saturation buildup vs. distance from fracture under three cases

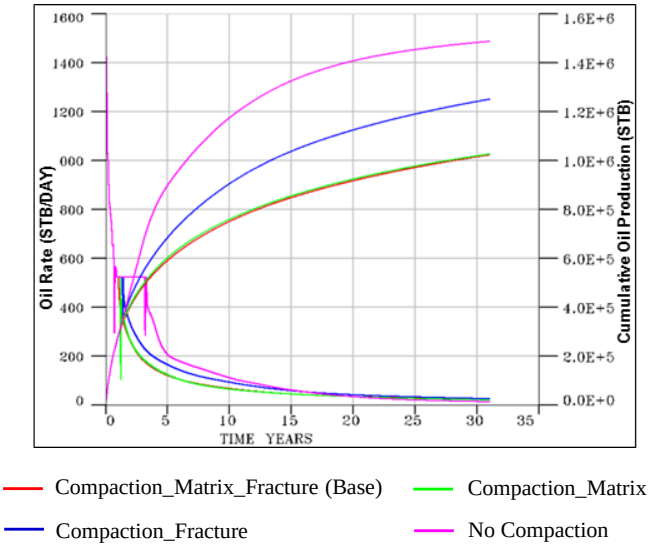

Fig. A.16 Oil rate and cumulative oil production under different rock compaction cases

A.4.3 Matrix Relative Permeability

There is not enough information about relative permeability in the literature for shale resources. We used General Corey's model and varied the coefficients and exponents in order to do a sensitivity check on relative permeability curves. **Table A.2** lists the parameters used for water-oil and gas-oil relative permeability curves.

Table A.2 Corey exponents used in sensitivity cases for matrix relative permeability

	n_o	n_w	n_g	n_{og}
Base case	3	4	4.5	3
Lower limit	0.25	0.25	0.25	0.25
Upper limit	5	5	5	5

Fig. A.17 presents the simulation results in different cases. Use of a Corey exponent of 0.25 is an extreme case for relative permeability. In this case, smaller changes in gas saturation cause larger change in gas relative permeability.

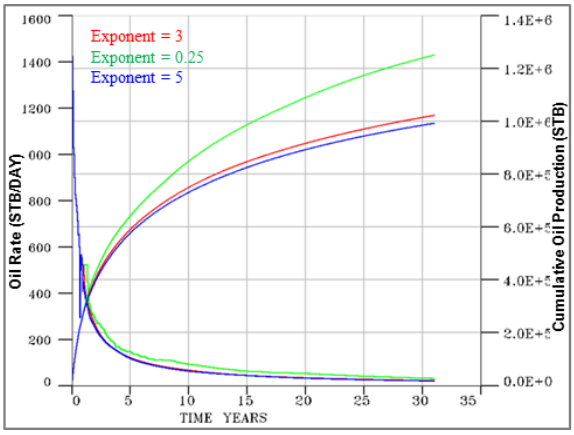

Fig. A.17 Oil rate and cumulative oil production for different matrix relative permeability curves

A.4.4 Enhanced Permeability Area (EPA)

As was mentioned in the introduction, one way of simulating the presence of natural fractures or artificially induced microfractures in the disturbed zone around hydraulic fractures is to increase the matrix permeability around planar fractures. We carried out a sensitivity run with and without the Enhanced Permeability Areas (EPA). Different half width of EPA is also considered during the sensitivity run. The permeability within EPA was increased by a factor of 100. Two cases of short (7 ft) and wide (14 ft) EPA were simulated. The production profiles under different cases are shown in **Fig. A.19**.

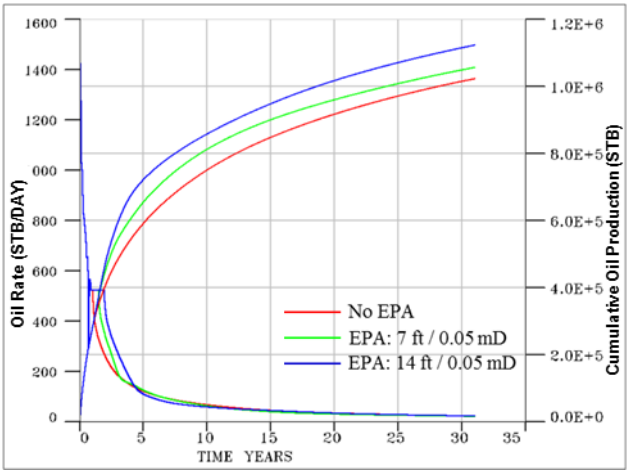

Fig. A.19 Oil production rate and cumulative oil production with or without EPA

A.4.5 Tornado Chart

Table A.3 summarizes the ranges in all 15 sensitivity parameters. The relative importance of each parameter on cumulative oil production or the bottom-hole pressure after 30 years of prediction is shown in **Fig. A.20**. It can be seen that matrix permeability, matrix relative permeability, fracture length, rock compaction and EPA have major impact on cumulative oil production and BHP.

Table A.3 Sensitivity parameters and their ranges

Uncertainty	Base	Low value	High value
Matrix permeability	~550 nD	10 nD	1000 nD
Fracture length	219 ft	117 ft	430 ft
Trans_multiplier vs. pressure	4E-4	2E-4	7E-4
Matrix porosity	~9.25%	7%	11%
Matrix relative perm.	~3	0.25	5
Rock compaction	Matrix & frac.	Matrix	Fracture
Phase behavior	High IFT	low IFT	High IFT
Enhanced perm. area	No EPA	14 ft as half width	7 ft as half width
S_{wi}	0.1265	0.1265	0.25
Compressibility	0	0	7 msip
Fracture permeability	30 mD	3 mD	300 mD
S_{or}	0.25	0.13	0.25
Fracture relative perm.	= matrix	Linear, 0~1	Linear, 0~0.1
Fracture porosity	= matrix	28.5%	33.3%
k_v / k_h	0.1	0	1

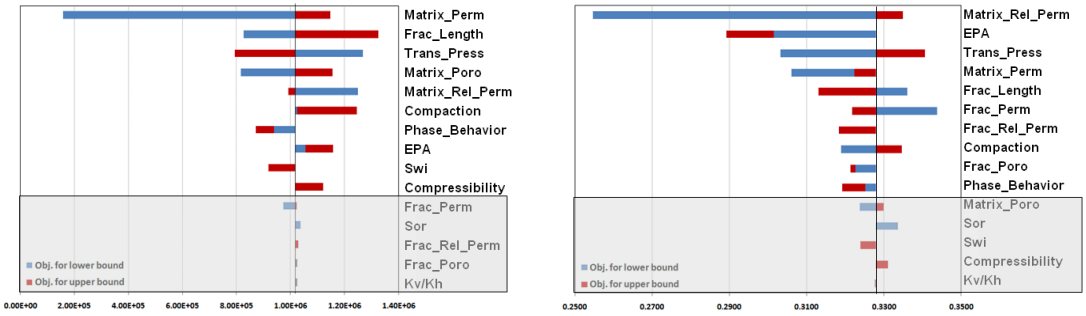

(a) (b)

Fig. A.20 (a) Impact of uncertainties on cum. oil production in 30 years, (b) Impact of uncertainties on bottom-hole pressure of 1 year history

A.5 History Matching and Production Forecasting Workflow Illustrated by Field Application

In this section we will illustrate the assisted history matching and production forecasting workflows applied to Well A. This includes building scenarios for geo-models followed by model calibration through assisted history matching using experimental design and genetic algorithm. Commercial simulators were used for assisted history matching and cluster analysis. The updated dynamic models were used for production forecasting.

A.5.1 Scenarios for Geo-model

Using the well logs for different wells in this area, three geological models can be built with different probability of occurrence. These are: a) blocky chalk, b) interbedded shale and c) marl carbonate. A typical log is presented in **Fig. A.21**. Reservoir properties and their ranges of each geo-model were estimated using our best available resources. Since these global reservoir properties were calibrated differently in our two proposed workflows to preserve geological realism, we call them realization parameters in our study.

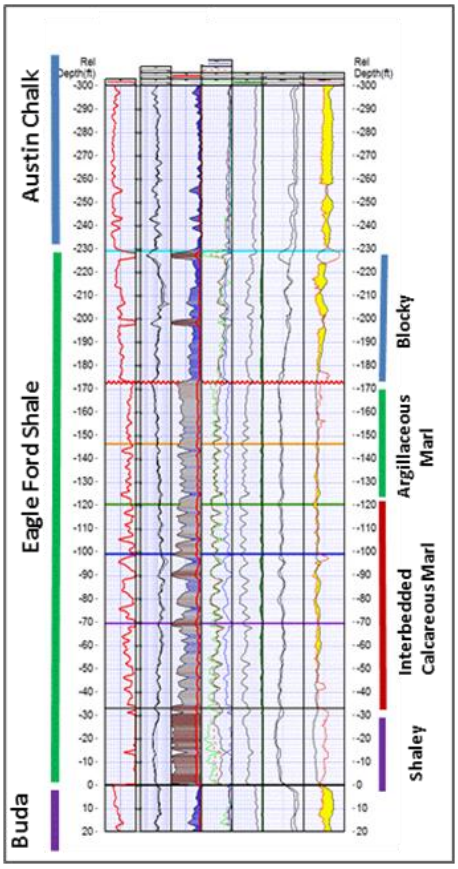

Fig. A.21 Geo-models selected in this area

- **Assisted history matching.** Realization parameters are evolved together with experimental uncertainties during history matching, and each geo-model is considered with same probability. The objective function is evaluated by single individual. **Fig. A.22** shows 40 good matches among all 140 experiments.

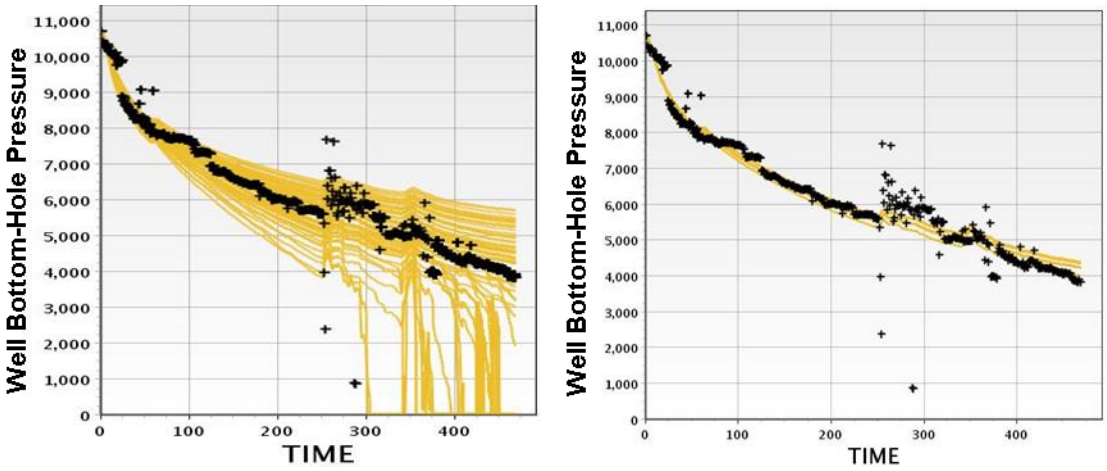

(a) (b)

Fig. A.22 (a) All 140 experiments from history matching, (b) 40 good matches selected from 140 experiments

A.5.2 Workflow I

In workflow I, geological uncertainties that represent three scenarios and key reservoir parameters from sensitivity analysis are calibrated together to update dynamic models, among which three updated models are selected by cluster analysis to be the representatives with respect to three geological scenarios. Production forecasting based on those three representative updated models will be performed afterwards.

- **Parameter selection.** In workflow I, porosity and initial water saturation are considered to be realization parameters. The ranges of realization uncertainty are given as a superset of those from three scenarios. Experiment parameters are the heavy-hitters from sensitivity analysis. The parameters and their ranges used in history matching process are listed in **Table A.4**.

Table A.4 Uncertainty ranges for Workflow I

	Uncertainty	Base	Min	Max
Geological Uncertainty	Porosity	11%	8%	14%
	Initial water saturation	0.13	0.13	0.25
Key Reservoir Parameter	PERMX in layer 4	1E-4 mD	1E-5 mD	1E-3 mD
	PERMX in other 5 layers	1E-4 mD	1E-5 mD	1E-3 mD
	Enhanced perm multiplier on k_m	100	1	1000
	Exponent in trans. vs. pressure	4E-4	0	7E-4
	Phase behavior	High	Low	High
	Exponent in SWOF, SGOF	3	0.25	5
	Exponent in compressibility vs. pressure	0	0	5E-6

- **Cluster analysis.** Based on 40 good updated models, we run cluster analysis to group models with similar sets of parameters using metric space method, and visualize the model similarity in MDS plot. Updated models are differentiated into three clusters (**Fig. A.23**) and select one model from each cluster, as shown in **Fig. A.24**. These three chosen models should also represent three different geo-models by the porosity and initial water saturation in three models fitting with our chosen scenarios: model 1 represents blocky chalk, model 2 represents interbedded shale, and model 3 represents marl carbonate.

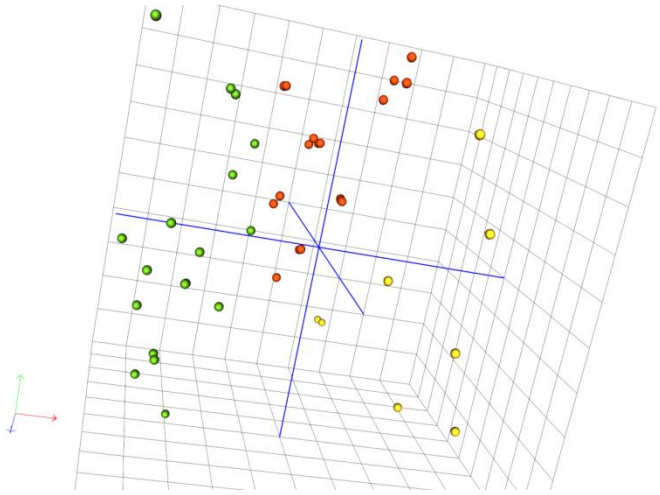

Fig. A.23 Cluster analysis for 40 good matches

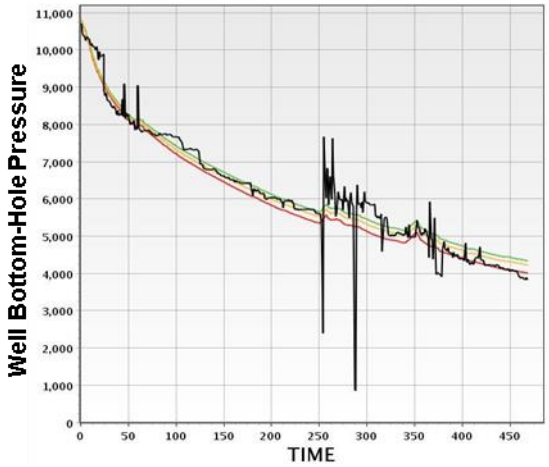

Fig. A.24 Representative model chosen from each cluster

- **Production forecasting.** Oil production in 30 years is forecast based on 40 matched models in **Fig. A.25**. The three representative models are highlighted by colored lines among all forecasting results. We can see that these three models can almost cover the range of all forecasting results. Therefore, when the simulation is quite time-

consuming, we can just run three representative models instead of all 40 updated models. **Table A.5** summarizes the forecasting results of cumulative oil production in 30 years under three models.

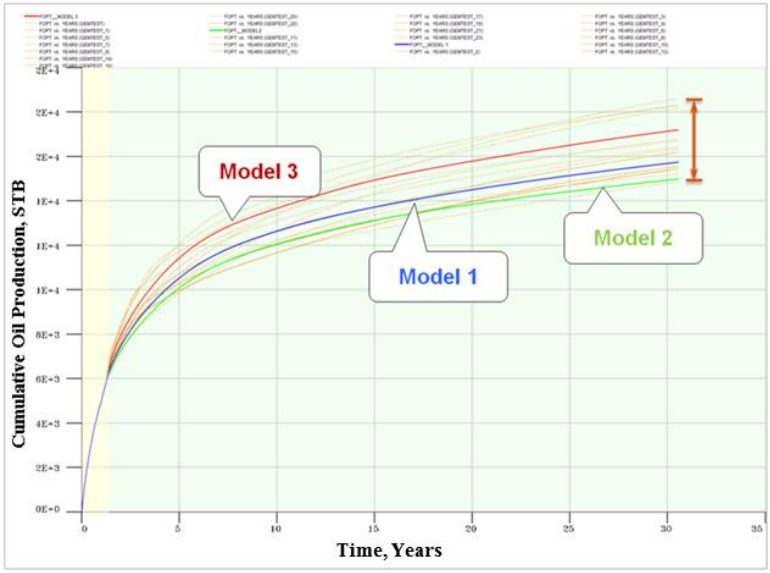

Fig. A.25 Forecasting of 30 years oil production using 40 good runs

Table A.5 Predicted EUR for three geo-models

	EUR_Element model (stb)	EUR_Whole model (Mstb)
Model 1 - Blocky chalk	16187	969
Model 2 - Interbedded shale	15426	923
Model 3 - Marl carbonate	17194	1029

A.5.3 Workflow II

In workflow II, experiment uncertainties are calibrated separately from realization parameters, so that the sub-objective from each geo-model will be calculated. The sub-objective will be evaluated together to obtain the total objective for each individual. Under each updated model, cluster analysis is applied to each geo-model for further production forecasting.

- **Parameter selection**. Porosity, initial water saturation, oil residual saturation and total pay are considered to be realization parameters. **Table A.6** gives the fixed realization parameters for each geo-model with their probability. **Table A.7** gives all uncertain parameters and their range that need to be adjusted during update.

Table A.6 Realization parameters and probability used in Workflow II

Realization parameter	Geo-model 1 Blocky chalk	Geo-model 2 Interbedded shale	Geo-model 3 Marl carbonate
Probability	0.30	0.40	0.30
Porosity	8%	12%	14%
S_{wc}	27.5%	30%	15.5%
S_{orw}	18%	20%	20%
S_{gi}	55%	50%	60%
Total pay, ft	45	40	100

Table A.7 Experiment parameters and their ranges used in Workflow II

Uncertain parameters	Base	Min	Max
PERMX in layer 4	1E-4 mD	1E-5 mD	1E-3 mD
PERMX in other 5 layers	1E-4 mD	1E-5 mD	1E-3 mD
Enhanced perm multiplier on km	100	1	1000
Exponent in trans. vs. pressure	4E-4	0	7E-4
Phase behavior	High	Low	High
Exponent in SWOF, SGOF	3	0.25	5
Exponent in compressibility vs. pressure	0	0	5E-6

- **Assisted history matching, cluster analysis and production forecasting**. Throughout the history matching process, three geological scenarios are evaluated separately with their probability to history match dynamic model. Cluster analysis and production forecasting of oil production in 30 years will be performed for each geo-model under updated models. The results of the whole process for every geo-model are demonstrated as follows.

Geo-model 1. Fig. A.26 shows 66 good matches out of all 140 experiments for geo-model 1. Then cluster analysis is run based on 66 good matches, as shown in **Fig. A.27**. We can see that for geo-model 1, within all good updated models, the parameters are scattered. Oil production in 30 years for geo-model 1 is calculated based on 66 good models. The highlighted red line is the forecasting of our chosen representative model (**Fig. A.28**).

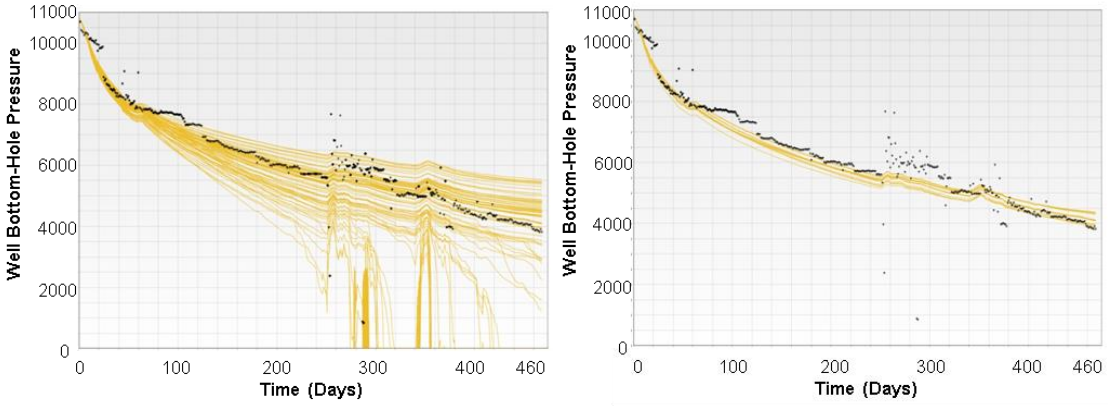

(a) (b)

Fig. A.26 (a) All 140 experiments from history matching for geo-model 1, (b) 66 good matches chosen from 140 experiments for geo-model 1

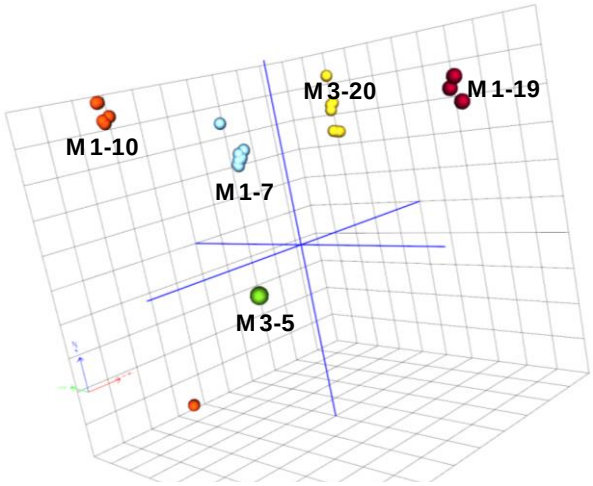

Fig. A.27 Cluster analysis over 66 good models for geo-model 1

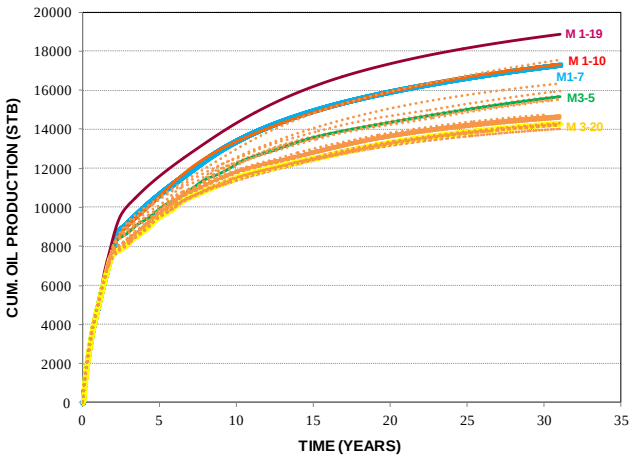

Fig. A.28 Production forecasting using 66 good matches for geo-model 1

Geo-model 2. 66 good matches are also chosen out of all 140 experiments for geo-model 2, as shown in **Fig. A.29**. Then cluster analysis is run based on 66 good matches, as shown in **Fig. A.30**. We can see for geo-model 2, within all good updated models, the parameters are scattered but less scattered than geo-model 1. Oil production in 30 years for geo-model 2 is calculated based on 66 good models. The highlighted green line is the forecasting of our chosen representative model (**Fig. A.31**).

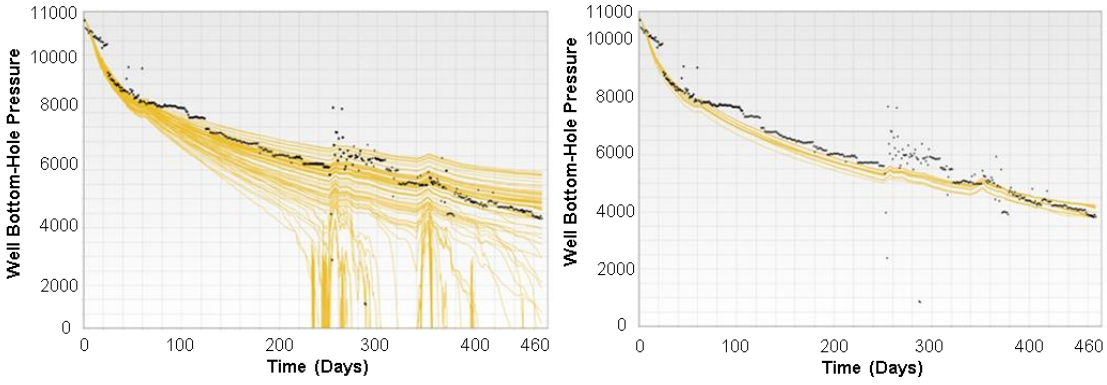

(a) (b)

Fig. A.29 (a) 140 experiments from history matching for geo-model 2, (b) 66 good matches chosen for geo-model 2

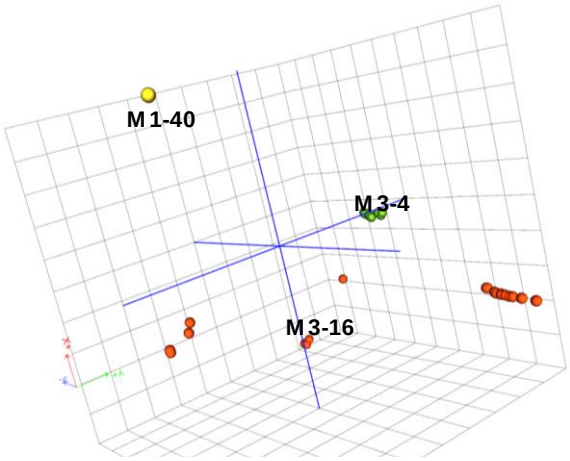

Fig. A.30 Cluster analysis using 66 good matches for geo-model 2

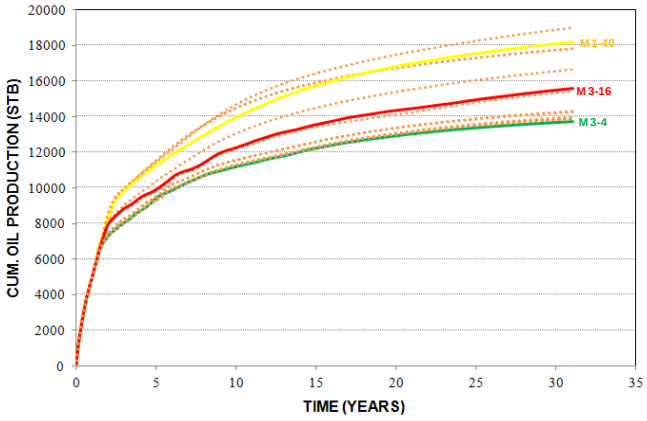

Fig. A.31 Production forecasting using 66 good matches for geo-model 2

Geo-model 3. For geo-model 3, only 9 good matches are also chosen out of all 140 experiments for geo-model 3, as shown in **Fig. A.32**. Then cluster analysis is run to group 9 good matches, as shown in **Fig. A.33**. We can see that for geo-model 3, within all good updated models, the parameters are scattered. The reason for much less good models for geo-model 3 is that geo-model 3 is a less probable scenario, which should be assigned small probability. Oil production in 30 years for geo-model 3 is calculated

based on 9 good models. The highlighted blue line is the forecasting of our chosen representative model (**Fig. A.34**).

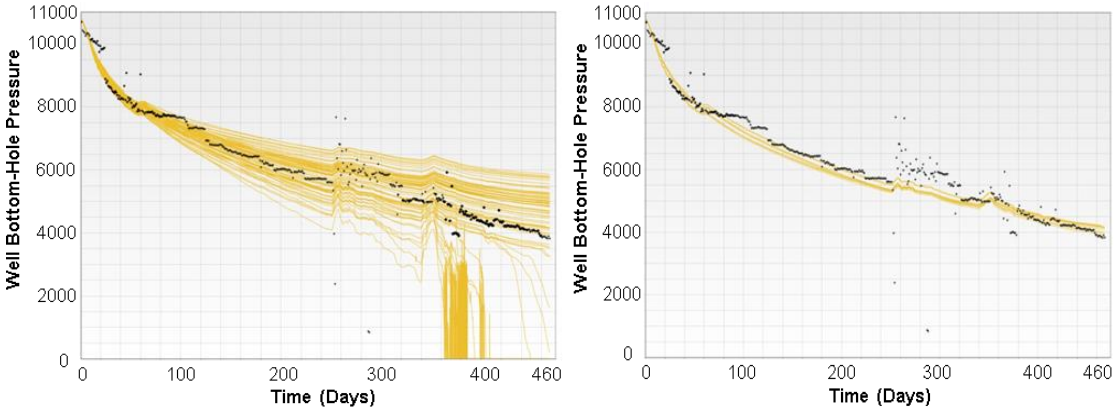

(a) (b)

Fig. A.32 (a) 140 experiments from history matching for geo-model 3, (b) 9 good matches chosen from all 140 experiments

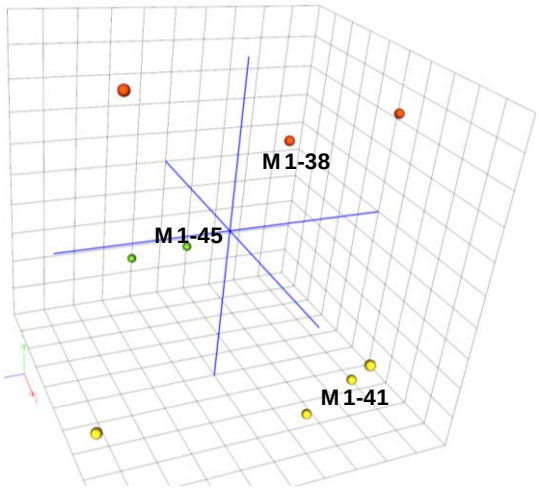

Fig. A.33 Cluster analysis using 9 good matches for geo-model 3

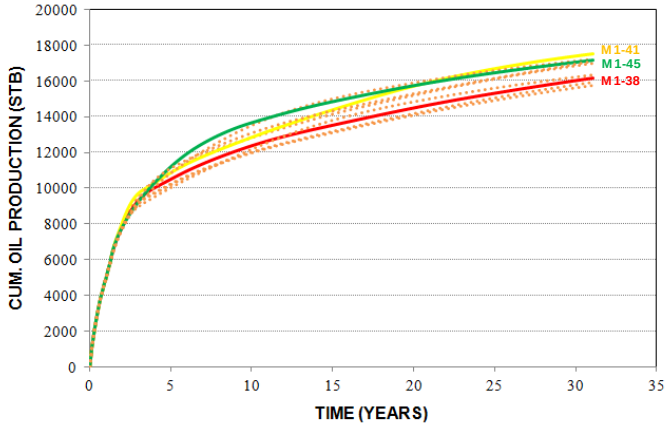

Fig. A.34 Production forecasting using 66 good matches for geo-model 3

Table A.8 summarizes forecasting results of three representative geo-models. The range is close to the range given by workflow 1, which also means we can just run the three representative models instead of all good models from each geo-model.

Table A.8 Summary on forecasting for three geo-models in Workflow II

	EUR_Element model (stb)	EUR_Whole model (Mstb)
Model 1 - Blocky chalk	17554	1110
Model 2 - Interbedded shale	16654	1054
Model 3 - Marl Carbonate	17241	1091

A.6 Comparison and Discussion

Application of the previously discussed workflows indicated their robustness. But, it also showed that each has its unique features. For Workflow I, a superset of realization parameters from geo-models evolve with experimental uncertainties to come up with one dynamic model during each evolution. Representative model for each geo-model is

selected from updated models by cluster analysis. So Workflow I does not require specific values for realization parameters and probability of each geo-model. However, it may not be able to find representative for some geo-model because of improper parameter ranges or evolution strategy finding local minima.

For Workflow II, realization parameters for each geo-model stay constant and only experimental uncertainties are evolved during history matching. So under each evolution, there is one dynamic model for each geo-model. The objective of each evolution is calculated as weighted-average of objective of each dynamic model. So, specific values for realization parameters and probability of each geo-model need to be provided for workflow II reasonably well, otherwise less proper geo-model with higher probability may filter out good dynamic models for the other geo-models during evolution. Cluster analysis is performed on updated models for each geo-model, so it may find more representatives cases for each geo-model. Compared with Workflow I, Workflow II generates more dynamic models which, in turn, requires more time for post-processing. **Table A.9** summarizes our observations for using these two workflows.

Table A.9 Comparison between Workflow I and Workflow II

	Workflow I	Workflow II
Features	• Dynamic model for each evolution • Each dynamic model has its own objective • Evolution individually • Equal geo-model probability	• Dynamic model for each geo-model, no model under each evolution • Objective is weighted-average of all geo-models • Evolution in group • Individual probability considered
Pros	• Good and quick way to forecast when probability is not determined • Fast post-processing	• May find more representatives for each geo-model
Cons	• May not be able to find representative for some geo-model (because of improper range, or local minima in evolution strategy)	• Less probable geo-model with higher probability may filter out good dynamic models for the other two geo-models • Slow post-processing
Requirement & Recommendation	• Proper parameter ranges • Good and quick answer	• Reasonable probability • More representatives for each geo-model

A.7 Summary and Conclusions

In this paper we discuss the impact of reservoir properties, hydraulic fractures, microfracs, phase behavior and rock characteristics on production behavior and present two workflows to utilize stochastic history matching method to a horizontal well in Eagle Ford shale oil reservoir. Some specific findings from this study are summarized below:

- For single porosity – single permeability model, matrix permeability and matrix relative permeability are critical parameters that affect oil production.
- Hydraulic fracture is the main conduit for flow. Hence, fracture compaction will impact the flow to the wellbore. However, rock compaction and its impact on

matrix permeability has a higher impact on flow from matrix.

- The rate of pressure depletion does impact the cumulative production.
- Based on the current application, Our Workflow I proved to be an efficient way for history matching and production forecasting. However, its inability to find representative cases for some geo-model due to improper parameter ranges or local minima evolution strategy makes it somewhat limited.
- Workflow II works better for situations where more information is available. However, reasonable values for realization parameters and probability distribution for each geo-model need to be provided beforehand, otherwise less probable geo-model with higher probability may filter out good dynamic models for the other geo-models. Workflow II generated more representative cases for each geo-model.

Both proposed workflows used different geological scenarios and ranges of uncertainty for reservoir parameters. However, the estimated range for the production forecast was comparable indicating the robustness of these workflows.